Dissertations, Master's Theses and Master's Reports

2021

New Horizons for Processing and Utilizing Red Mud

M. Archambo

Michigan Technological University, msarcham@mtu.edu

Recommended Citation

NEW HORIZONS FOR PROCESSING AND UTILIZING RED MUD

By

Michael Scott Archambo

A DISSERTATION

Submitted in partial fulfillment of the requirements for the degree of

DOCTOR OF PHILOSOPHY

In Chemical Engineering

MICHIGAN TECHNOLOGICAL UNIVERSITY

2021

This dissertation has been approved in partial fulfillment of the requirements for the Degree of DOCTOR OF PHILOSOPHY in Chemical Engineering.

Department of Chemical Engineering

Dissertation Co-Advisor: Dr. *S. Komar Kawatra*

Dissertation Co-Advisor: *Dr. Timothy C Eisele*

Committee Member: *Dr. Tony N Rogers*

Committee Member: *Dr. Gowtham*

Department Chair: *Dr. Pradeep Agrawal*

Table of Contents

List of Figures

List of Tables

Preface

"Red mud: Fundamentals and new avenues for utilization" was published in the journal *Mineral Processing and Extractive Metallurgy Review* in 2020. The article was slightly modified and used as Chapter 2. The first author performed all experiments and wrote the article. The second author provided assistance in understanding experimental data and writing review.

"Utilization of Bauxite Residue: Recovering Iron Values Using the Iron Nugget Process" was published in the journal *Mineral Processing and Extractive Metallurgy* in 2020. The article was slightly modified and used as Chapter 5. The first author performed all experiments and wrote the article. The second author provided assistance in understanding experimental data and writing review.

"Extraction of rare earths from red mud iron nugget slags with oxalic acid precipitation" was submitted for review to the journal *Mineral Processing and Extractive Metallurgy Review* in 2021. This article was slightly modified and used as Chapter 7. The first author performed all experiments and write the article. The second author provided assistance in understanding experimental data and writing review.

Acknowledgements

I would like to give thanks to Dr. Kawatra for giving me this fantastic opportunity to pursue my doctorate degree. I appreciate him for always pushing me to do my best and everything he does for his family of graduate students.

I would like to thank my parents Scott and Beth Archambo for doing everything they could to ensure that I was able to achieve my goals. Having your support has always given me strength.

Abstract

Red mud is an industrial slurry waste that is produced as a byproduct of the Bayer process for alumina. The waste is generated in large quantities, up to a ratio of 2:1 against the valued product alumina. Red mud exhibits many chemical and physical properties that categorize it as a hazardous material. Due to the addition of sodium hydroxide in processing, the pH is typically at values close to 13. Small particle size discourages separation from water for disposal, so drying red mud happens over many years.

The pH of red mud can be reduced with inexpensive reagents. Carbon dioxide is a greenhouse gas that is finding a great deal of research into potential sinks to reduce the footprint on the atmosphere. Combining carbon dioxide with red mud can effectively reduce the pH while also providing a sink for the greenhouse gas. Carbon dioxide is able to reduce the pH of red mud from 13 to 10 over long periods of time.

Red mud can be utilized to produce a variety of value-added products. Most red muds around the world contain a large quantity of iron, titanium, aluminum, and rare earth elements. One method of removing the iron is through the iron nugget process which reduces iron and removes impurities in a single step. The iron nugget process is able to produce blast furnace quality pig iron (over 90% iron purity) with the addition of a carbonate flux material. Rare earth elements are concentrated in the slags from the iron nugget process and can be removed with acid leaches.

The current view of red mud as a waste material is misleading. The proposed work will investigate methods to reduce the hazardous nature of red mud by reducing the pH and

also remove valuable minerals. This will effectively give value to the waste product while simultaneously reducing the overall amount of red mud waste that needs to be disposed.

1 General Introduction

The waste created from alumina processing poses a large threat to the world and a problem for the mining industry has yet to solve. Its estimated that red mud is produced at a rate of 120 million tons per annum (Power et al, 2011). This red mud doesn't disappear once its produced, it gets sequestered away to land based impoundments or lagoons where it sits for years as it dries slowly. The stockpiled of red mud around the world is estimated to be near 4 billion tons, including waste from 84 active plants and over 50 legacy site that are not shut down (Evans, 2016), (Wang et al, 2019). Red mud is an environmental and storage issue that continues to compile every year as aluminum demand increases.

Red mud is composed of fine particles in a slurry which contain a multitude of different minerals. The particle size is typically in a range near 10 microns or smaller (Paramguru et al, 2004). Red mud also is recognized for its signature high alkalinity, which typical gives a pH over 13. This material is created with the Bayer process as seen in Figure 1-1. The bauxite ore is first crushed to the liberation size and then sent through the desilication step. Desilication dissolves silicates and reprecipitates them in an insoluble form so that they do not contaminate the aluminum liquor. The ore is then fed to digestion, where caustic sodium hydroxide dissolves the aluminum bearing minerals. The aluminum rich liquor is given to a precipitator to crystallize aluminates in a pure form. Calcining removes water molecules to yield the final product, alumina. Any material that did not dissolve in digestion is separated along with residual sodium hydroxide and thickened to yield red mud.
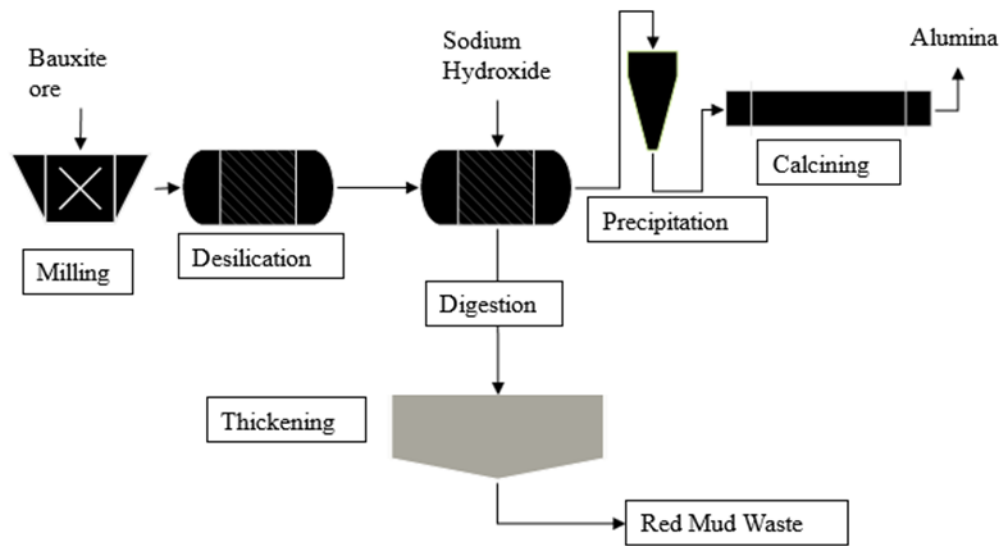
Figure 1-1: The Bayer Process, the generation of valuable alumina and red mud from bauxite ore.

The current strategy for red mud disposal and storage is not working and needs to be adapted. Waste reservoirs for red mud do not effectively contain the hazardous material. For example, the red mud spill in Hungary on October 4th, 2010 saw a breach in the wall of its waste pond. The satellite image of the incident can be seen in Figure 1-2. 700,000 cubic meters of red mud crashed into nearby towns and coated them with the fine slurry of residue. The tragedy that day killed 10 people and many others required medical attention for chemical burns (Rutyers et al, 2011). Longer term environmental risks were also caused by the spill including overwhelming the soil with high pH material, and the release of dangerous metals such as Al, As, Cr, Mo, and V (Mayes et al, 2016). 40 square kilometers were immediately affected by the spill, including the Marcal river (Khairul et al, 2019). More area is at potential risk as the red mud dries and fine dust is allowed to

travel by air farther from the spill. The reduction of material stored in these red mud ponds is critical for the environmental safety of the ecosystem and its people.

Figure 1-2: Satellite image of the red mud spill in Ajka, Hungary in 2010. Jesse Allen, Devecser és Kolontár térsége a vörösiszap katasztrófa után, marked as public domain, more details on Wikimedia Commons

Red mud can be utilized to remove minerals which possess value and could be sold. Most red muds contain a large weight percentage of iron that ranges from 20- 60% (Paramguru et al, 2004). Removing iron from red mud waste can potentially reduce the amount of waste by 60%. Red mud also contains a concentrated amount of rare earth elements. Akcil et al (2018) found that red muds around the world can contain total rare earth concentrations up to 1700 ppm. This puts red mud in a unique position to be able to produce critical materials that are necessary for the independence of the economy from China, who controls more than 95% of current rare earth element production (Akcil et al, 2018).

This dissertation will investigate methods to reduce the amount of red mud as well as reduce its hazardous properties. Chapter 2 explores the current state of alumina and red mud production around the world and the current state of research into neutralization and element extraction. Carbon dioxide is used to neutralize red mud in Chapter 3. This chapter investigates how well carbon dioxide can reduce the pH of red mud and what materials can be generated from the reaction. In Chapter 4 iron is removed from red mud using the iron nugget process. This chapter focuses on optimizing the removal of iron using a heating process by changing variables such as residence time and carbon content. Chapter 5 goes further in the iron nugget process by investigating the role that flux additions play in the separation of iron. Chapter 6 will show potential to remove flux additions altogether by using CO_2 neutralized red mud as feed material. Chapter 7 focuses on rare earth elements and the potential to use red mud nugget slags as a feed stock for rare earth production in the United States.

2 Red mud: Fundamentals and new avenues for utilization[1]

2.1 Abstract

Red mud is generated at a rate of up to 175.5 million tons per year. The global stockpile of red mud is near 4 billion tons. This material is hazardous with pH values from 11 to 13. Reduction of this waste is critical. Current industry practices for disposal of red mud involves different stockpiling techniques on valuable land area or disposing into critical bodies of water. This review studies processes which can reduce the negative environmental impact of red mud in an economic way. For instance, neutralization of red mud with CO_2 can decrease the pH from 12.5 to 7. Treatment of red mud by this method lessens the negative environmental impact and prepares it for further processing for utilization. The current utilization rate of red mud is very low, only about 3 million tons per year are used as an additive for cement and construction. Red mud contains a large quantity of valuable minerals that can be extracted to both reduce the amount of red mud and provide value to the waste. This review investigates novel methods for treating red mud and extracting minerals like iron, titanium, and rare earth elements using a variety of smelting, direct reduction, and leaching processes. For example, the iron nugget process is a single step method to reduce iron oxides to metallic iron and separate them from red mud. Iron nuggets produced from red mud have an iron grade above 90%, which is comparable to pig iron generated by the blast furnace.

2.2 Introduction

The increase in demand for products containing aluminum has led to a sharp increase in production of aluminum around the world. Only one method is suitable for economically producing alumina at such a large scale, which is the Bayer process. The byproduct of this process, known as red mud, has been considered a waste product for many years. Typically, industry disposes the red mud into landfills or into bodies of water over long periods of time. The total stockpile of red mud in the world is estimated to be near 4 billion tons (Wang et al, 2019). Every year the stock grows and red mud is added at a rate of at least 120 million tons per year (Power et al, 2011).

Red mud is a hazardous material with high pH ranges. These caustic sludges are dangerous to environments near red mud disposal sites and people that live near them. Reducing the risk of contamination is crucial and many research projects have investigated ways to lessen the negative impact of red mud. Many of these new projects are pH neutralization experiments. The most novel of these processes is the use of carbon dioxide to neutralize red mud. Since carbon dioxide is a greenhouse gas, there is incentive to sequester it. This effective method can reduce the pH of red mud and provide a sink for carbon monoxide (Archambo et al., 2020).

Total utilization of red mud is only 3 million tons per year, mainly as an additive into cements (Pontikes and Angelopoulos, 2013). This equates to less than 1 percent of red mud being utilized which is shocking because red mud contains many valuables that could be recovered at a profit. Iron can be found in large quantities in most red muds with iron grades varying from 20 to 60% (Paramguru et al, 2004). Red mud has the potential

to be an excellent iron feedstock as its iron content is comparable to the iron range of North America. Steel plants in close proximity to Bayer process alumina plants have the potential to utilize the red mud as feed for iron and steel making and cut down on the large cost of shipping iron ore pellets over great distances. This review investigates novel methods for extracting iron from red mud that are not available in prior red mud review publications. One example is the red mud iron nugget process which generates pig iron of blast furnace quality in a single step using only red mud and powdered wood as feed material (Archambo and Kawatra, 2020). This is the first time that iron nuggets have been generated from red mud by using powdered wood as the reducing reagent. Steel plants are often in close proximity to alumina plants. Implementation of a nugget process from red mud could reduce the distance that iron pellets have to travel to be processed.

Many red muds also contain elevated concentrations of rare earth elements, which are strategically critical resources that are becoming of even more vital importance to the world in recent times. China controls the market on rare earth elements at 78.7% of total worldwide production in 2017 (Balaram, 2019). Finding usable rare earth concentrates, such as red mud is essential for the health of the United States economy as well as the worlds. New research shows that these elements can be extracted from red mud (Wang et al., 2013; Abhilash et al., 2014; Alkan et al., 2017, 2018; Davris et al., 2018; Rivera et al., 2018; Zhang et al., 2019).

Understanding how red mud is generated and the physical and chemical properties associated with it helps to drive the investigation on extracting values from red mud while reducing the environmental risk and shrinking the total stockpile of red mud. This

review demonstrates the need to utilize red mud by investigating new up to date research on the neutralization of red mud pH as well as novel processes for the extraction of valuable minerals such as iron, titanium, and rare earth elements. If red mud can be viewed as a feed material rather than a waste product, the incentive to process it further will undoubtedly reduce its impact on the environment while increasing profit.

2.2.1 Bauxite ore, mineral precursor to red mud

Bauxite is the main feed ore that is used in alumina production. It can be found in different ore bodies around the world. Many countries have been mining bauxite to produce alumina and based on the U.S. Geological Survey in 2020, the worldwide bauxite resources are estimated to consist of Africa (32%), Oceania (23%), South America and the Caribbean (21%), Asia (18%), and elsewhere (6%); an estimated 55 to 75 billion tons of total resources (U.S.G.S 2020). Table 2-1 shows the production of alumina from bauxite around the world based on country. The estimated reserves for each country are also reported. The top 5 reserves for bauxite ore are located in China, Jamaica, Brazil, Australia, and Guinea. China is the number five spot and is currently the third largest producer of bauxite on the planet behind Guinea and Australia.

Table 2-1:Bauxite ore reserves and production worldwide (U.S.G.S, 2020)

Country	2019 Bauxite Production (x1000 tons)	Estimated Reserves (x1000 tons)
Australia	100,000	6,000,000
Guinea	82,000	7,400,000
China	75,000	1,000,000
Brazil	29,000	2,600,000
India	26,000	660,000
Indonesia	16,000	1,200,000
Jamaica	8,900	2,000,000
Russia	5,400	500,000
Vietnam	4,500	3,700,000
Saudi Arabia	4,100	200,000
Malaysia	900	110,000
Other Countries	15,000	5,000,000
World Total	**370,000**	**30,000,000**

Bauxite is not one mineral, but rather a conglomerate of multiple aluminum bearing minerals with other gangue minerals. These gangues consist of iron oxides (Fe_2O_3 and $FeO(OH)$), clay minerals like silica and kaolinite, and titanium minerals such as rutile and anatase. Bauxite is mined for aluminum production because of high amounts of the following aluminum bearing minerals:

1. Gibbsite: $Al(OH)_3$

2. Boehmite: $AlO(OH)$

3. Diaspore: $AlO(OH)$

In terms of worldwide alumina production, 69.6% of ore mined is gibbsite, 24.6% is boehmite, and 5.8% is diaspore (Paramguru et al, 2004). These materials vary in their crystal structure and stability, resulting in differing difficulties in processing. Gibbsite requires the mildest conditions to process while boehmite and diaspore require considerably more energy. Table 2-2 outlines which areas of the world contain each of the three types of bauxite ore. The type of ore determines how aggressive the processing conditions are required during the Bayer Process.

Table 2-2: Bauxite ore types found in each producing country of alumina (Paramguru et al, 2004)

Country	Bauxite Ore Type		
	Gibbsite	**Boehmite**	**Diaspore**
Australia	X	X	
Guinea		X	X
China			X
Brazil	X		
India	X		
Indonesia	X		
Jamaica	X		
Malaysia	X		
Greece			X
Ghana	X		
Guyana	X		
Hungary		X	
Romania			X
Sierra Leone	X		
Suriname			
Turkey			X
Venezuela	X		

2.2.2 The Bayer Process

The Bayer process is the most commonly used method of producing alumina from bauxite on a large scale. The process consists of a series of unit operations that are chemically and energy intensive. Red mud is generated during this process in large quantities, each ton of alumina processed results in between 1.5 to 2.5 tons of red mud byproduct (Borra et al, 2016). The product of the Bayer process, alumina, is then sent to electrochemically produce aluminum metal using the Hall-Heroult process. Below is a summary of each of the steps of the Bayer process and Figure 2-1 shows a simplified process flow diagram for the Bayer process.

Crushed Ore

```
                              ┌──────────┐          ┌────────────┐
        ───────────────────▶  │ Milling  │  ─────▶  │ Desilication│  ─── Desilication
                              └──────────┘          └────────────┘       Product
                                                                            │
                                                                            ▼
         ┌─────────────┐          ┌──────────────┐          ┌──────────┐
Red Mud ◀│ Clarification│ ◀───────│              │◀─────────│ Digestion│
         └─────────────┘          └──────────────┘          └──────────┘
                │
             Alumina
                │
                ▼
         ┌──────────────┐          ┌────────────┐
         │ Precipitation│ ──────▶  │ Calcination│ ──────▶
         └──────────────┘          └────────────┘
```
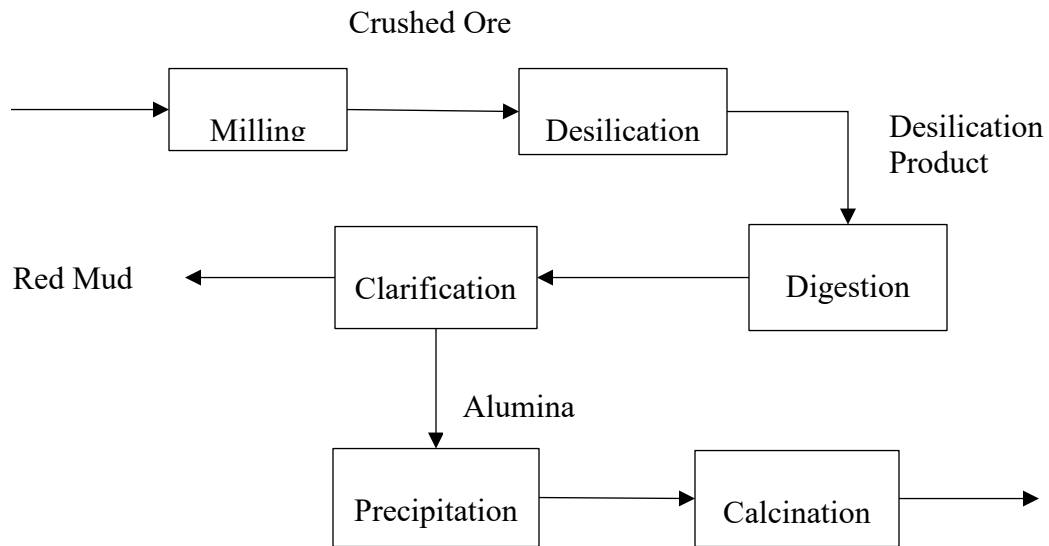
Figure 2-1: Simplified process flow diagram for the Bayer process

2.2.2.1 Milling and Desilication

To increase the available surface area for digestion, the first step of the Bayer process is a fine grinding step. This grinding aims to reduce the bauxite ore to a particle size of less than 150µm.

The desilication step occurs before the dissolution of bauxite in order to transform chemical species that will react with caustic at the high pH range of the digestion tanks. The goal is to dissolve reactive species that would contaminate the product liquor and re-precipitate them as an insoluble mineral that won't interfere in the digestion stage. This includes many clay minerals such as kaolinite that will react with caustic at low temperatures and even quartz that will begin to react as the temperature increases. To avoid impurities in the aluminum bearing liquor later in the process, this step dissolves the soluble clay minerals and then precipitates them in an insoluble form. The dissolution reaction for these minerals is shown in Equation 2-1 (Kotte, 1981). The parameters that affect this dissolution are temperature, kaolinite surface area, caustic concentration, silica concentration, and alumina concentration.

$$(2H_2O \cdot Al_2O_3 \cdot 2SiO_2) + 6OH\text{-} \leftrightarrow 2SiO_3^{-2}(aq) + 2Al(OH)_4\text{- } (aq) + H_2O \qquad \text{(2-1)}$$
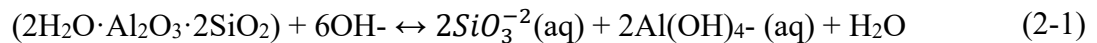
Precipitation occurs via Equation 2-2 where Desilication product (DSP) is formed (Kotte, 1981). Parameters that affect this reaction are temperature, silica concentration, alumina concentration, caustic concentration, and DSP surface area.

13

$$2SiO_3^{-2}(aq) + 2Al(OH)_4\text{-}(aq) + 2Na^+(aq) \leftrightarrow (Na_2O \cdot Al_2O_3 \cdot 2SiO_2) + 4OH\text{-} \quad (2\text{-}2)$$

$$(aq) + 2H_2O$$
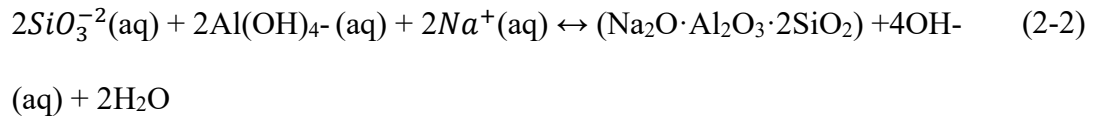
The ratios of different species are important to maximize efficiency of the process, high caustic concentration increases dissolution but decreases precipitation, and high alumina concentration decreases dissolution but increases precipitation (Kotte, 1981). This process generally occurs at moderate temperatures near 100 °C with residence times ranging from 6 to 12 hours in order for the reaction to achieve high enough conversion. With this long residence time, the desilication step is usually the limiting factor in determining total residence times of bauxite in the process (Thomas and Pei, 2007). Since the DSP is precipitated in this step, the particle size of these new insoluble minerals is very small, which contributes to the very fine particle size of red mud down the line of the process.

2.2.2.2 Digestion and Clarification

The desilication product is fed into the digestion tanks for dissolution. The conditions inside the tank vary depending on the primary type of bauxite being digested, as mentioned earlier the three most common types of bauxite ore are gibbsite, boehmite, and diaspore. The aluminum-bearing mineral is dissolved at a high pH using sodium hydroxide. The digestion occurs at pressures between 1 and 6 atm and at temperatures from 150- 250 °C. Dissolution of gibbsite is the easiest because this mineral is a monohydrate and can be extracted at lower temperatures with weaker caustic solutions, while boehmite and diaspore require higher temperatures and more concentrated

solutions because they exist as trihydrate minerals (Adamson et al, 1963). Equations 2-3, 2-4, and 2-5 show the dissolution reactions for each of the bauxite minerals (Wargalla and Brandt, 1981; Paramguru et al, 2004).

$$\text{Gibbsite (135-150 °C)} \qquad Al_2O_3 \cdot 3H_2O + 2NaOH \leftrightarrow 2NaAlO_2 + 4H_2O \qquad \text{(2-3)}$$

$$\text{Boehmite (205-245 °C)} \qquad Al_2O_3 \cdot H_2O + 2NaOH \leftrightarrow 2NaAlO_2 + 2H_2O \qquad \text{(2-4)}$$

$$\text{Diaspore (220-255 °C)} \qquad Al_2O_3 \cdot H_2O + 2NaOH \leftrightarrow 2NaAlO_2 + 2H_2O \qquad \text{(2-5)}$$
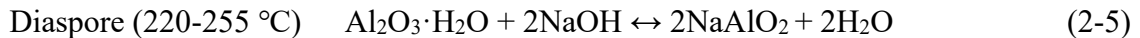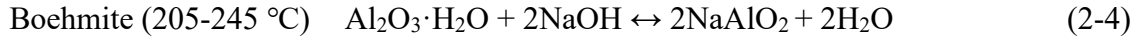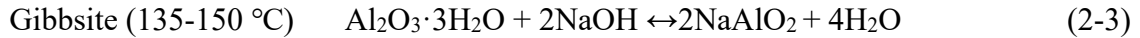
At these temperatures and pressures the alumina-bearing minerals can be dissolved in highly alkaline solutions, but the other oxide minerals (including hematite and rutile) will remain insoluble. Silica can be dissolved depending on the type that is present in the bauxite ore. kaolinite for example is a reactive silica mineral and is susceptible to reaction with sodium hydroxide, this causes losses in caustic in the process (Adamson et al, 1963).

The clarification process separates the pregnant liquor solution of aluminates from the remaining undissolved solids. This is the step of the Bayer process that generates red mud and it is a large aspect of alumina production as a whole. The separation of red mud and subsequent discharge from the facility can account for up to 50% of total plant operations (Paramguru et al, 2004). Plants process and discharge red mud based on local environmental regulations, the location of the plant, and economic considerations of disposal.

The solids are put through a series of filters and thickening tanks to increase the solid/water ratio of the waste and remove the aluminate liquor. Filtration of red mud must remove all solids from the aluminate liquor so that impurities do not persist later in the precipitation step of the process. The filters usually operate at elevated temperatures from 95 to 110 °C, at pressures from 4-5 bar, with a feed of solids content 200- 300 mg/L (Bott et al, 2008). Additives such as tricalcium aluminate (TCA) are added to the filter slurry feed to improve filtering behavior (Bott et al, 2008). Red mud is thickened with the aid of flocculants such as starch or synthetic polyacrylamides (Ballentine et al, 2011).

2.2.2.3 Precipitation and Calcination

After the red mud has been removed from the system, the purified pregnant aluminate solution is crystallized into a pure solid aluminum hydroxide. Reactions relevant to precipitation of solid aluminum hydroxides from the liquor solution can be seen in Equations 2-6 and 2-7 (Chaubal, 1990).

$$\text{Al(OH)}_4\text{- (aq)} + \text{H}_3O^+(aq) \leftrightarrow \text{Al(OH)}_3 \text{ (s)} + 2\text{H}_2\text{O} \qquad (2\text{-}6)$$

$$Al^{3+}(aq) + 6\text{H}_2\text{O (aq)} \leftrightarrow \text{Al(OH)}_3 + 3\text{H}_3O^+(aq) \qquad (2\text{-}7)$$
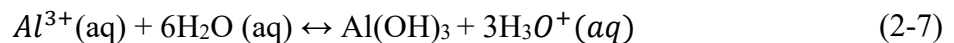
The next step of the process requires carefully controlling the precipitate's size distribution. Within the precipitation unit operation, the seed crystal size distribution must be carefully controlled to keep the product size consistent. Within the precipitation unit operation, a size classification of the seed particles is also occurring in order to meet the required particle size distribution as seen in Figure 2-2.
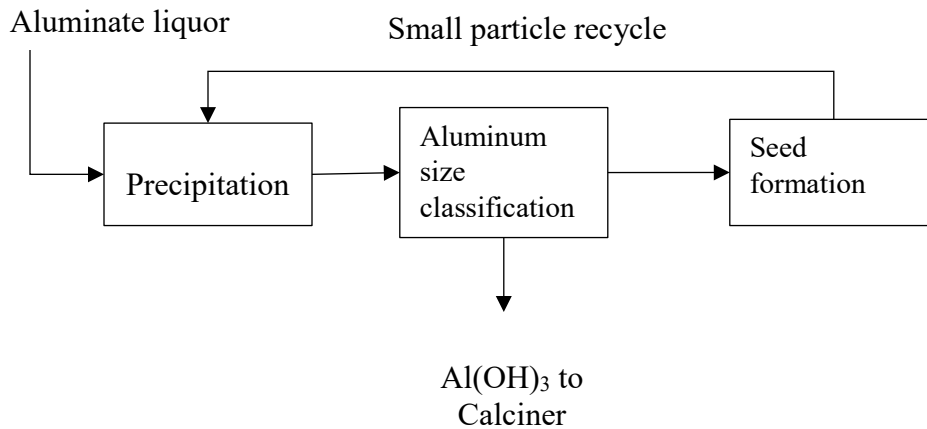
Figure 2-2: Flow diagram for aluminum hydroxide precipitation and size classification in the Bayer process

The solid product from precipitation is fed into the calciner to drive off moisture and yield solid alumina (Al_2O_3). Calcination of alumina is performed using rotary kilns, fluidized bed calciners, or other similar technologies. The chemical reaction of calcining aluminum hydroxide can be seen in Equation 2-8 (Hind et al, 1999).

$$2Al(OH)_3 \text{ (s)} \leftrightarrow 2Al_2O_3 \text{ (s)} + 3H_2O \qquad (2\text{-}8)$$
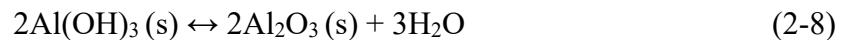
This is the final product of the Bayer process. The total energy expended in the Bayer process to produce 1 kg of alumina is 12.77 MJ (Balomenos et al., 2011). The produced Alumina can be further processed by the Hall-Heroult process to electrochemically produce Aluminum. The Hall-Heroult process is very energy intensive, requiring 212.92 MJ to produce 1 kg of metal aluminum (Balomenos et al., 2011). With such a large consumption of energy, there is incentive to innovate a new process to produce aluminum more energy efficiently. One such process is the carbothermic reduction of alumina under

a vacuum (Halmann et al., 2014). Under atmospheric pressures, the carbon reduction of alumina can only occur at temperatures above 2200 °C, but performing the reduction under a vacuum shifts the energy curve down and the reduction is allowed to occur at lower temperatures around 1400 to 1800 °C (Halmann et al, 2014). Another setup attempted to utilize carbothermic reduction from bauxite ore to metal aluminum, which would eliminate both the Bayer process and the Hall-Heroult process (Halmann et al., 2012). These processes seem to have issues with purity of the resulting aluminum, along with large amount of iron in bauxite needing to be removed before the process can start to be effective. Table 2-3 shows the worldwide production of alumina based on country. Leading producers of alumina in 2019 were China, Australia, and Brazil with China in the lead for alumina production by 53 million tonnes.

Table 2-3: Worldwide alumina production in 2019 (USGS, 2020)

Country	2019 Alumina Production (x1000 tons)
China	73,000
Australia	20,000
Brazil	8,900
India	6,700
Russia	2,700
Jamaica	2,100
Saudi Arabia	1,800
United States	1,600
Canada	1,500
Vietnam	1,300
Indonesia	1,000
Guinea	300
Other Countries	12,000
World Total	**130,000**

2.2.3   Characterization of red mud

The solid residue that is rejected after digestion in the Bayer process is known as red

mud. These are the materials which did not dissolve during the dissolution step. The

mineral phase composition of red mud varies very widely depending on the source of the

ore body that it originated from. The typical deviation of mineral compositions is shown

in Table 2-4. Red mud typically contains a large fraction of hematite, an iron-bearing

mineral which may be worth extracting. Residual aluminates usually combine with silica

to form aluminosilicates which could be useful for construction materials. Other

noteworthy minerals are the potential titanium and rare earth elements, which are other

valued minerals that could be extracted.

Table 2-4: Mineral oxide composition ranges of red mud

Mineral Component	Weight % Range
Fe_2O_3	4-55
TiO_2	2-17
Al_2O_3	6-27
SiO_2	3-24
Na_2O	0-10
CaO	0-40
Rare Earth Elements	500- 1700 ppm (Akcil et al, 2018)

Table 5 shows the various composition of red mud around the world. The key takeaway

from Table 2-5 is that red mud composition varies significantly from location to location,

and characterization at the scale of individual plants is important for characterizing

potential valuable extraction targets. In general, the two major components tend to be

iron oxides and aluminum oxides, which usually account for half of the weight

composition for red mud, though that is not true for all cases. The remaining oxides of

silicon, titanium, sodium, and calcium typically play a smaller role in total composition

of red mud.

Table 2-5: Mineral phase compositions of various red mud sources worldwide

COUNTRY	PLANT	MAJOR COMPOSITION					
		Fe_2O_3	Al_2O_3	TiO_2	SiO_2	Na_2O	CaO
CHINA	Chalco (Grafe et al, 2011)	6.81	18.36	10.45	14.49	5.53	25.22
CHINA	Pingguo (Grafe et al, 2011)	26.9	26.8	7.3	13.1	0	23.5
CHINA	Henan (Zhang et al, 2016)	11.77	25.48	4.14	20.58	6.55	13.97
CHINA	Guizhou (Zhang et al, 2016)	4.03	7.64	3.63	19.03	2.1	34.0
CHINA	Shandong (Zhang et al, 2016)	6.24	5.91	2.1	19.18	2.1	39.52
AUSTRALIA	AWAAK (Snars and Gilkes 2009)	28.5	24	3.11	18.8	3.4	5.26
AUSTRALIA	Pinjarra (Grafe et al, 2011)	36.2	17.1	3.9	23.8	1.6	3.9
BRAZIL	Alunorte (Snars and Gilkes 2009)	45.6	15.1	4.29	15.6	7.5	1.16
INDIA	Korba (Grafe et al, 2011)	27.9	19.4	16.4	7.3	3.3	11.8
INDIA	Damanjodi (Grafe et al, 2011)	54.8	14.8	3.7	6.4	4.8	2.5

INDIA	Hindalco (Paramguru et al, 2004)	35.46	23.00	17.20	5.00	4.85	0
INDIA	NALCO (Shamshad et al, 2018)	51.04	17.57	3.24	8.65	8.03	1.64
JAMAICA	Kirkvine (Grafe et al, 2011)	49.4	13.2	7.3	3.0	4.0	9.4
GREECE	Alumine de Greece (Grafe et al, 2011)	42.5	15.6	5.9	9.2	2.4	19.7
ITALY	Eurallumina (Sglavo et al. 2000a)	35.2	20	9.2	11.6	7.5	6.7
FRANCE	Aluminium Pechiney (Pera et al. 1997)	26.62	15	15.76	4.98	1.02	22.21
UNITED KINGDOM	ALCAN (Srikanth et al. 2005)	46	20	6	5	8	1
HUNGARY	Ajka (Grafe et al, 2011)	42.1	14.8	5.2	13.5	8.9	6.1
CANADA	ALCAN (Vachon et al. 1994)	31.6	20.61	6.23	8.89	10.26	1.66
TURKEY	Seydisehir (Altundoğan et al. 2002)	36.94	20.39	4.98	15.74	10.1	2.23
SPAIN	Alcoa (Snars and Gilkes 2009)	37.5	21.2	11.45	4.4	3.6	5.51

GERMANY	AOSG (Snars and Gilkes 2009)	44.8	16.2	12.33	5.4	4	5.22
USA	RMC (Snars and Gilkes 2009)	35.5	18.4	6.31	8.5	6.1	7.73
USA	Alcoa Mobile (Paramguru, 2004)	30.40	16.20	10.11	11.14	2	0

Red mud mineral composition is not limited to what is shown in Table 4 and Table 5, depending on the source of the ore, a plethora of other elements could also be present in red mud waste. The red mud might have high content of valuable metal elements such as vanadium, gallium and other elements that are radioactive. It may also contain the oxides of manganese, magnesium, zirconium, zinc and chromium though at lower levels (Damayanti and Khareunissa 2016). Depending on the origin of bauxite trace quantities of barium, cadmium, mercury and nickel may be present (Borra et al. 2015). It has been demonstrated that REE's in the red mud are twice as pure to that found in the bauxite ore. Red mud may contain the REE's like Sc, Y, La, Ce, Pr, Nd, Sm, Gd, Tb, Dy, Ho, Er, and Yb (Damayanti and Khareunissa 2016). The average REE concentration found in red mud in Greece and Turkey is 900 ppm (Damayanti and Khareunissa 2016). The Bayer process concentrates rare earths present in the red mud by selectively removing aluminum-bearing minerals. In most cases, the rare earth concentration in red mud is considerably more concentrated than the average of earth's crust. The content of rare earth elements in red muds around the world is shown in Table 2-6. From the table, most

cases show a significant increase in rare earth concentration compared to the average REE content in the earth's crust.

Table 2-6: Rare earth element concentration of red mud comparison with earth average crust composition. Concentrations in parts per million (ppm). (Elements not tested for in each study are represented with a "-")

Location	Rare Earth Elements. Concentrations in parts per million (ppm)													
	La	Ce	Pr	Nd	Sm	Gd	Tb	Dy	Ho	Er	Yb	Y	Sc	Ga
Average in earth's crust (Balaram, 2019)	*39*	*66*	*9*	*41*	*7*	*6*	*1*	*5*	*1*	*3*	*3*	*33*	*22*	*-*
Chinalco, China (Ujaczki et al., 2018)	416	842	95	341	64	56	184	48	25	28	28	266	158	570
Australia (Wang et al., 2013)	-	-	-	-	-	-	-	-	-	-	-	68	54	89
Brazil (Barbosa Botelho et al., 2019)	-	-	-	-	-	-	-	-	-	-	-	24	43	-
India (Abhilash et al., 2014)	110	70	0.5	-	-	-	-	-	-	-	-	1	5	-
India (Singh et al., 2019)	58	98	-	-	-	-	-	-	-	-	-	-	48	-
India (Ujaczki et al., 2018)	112	191	18	48	9	7	-	4	-	1	2	13	58	91

Jamaica (Narayanan et al., 2019)	287	366	74	69	0	37	0	37	5	21	16	373	55	0
Greece (Borra et al., 2015)	114	386	28	98	21	22	-	16	4	13	14	75	121	-
Alumine de Greece Greece (Vind et al., 2018)	130	480	29	107	19	22	3	20	4	13	13	108	-	-
Greece (Deady et al., 2016)	127	409	28	103	20	18	2	19	3	11	13	98	-	-
Ajka, Hungary (Ujkazki et al., 2014)	114	368	-	-	-	-	-	-	-	-	-	68	-	89
Turkey (Deady et al., 2016)	169	480	47	161	32	4	26	23	4	13	14	113	-	-
Russian Federation (Martoyan et al., 2016)	-	-	-	-	-	-	-	-	-	-	-	53	25	35
Russian Federation (Ujaczki et al., 2018)	-	-	-	-	-	-	-	-	-	-	-	-	90	-
Iran (Martoyan et al., 2016)	-	-	-	-	-	-	-	-	-	-	-	1	19	30

Red mud is also characterized by its high alkalinity that comes from residual sodium

hydroxide that was used to dissolve bauxite in the digestion stage of the Bayer process.

As mentioned previously, the desilication product which removes soluble silicates from

solution is stable at high pH. When red mud is neutralized, the DSP products begin to

dissolve and they release sodium hydroxide anions back into solution which act as a

buffer (Power et al, 2011). The particle size for red mud is another very important factor

to acknowledge when characterizing this material. The DSP that was precipitated in the

Bayer process are of a very small particle size, which can be less than 10 ums. Red mud

slurries are also characterized as thixotropic, which means that its resistance to flow, or

viscosity, increases with the amount of mixing energy applied (Power et al, 2011). This

thixotropic property combined with the small particle size make red mud a formidable

material to handle and dewater.

Another major concern is the possibility of concentrating radioactive and toxic elements

within the red mud, similar to how the rare earths can be concentrated. Elements such as

uranium and thorium can be present in bauxite ores with radio activities reported to be

120-350 Bq/Kg for U238 and 450-1000 Bq/Kg for Th232 (Damayanti and Khareunissa,

2016). These quantities are greatly concentrated in red mud after it has left the Bayer

process. Soil tests performed at red mud spill sites has confirmed elevated concentrations

of toxic elements such as arsenic, chromium, mercury, lead, and zinc at concentrations

above 100mg/kg of water (Rutyers et al, 2011). One study found that the soil contained

high amounts of $Al(OH)_4$ ions that were mobile in solution at toxic levels around 175

mg/L; Cr(IV) was also present at dangerous levels of 0.15 mg/L (Milacic et al, 2012).

Responsible disposal of red mud should account for not only the caustic nature of red mud, but the toxicity or radioactivity of the red mud as well.

2.2.4   Worldwide production of red mud

The stockpile of red mud is only due to increase, due to continuously increasing demand for aluminum production around the world and a lack of competitive alternatives to the Bayer process. There were 130 million tons of alumina produced in 2019, as was shown in Table 3. This large number is coupled with the fact that for every ton of alumina that is produced around the world, 1-2.5 tons of red mud are generated (Patel and Pal, 2015). The worldwide average amount of red mud produced per ton of alumina produced is 1.35 (Evans, 2016). This means that the growth of the red mud stockpile is estimated at a rate of at least 175.5 million tons per year in 2019, but the number is likely on the larger end of the estimate. It is estimated that since the alumina industry began in the late 1800s, the stockpile of red mud has grown considerably in recent years. In 1985, it was estimated that the global stockpile of red mud had reached 1 billion tons and in 2007 the stockpile was reported to be 2.6 billion (Power et al, 2011). In 2015, the estimated stockpile of red mud was as high as 4 billion tons (Wang et al, 2019). The production of red mud is growing every year and space to dispose of red mud is becoming more limited. It is more critical than ever to develop solutions for utilization of red mud to reduce the global stockpile.

Currently, there are 84 alumina plants around the world that operate and produce red mud (Patel and Pal, 2015). Most of these plants still utilize the Bayer process with some exceptions in countries like Russia, Iran, and China which use alternative processes

(Evans, 2016). In addition to the currently operating plants, there is a number of closed alumina plants which still contain their produced red mud stockpile with around fifty of these sites worldwide paired with actively producing sites, there is an estimated 3,000 million tons of red mud (Evans, 2016).

China is by far the largest producer of alumina and subsequently red mud in the world. In 2019, China produced 73 million tons of alumina, from Table 3. On a red mud basis, China produced 88 million tons annually, 1.2 times the amount of alumina (Wang et al, 2019). Of the 80 plus alumina plants that are in operation today, around 30 of them are located in China (Evans, 2016). Five of China's provinces account for 77% of the total production of red mud; these provinces are Shanxi, Shandong, Guangxi, Henan, and Guizhou with production of red mud at 14.14, 18.50, 9.06, 12.13, and 4.50 million tons per year, respectively (Wang et al, 2019). Chinese bauxite ores are mostly comprised of diaspore which are the most difficult to process and require intensive energy and reagent dosages (Liu et al, 2014). With such a large amount of dangerous red mud in the country of China, the utilization of this material is important to ensure that disposal areas take up minimum land area. Between 2011 and 2013, the utilization rate of red mud decreased from 5.2% to 4% (Wang et al, 2019). Current utilization is estimated to be around 10% as of 2015, but the government of China is aiming to expand that to 20% (Liu et al, 2014; Patel and Pal, 2015).

Australia is currently the number 2 producer of alumina in the world with a 2019 production of alumina of 20 million tons. The annual production of red mud for this country is reported to be 30 million tons, 1.5 times the amount of alumina produced in the

country, while the global average production ratio is around 1.35 (Evans, 2016; Wang et al, 2019). Primary producers of red mud in Australia are from the following plants:

• Yarwun (Queensland) – Rio Tinto Alcan

• Kwinana (Western Australia) – Alcoa of Australia

• Pinjarra (Western Australia) – Alcoa of Australia

• Queensland Alumina Limited (Queensland)- Rio Tinto Alcan, Rusal

• Wagerup (Western Australia) – Alcoa of Australia

• Worsley (Western Australia) – South 32- Worsley Alumina

Australia has dealt with its red mud issue by processing the waste so that it has a lower and less caustic pH. The neutralization method is with seawater to drive down the pH so that it can be used more easily in other projects or for extraction of other materials. This technology was developed by Queensland Alumina Limited (QAL) (Cristol and Greenhalgh, 2018) and will be discussed in more detail later in the review.

In India, red mud is generated at six different plants; NALCO, HINDALCO, VEDANTA, UTKAL, RAYKAL, ADITYA, and JSW. The total production of red mud for these Indian plants is summarized in Table 2-7. Its estimated that India accounts for 6.25% of the world generation of red mud (Patel and Pal, 2015).

Table 2-7: Yearly generation of red mud in India by alumina plant (Patel and Pal, 2015)

Indian Alumina Plant	Red mud generation per year (million tons)
NALCO	2.697
HINDALCO	2.062
VEDANTA	1.82
UTKAL	1.95
RAYKAL	1.82
ADITYA	1.82
JSW	1.82
Total	**13.73**

There is a strong push in European alumina plants to minimize the production of red mud, due to geographic necessity. Many European alumina plants do not have access to large amounts of land space for reservoirs. This results in two things, reduction in the total amount of produced alumina and the disposal of red mud into the nearby ocean. In order to reduce the amount of red mud produced, many European countries import higher quality bauxite ores from around the world to extract them under more rigorous process conditions which results in an average European ratio of red mud produced vs alumina to be 0.67, considerably lower than the global average ratio of 1.35 (Evans, 2016). Greece, for example has one alumina plant, Alumine De Greece and that produces yearly 0.7 million tons of red mud (Wang et al, 2019).

The major producers of alumina and red mud in the Americas are Brazil and Jamaica.

These countries have high amounts of bauxite ore reserves at 2.6 and 2.0 billion tons

respectively from Table 1. Alunorte in Brazil produced 6 million tons per year in 2011

(Power et al, 2011) and the current amount of bauxite residue generated by Brazil has

reached 10.6 million tons (Wang et al, 2019).

2.3   Disposal Practices for red mud

Lagoon impoundments were common for red mud disposal before the 1980s. Dry

stacking methods began to replace lagooning methods as land space for lagoons became

scarce. Dry stacking reduces the land area required at the same time reducing the liquor

release to the surrounding environment (Balomenos et al, 2018). Filter press technology

was first employed in red mud disposal in 2006, allowing for the reduction of red mud

moisture content below 28%. The filter press saw widespread adoption throughout the

alumina industry between 2006 and 2012. Dry stacking is presently the predominant

technology for red mud disposal, as it significantly reduces waste volume and land area

requirements, and completely eliminates dam failure. Furthermore, the dried red mud is

much easier to transport and utilize in other applications, such as construction or cement.

Disposal of red mud is one of the key aspects of any aluminum processing operation.

Between 1.9 and 3.6 tonnes of bauxite ore is required to generate 1 ton of alumina

product and the rest becomes red mud (Hind et al, 1999). With the large environmental

risk that is associated with red mud, disposal practices are essential for an operating

alumina plant. Removal and disposal of red mud at any given plant can account for 30-

50% of total operations (Paramguru et al, 2004). Many different techniques have been implemented around the world for red mud disposal. Factors that play into which disposal method is chosen for each plant are things like annual rainfall, topography of the surrounding land, the size of the refinery (production rate of red mud), and availability of land (Power et al, 2011). Table 2-8 shows aluminum plants around the world and which method they use for red mud disposal.

Table 2-8: Red mud disposal practices by plant

Plant Name	Country	Disposal Method
Kwinana (Evans, 2016)	Australia	Dry Stacking with CO_2 Neutralization
Kirkvine (Power et al, 2011)	Jamaica	Lagoon
Aluminum De Greece (Balomenos et al, 2018)	Greece	Dry Stacking
Gardanne (Power et al, 2011)	France	Marine Disposal
Ajka (Evans, 2016)	Hungary	Lagoon
Pinjarra (Evans, 2016)	Australia	Dry Stacking
Queensland Alumina (Power et al, 2011)	Australia	Lagoon with Seawater neutralization
Gove Alumina (Power et al, 2011)	Australia	Dry Stacking
VAW Stade (Evans, 2016)	Germany	Lagoon
Alunorte (Power et al, 2011)	Brazil	Dry Stacking

Dhamanjodi (Power et al, 2011)	India	Dry Stacking
Nalco (Rai et al, 2020)	India	Thickened Tailings Disposal
Hindalco (Rai et al, 2020)	India	Filter Pressure followed by dry stacking

2.3.1 Seawater disposal and lagooning

Seawater disposal of red mud is currently regarded as a method of last resort. The red mud is released directly into a nearby water source once it is separated from the alumina liquor. Marine ecosystems are greatly affected by red mud disposal because it creates an increase in turbidity seawater with ultrafine colloidal magnesium and aluminum compounds (Rai et al, 2012). Due to available land constraints for any kind of land-based storage, some plants must resort to this method for removal of red mud. Seven plants in the world (out of eighty-four total) utilize seawater disposal (Khairul et al, 2019). Plants located in countries with comparatively small land area like France, Greece, and Japan all currently dump their red mud wastes into the sea. The plants of Gardanne Alumina (France) and Aluminum De Greece (Greece) use seawater disposal due to economic and environmental reasons (Rai et al, 2012). Overall, the enormous negative effect that red mud disposal has on ocean life and ecosystems in general has led to seawater disposal of red mud to be a last resort.

The second method of red mud disposal is referred to as lagooning. Red mud is pumped into land-based storage areas after it is removed from the Bayer process. Figure 2-3

shows an example of a red mud tailings reservoir in Germany. Lagooning requires a large amount of land area in order to sequester the red mud. Each tailings lagoon or dam is constructed based on many different factors such as; the amount of tailings expected, characteristics of the red mud, and topographic and geological considerations for the potential site of the reservoir (Gawu et al, 2012). To determine how much waste a given area of disposal land can sequester, it is important to be able to determine the yield stress of the material that is being disposed. A common and simple test to accurately determine yield stress, called the slump test, relates the height of the waste pile to the stress exerted on the material (Pashias et al., 2000). Techniques like this allow for more efficient disposal of waste piles.

All parameters of importance must be considered when designing and installing tailings reservoirs. Doing so can prevent a breach in containment and spill caustic waste into the environment. In addition, the construction of the reservoirs usually includes a sealant or a layer or impermeable clay at the bottom of the reservoir in order to prevent any liquid from seeping into the soil beneath and potentially contaminating the groundwater. Research has gone into different type of sealants for reservoirs; multiple layers of impermeable clay along with geo-membrane and plastics have all been utilized to keep the red mud separate from the layer of soil. These seals are made more effective by decanting the surface water to minimize the hydrostatic pressure of the dam on the seal (Power et al, 2011). Benefits that lagooning provides over other methods are of lower capital cost to install as compared to the dry methods and a greater ability to suppress red mud dust escaping into atmosphere (Rai et al, 2012).

Figure 2-3: A red mud tailings reservoir in Stade, Germany. Ra Boe / Wikipedia

(https://commons.wikimedia.org/wiki/File:Luftaufnahmen_Nordseekueste_2012-05-by-

RaBoe-478.jpg), "Luftaufnahmen Nordseekueste 2012-05-by-RaBoe-478",

https://creativecommons.org/licenses/by-sa/3.0/de/legalcode

The careful consideration of the requirements for the construction of lagoons are very

important for the consideration of the local communities. One example of a catastrophic

failure of a red mud impoundment was the disaster at Ajka, Hungary. 700,000 cubic

meters of red mud spilled into the town on October 4th, 2010. This tragedy killed 10

people and many others were treated for chemical burns for being in contact with the

hazardous material (Ruyters et al, 2011). This spill contaminated 40 square kilometers of

land and the marine life of the nearby Marcal river was negatively affected (Khairul et al,

2019).

A study done in central China showed the effects of red mud reservoirs on the

surrounding environment. Concentrations higher than China's standard for surface water

of dangerous ions such as fluorine ions, sulfate ions, mercury, and arsenic were reported.

The radioactivity of the red mud also contributes to disaster when it can be released into the environment (Wen et al, 2012).

The lagooning of red mud has been a good way to dispose of red mud in the earlier years of alumina production, before demand became so high. For red mud disposal today, lagooning requires more land area to sequester mine waste that could be more effectively used for other purposes. With the aftermath of the accident in Hungary, the correct construction of these dams is critical for this disposal technology to be successful. Structural failures or leaks and seepages into the ground can cause disastrous effects. The incentive to reduce the amount of land area required to store these tailings has led to recent innovation in dry red mud disposal technology.

2.3.2 Dry methods- Thickened tailings disposal

Multiple factors have led to the development of improved disposal methods for red mud. These processes are named thickened tailing disposal (TTD) because generally the main objective is to decrease moisture content of the slurry. Lowering the moisture content reduces the volume and land area required to store the red mud, and the recovered liquid can be recycled back into the process. If enough water can be removed, the slurry can become stably dispersed and readily dried by spreading it into a thin layer. A combination of air drying and water drainage systems in the pond continue to dry the red mud (Glenister and Abbot, 1989). For red mud of Jamaican origin, it was found that dewatering by use of centrifuging was more effective than gravity dewatering and a solid content of 40 percent was achievable (Good and Fursman, 1968).

For dry stacking technologies, the rheology of the red mud slurry plays a substantial role in the effectiveness of the process. Red mud slurries are thixotropic, which means that the surface viscosity decreases as stress on the fluid increases. Therefore, a slurry that has been settled to a higher solids content will not be pumpable due to the high viscosity. Mixing the slurry will in turn lower the viscosity and allow the fluid to be pumped (Power et al, 2011). Alcoa's refinery at Pinjarra noted that the yield stress from the thickener underflow varied from 280 to 550 N/m, but when the red mud was passed through a centrifugal underflow pump that supplies sufficient shearing stress, the yield stress was reduced to between 60 and 100 N/m (Glenister and Abbot, 1989).

2.3.2.1 Thickening/Flocculants

The particle size of red mud slurries proves to be one of the most difficult aspects of handling the material. With most red mud slurries containing particles smaller than 10 microns at 80% passing, the settling rates for the solids in these slurries are intolerably slow. In order to improve the recovery of liquor in the plant along with reducing the moisture content of the red mud discharge, the particles must be settled or thickened to a higher solids content. This is widely done in industry using thickener tanks along with the aid of chemical flocculants. Many different types of thickeners have been designed specifically for the dewatering of red mud. Figure 2-4 shows a general flow diagram for the process thickening of red mud. The deep thickener along with other types of super thickeners was developed by Alcan, which provides a higher length to diameter ratio for better performance of red mud generation (Paramguru et al, 2004).
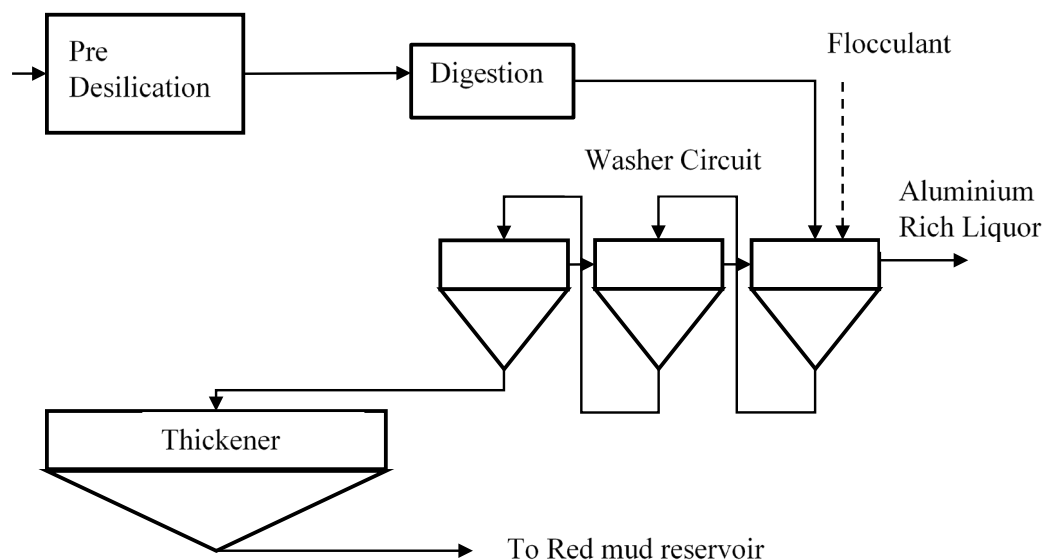
Figure 2-4: The thickening circuit for red mud before disposal discharge

Chemical additives are introduced in order to increase the speed of sediment settling. These flocculants attach to many small particles like a glue and agglomerate to larger diameter particles which settle much faster. The flocculant bridges across many particles of fine red mud and increases the effective particle diameter and particles of higher diameter settle faster. Figure 2-5 illustrates the effect that flocculants have on fine particle slurries. The typical types of flocculants used in the Bayer process are starches, polyacrylamide, and polyacrylates.
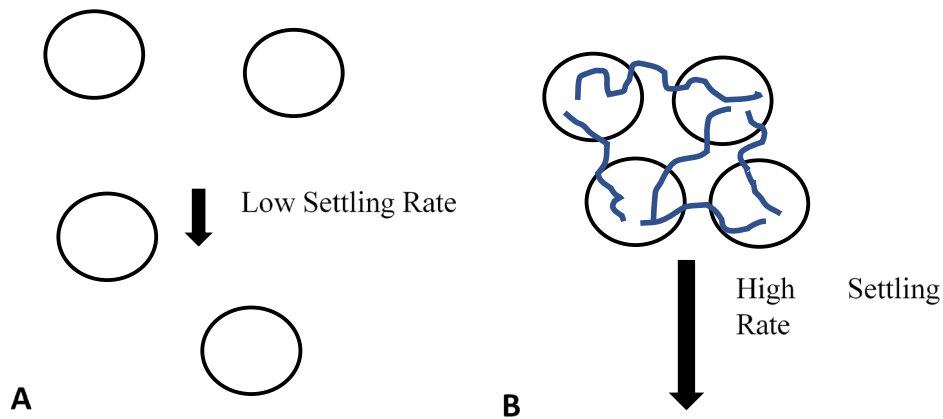
Figure 2-5: Flocculation of Ultrafine Red Mud Particles. A) Red mud slurry suspension without flocculant B) Red Mud slurry suspension with the aid of flocculants

The structures of each of these molecules can be seen in Figure 2-6. The starches amylose and amylopectin are used less frequently today because they have a limited charge density and a small molecular weight for an effective flocculant (Ballentine et al, 2011). This means that the starch does not adsorb very strongly onto the surface of the particle and the small molecular volume limits the amount of available spaces for attachment of particles. The synthetic flocculants do not have the disadvantages that starch has; they can be made to a specific molecular weight tailored to a specific plant's needs (Ballentine et al, 2011). The polyacrylate also contains a very high surface charge in contrast to starches which can more effectively adsorb onto particle surfaces (Ballentine et al, 2011).

Traditionally, starch had been the primary flocculant in thickening operations of red mud, but the industry has moved to using acrylamide and polyacrylate polymers as a means to settle red mud. The reasons for this are the lower dosages required for polymers

compared to starch and the ability to alter the molecular weight of the polymers to optimal size for each process (Sankey and Schwarz, 1982).
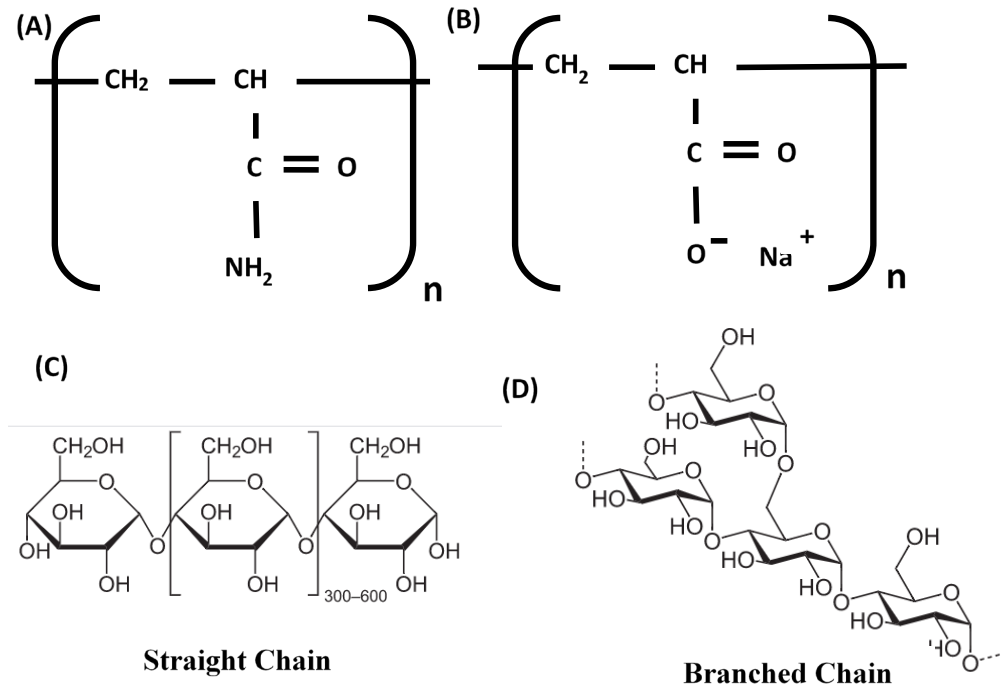
Figure 2-6: Chemical structures of flocculants used to clarify Bayer process liquor and thicken red mud. (A) polyacrylamide (B) Polyacrylate (C) Amylose starch (D) Amylopectin starch

2.3.2.2 Dry Stacking Slurry

Dry stacking the red mud slurry involves thickening to between 45-55% solids and depositing it in thin layers in drying cells between 300 mm and 500 mm thick. At this moisture, the slurry is still pumpable and needs to evenly coat the drying cell. The red mud dries over the course of 30 to 60 days through a combination of solar heating and

water drainage. The target solids content by the end of the drying period is 65-70% (Mitsopoulus and Belanger, 2006).

2.3.2.3 Dry Stacking Cake

With the use of filtration alongside thickening, red mud can be thickened to up to 60% solids. Red mud of this moisture content no longer acts as a flowable fluid but as a wet solid. The red mud behaves non-thixotropically at this moisture content because it's no longer behaving like a fluid. This enables the material to be hauled to impoundments by heavy machinery such as dozers and dump trucks. Multiple plants around the world have begun to utilize this method for bauxite residue disposal. The Hindalco plant in Renukoot, India uses vacuum drum filters; the plant in Stade, Germany along with the CVG plant in Venezuela have had success using hyperbaric filters (Power et al, 2011). The drawback to this method of disposal is that the extremely small dry particles are prone to dusting, which can cause the particles to travel distances beyond the disposal site through the air. With the harmful toxic elements that red mud contains, the contamination of nearby ecosystems through dust is more probable here. Ultimately, this method is most desirable, dry red mud can easily be transported with heavy machinery to a dump site. The dry material can also be transported elsewhere to be used in other processes as an additive, in processes such as cement or ceramic making.

2.4 Neutralization techniques of red mud

The high alkalinity of red mud is the most significant factor contributing to its classification as a hazardous waste. The typical range of pH for red mud discharged from

an alumina plant is between 11 and 13 due to residual strong bases and partially soluble metal hydroxides which tends to have long lasting nature. This is detrimental to any life and ecosystems that exist at or near a red mud waste pond. Disposing red mud at a pH of 9 or lower would significantly decrease the environmental risk it would pose (Hanahan et al, 2004). The incentive to neutralize red mud comes from a need to make the process more environmentally friendly and treat the material for further processing to remove other valuable minerals. Many methods for red mud neutralization have been studied and some have seen some utilization on an industrial scale, such as seawater neutralization, carbon dioxide neutralization, and acid neutralization.

2.4.1   Seawater neutralization

As stated previously, red mud has a high pH once it exits the process to the disposal area. Much research has gone into methods to reduce the risk of red mud waste to the environment and the human population centers around it. One such method is to mix red mud with seawater to reduce the pH to an acceptable level so that the land can be reclaimed by vegetation. With this method, the seawater is mixed with red mud for neutralization, the solid particles then are allowed time to settle and the used seawater is decanted back into the ocean environment. Seawater has a high buffering capacity for alkaline materials, which makes it a good component to neutralize red mud (McConchie et al, 1996). Seawater neutralization converts highly caustic, soluble hydroxide compounds into less caustic, insoluble weakly alkaline solid compounds (Rai et al, 2012). The free calcium and magnesium ions in seawater react with red mud ions such as hydroxyls, carbonates, and aluminates to form precipitates. The neutralization is a very

complex process, the generalized reaction is shown in Equation 2-9 (Cristol and Greenhalgh, 2018).

$$6MgCl_2 + 2NaAl(OH)_4 + Na_2CO_3 + 8NaOH + 4H_2O \leftrightarrow \qquad (2\text{-}9)$$

$$Mg_6Al_2CO_3(OH)_{16} \cdot 4H_2O + 12NaCl$$
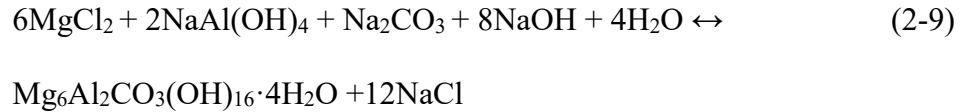
The neutralized red mud exhibits a tendency to settle its fine particles more quickly than general red mud waste. Regular red mud waste contains high sodium concentrations, which can become bound to aluminosilicate and aluminum oxide minerals which cause mineral dispersion (Hanahan et al, 2004). The dispersed particles at high pH combined with the extremely fine particle size cause the settling times of these solids to be very large. With the addition of seawater, exchange cations, Ca and Mg act to flocculate the aluminosilicates and aluminum oxides by forming electrostatic bridges around them; the more agglomerated solids display increased settling times (Hanahan et al, 2004).

Many are concerned that neutralizing red mud with seawater will contaminate the water with alkaline ions and concentrated toxic elements. McConchie et al. (1996) found that the seawater discharge from red mud contained concentrations that are very comparable to the world average seawater values. At a neutralization pH around 8, toxic metals are insoluble and will not be a hazard to the environment (Hanahan et al, 2004). Soil sediment around the release area of utilized bauxite residue seawater are within the limits of what would be considered an unpolluted estuarine sediment, based on trace element concentrations; also, no change in biodiversity was noted to be in the area (McConchie et al, 1996). One study looked at adding additions of gypsum and organic matter to remove

alkaline sodium ions after seawater neutralization. The study found that 5% gypsum addition would be needed to exchange free sodium ions and remove the alkalinity while additions of organics were useful in increasing microbial activity (Li et al, 2018). Queensland Unlimited Alumina (QAL) has begun to adopt this as a viable method for neutralizing its bauxite waste. The plant used seawater to neutralize red mud and stored it in lagoons until 2007 where they added a clarifier to dry the red mud and make use out of it as a construction material. According to Cristol and Greenhalgh (2018), the plant is able to reduce the pH of the red mud to under 9 and considers the clarifier overflow and underflow non-hazardous. The plant can treat 5,800 m^3/h of waste containing nearly 520 t/h of solid waste (Cristol and Greenhalgh, 2018).

In the process developed by Queensland Alumina Limited (QAL), the mud from the last washer underflow is pumped to the residual disposal area using seawater (Cristol and Greenhalgh, 2018). The mud is allowed to mix with the excess of sea water in an agitated reactor to neutralize the caustic content. Insoluble precipitates settle out as a result of reaction of calcium and magnesium on hydroxides and carbonate minerals. The chemical reaction leading the precipitation are:

$$6MgCl_2 + 2NaAl(OH)_4 + Na_2CO_3 + 8NaOH + 4H_2O \rightarrow 12\ NaCl \qquad (2\text{-}10)$$
$$+Mg_6Al_2CO_3(OH)_{16}\ 4H_2O(s)$$

$$MgCl_2 + 2NaOH \rightarrow Mg(OH)_2(s) + 2NaCl \qquad (2\text{-}11)$$

$$CaCl_2 + 2NaOH \rightarrow Ca(OH)_2(s) + 2NaCl \qquad (2\text{-}12)$$
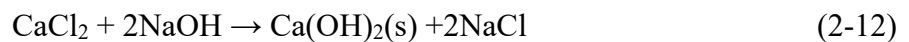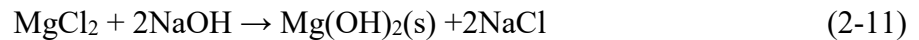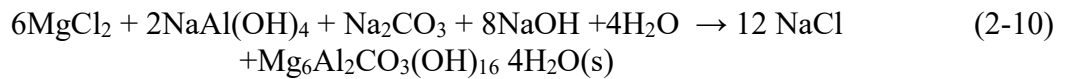
The precipitates from the neutralization process and the red mud are separated using the clarifier. Clarifier underflow consists of neutralized red mud and the overflow consists of magnesium deficient sea water is fed to decant pond to recover any solid content before discharging it to sea. The two streams produced from the clarifier are non-hazardous and can be disposed as per environmental norms. The schematic of the process used at QAL is shown in Figure 2-7 (Scarsella et al, 2012).
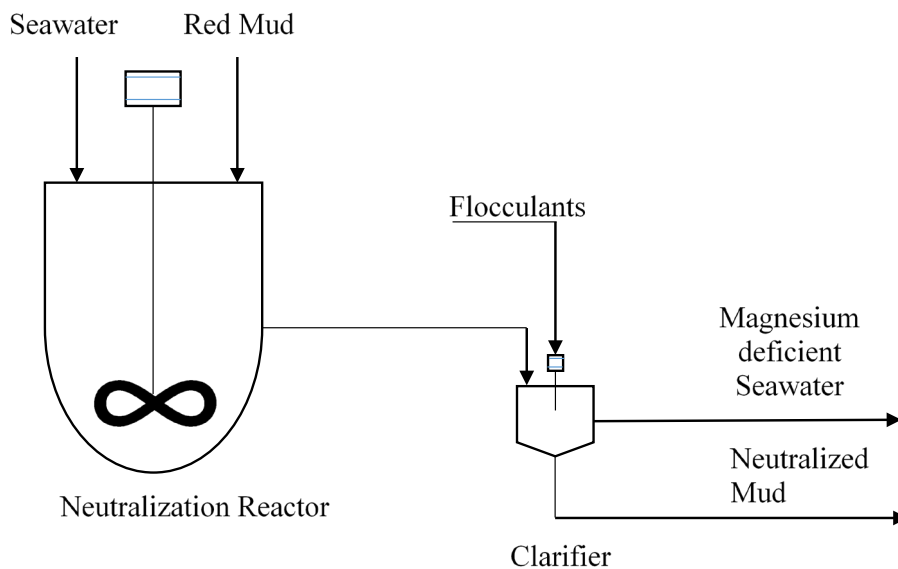
Figure 2-7: Process Flow diagram of Seawater Neutralization at QAL

This process offers several advantages such as low cost of seawater addition, good quality of decanted water meeting regulatory expectations, low risk of ground water contamination due to seepage from the dam and low risk to employees due to non-hazardous residue and discharge water.

2.4.2 Carbon dioxide neutralization

Carbon dioxide is a byproduct of industry which majorly contributes to environmental pollution. Carbon dioxide that is released into the air is an unutilized source of material that can be used in other material processes. Research has gone into finding a use for this greenhouse gas which is significant enough to use on the large scale of CO_2 production. Since CO_2 is an acid gas, it has the potential to react with red mud and reduce the high pH so that the material in no longer hazardous and can be utilized or disposed of safely. CO_2 has the advantage for neutralization over conventional acids because acids are generally more expensive and a plant can easily implement CO_2 from wastes generated elsewhere in the process (Rivera et al, 2017).

Carbon dioxide reacts in red mud primarily with its most prevalent alkaline component, Tri-calcium aluminate (TCA). Dissolution of TCA is what liberates the alkalinity in red mud by exposing OH anions. The following reactions show the interaction between CO_2 and TCA. (Smith et al, 2003). Equations 2-13 and 2-14 are the interaction with the CO_2 and the hydroxide ions from the caustic liquor and Equations 2-15, 2-16, and 2-17 are the dissolution of TCA in CO_2. It should be noted that the liquor reactions are fast and the dissolution of TCA is slow; TCA transforms into minerals like calcite, dawsonite, and aluminum hydroxide and the pH will rebound if the reactions are incomplete since all of these equations are reversible and will push to equilibrium (Smith et al, 2003).

$$CO_{2\,(aq)} + OH^-_{(aq)} \leftrightarrow HCO_3^-{}_{(aq)} \qquad (2\text{-}13)$$

$$HCO_3^-{}_{(aq)} \leftrightarrow H^+_{(aq)} + CO_3^{-2}{}_{(aq)} \qquad (2\text{-}14)$$

$$Al(OH)_4^-{}_{(aq)} \leftrightarrow Al(OH)_{3(s)} + OH^-_{(aq)} \qquad (2\text{-}15)$$

$$NaAl(OH)_{4(aq)} + CO_{2(aq)} \leftrightarrow NaAl(OH)_2CO_{3(s)} + H_2O_{(l)} \qquad (2\text{-}16)$$

$$Ca_3Al_2(OH)_{12\,(s)} + 3CO_2 \leftrightarrow NaAl(OH)_{3\,(s)} + H_2O_{(l)} \qquad (2\text{-}17)$$
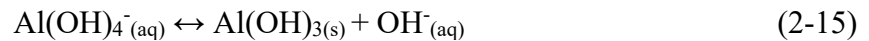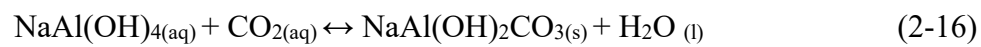
The pH of red mud is known to rise again after the CO_2 gas has been added. The pH of red mud continues to change over large periods of time after the addition of CO_2. Rivera's work on CO_2 neutralization before acid leaching for metal recovery was able to obtain a red mud pH of 8.6 (Rivera et al, 2017). His work shows that following neutralization, the compounds formed are water soluble and leachable. Patel achieved similar results with CO_2 neutralization using multiple CO_2 cycles, he achieved a red mud pH of 8.45 (Patel and Sahu, 2018).

Archambo et al. (2020) neutralized red mud with CO_2 in 1-hour cycles at a gas flow rate of 10 ml/min; the pH of the red mud was reduced down to as low as 7. The experimental setup is described in Figure 2-8. 1 Kg of Red mud was placed in an open 2000 mL beaker and mixed with 1 L of water in order for the red mud to be mixed homogeneously. A mixer was used to keep the particles suspended and a CO_2 bubbler was inserted into the bottom of the cell. A pH probe was inserted into the cell to measure the pH periodically.
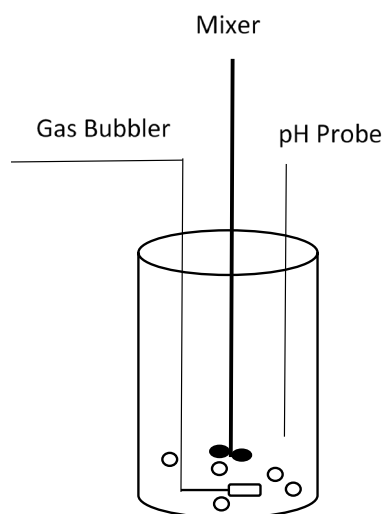
Figure 2-8: Process flow diagram for red mud pH neutralization using CO_2 gas

Nearly as soon as the CO_2 stream was shut off from the experimental cell, the pH began to rise again as seen in Figure 2-9. Experiments were also done to determine a final pH for neutralized red mud, the red mud was neutralized for 1 hour and then the pH was recorded over a period of 7 days. Figure 2-10 shows the results of the pH initial neutralization followed by the pH rebound over 7 days. Ultimately, the pH rose to a pH near 10, which is an overall pH reduction of 2.5, from 12.5 to 10.5.
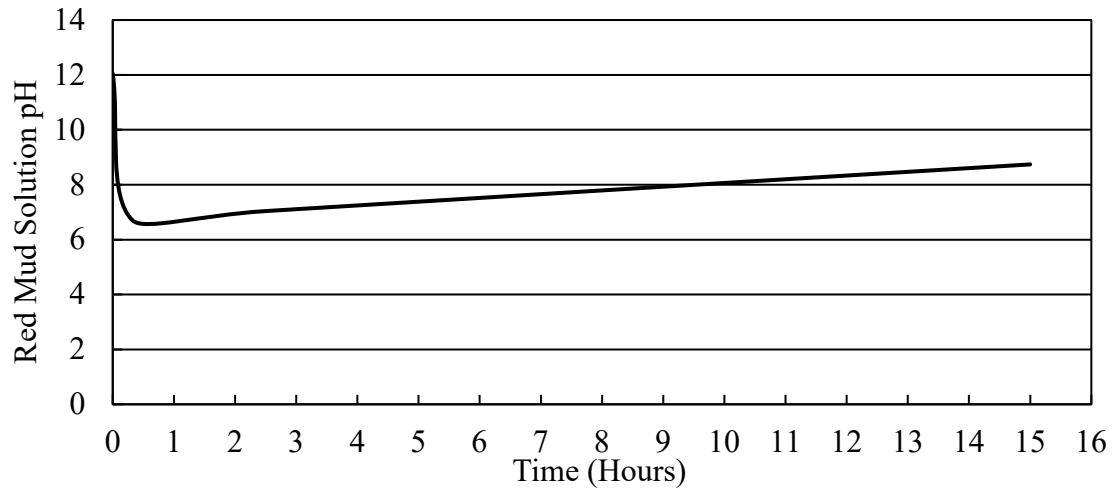
Figure 2-9: Red mud neutralized with CO_2. pH recorded over a period of 15 hours.
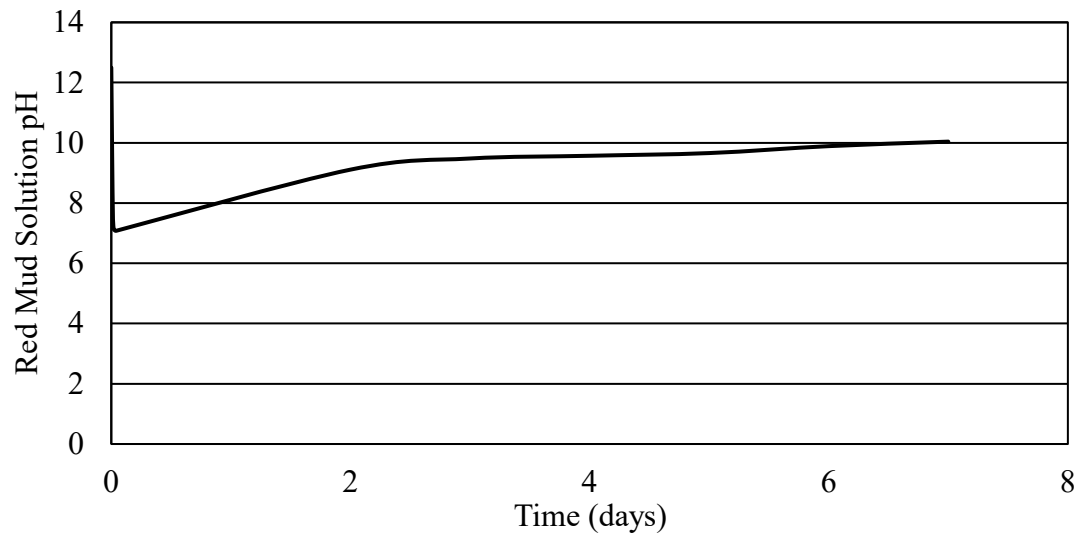
Figure 2-10: Red mud neutralized with CO_2. pH recorded over a period of 7 days

Over a longer period of 7 weeks, Rai et al. (2013) reduced the pH of red mud to around 7 and allowed the pH to rebound for a week and then neutralized it again. For 7 neutralization cycles, it was observed that the pH would always rise to 9-9.5 over the period of one week (Rai, 2013).

In order to determine which size fraction of red mud was most effective at sequestering carbon dioxide, neutralizing experiments of red mud were performed on three different average size fractions of 5 microns, 30 microns, and 50 microns (Yadav et al, 2010). The average size fraction of 30 microns proved to be the most effective due to a higher presence of cancrinite phases; sequestering CO_2 at a maximum capture rate of 5.3g CO_2/100 g red mud (Yadav et al, 2010). Rai et al. (2013) attributes the pH rise to the fact that the CO_2 only interacts with and neutralizes the aqueous phase of the red mud slurry, the solid fraction of red mud remains largely undissolved due to the short contact time between the reactants. The solid phase contains alkaline solids that release alkaline hydroxide ions as they dissolve and if these minerals don't completely react with CO_2, the alkalinity of red mud will continue to be an issue.

The Kwinana refinery in Australia conducted pilots scale experiments and eventually was able to implement a full-scale CO_2 neutralization of red mud. They were able to initially achieve pH of 8.5 while under pressure, but over time once the red mud was released from the pressure vessel the pH rebound to 10.5 (Power et al, 2011). In all of these neutralization experiments, the pH rises again after each sequestration cycle. pH rebound can be attributed to the dissolution of compounds like TCA, which are unstable in the neutral pH range and they release hydroxide ions which buffer the red mud at a higher pH (Power et al, 2011). The use of CO_2 as a solution for red mud alkalinity has the benefit of being able to reduce the overall pH and sequestering a small amount of CO_2. Due to the buffering ability of minerals like TCA and kaolinite which bring the pH back into the

alkaline region after a small period of time, it's unlikely that $CO^{-}2$ neutralization will be enough to remove the hazardous properties of red mud alone.

A far more likely scenario is one where CO_2 neutralization is used as a pretreatment for the extraction of minerals from red mud where the red mud is processed soon after neutralization and the pH rebound does not occur. Important chemical phases are formed during neutralization that can be used in further processing, but the pH rebound may cause them to react further. Table 2-9 shows and X-ray diffraction pattern for neutralized red mud.

Table 2-9: X-Ray Diffraction of red mud that has been neutralized with CO_2

Chemical Component	Weight Percent, %
Calcium Carbonate, $CaCO_3$	2.4
Hematite, Fe_2O_3	29.0
Goethite, FeOOH	19.0
Gibbsite, AlO_3	5.6
Anatase, TiO_2	5.0
Rutile, TiO_2	6.5
Sodalite, $Na_4Al_3(SiO_4)_3Cl$	6.1
Sodium Aluminum Silicate Hydrate, $1.08Na_2O \; Al_2O_3 \; 1.68SiO_2 \; 1.8H_2O$	26.5

After a neutralization cycle, from the table, an XRD of red mud showed an increase in calcium carbonate content by 2%. Calcium carbonate, or limestone is a material used in iron and steelmaking as a flux material in order to enhance separation of impure slags

from the iron. This newly formed material can be utilized as a fluxing material in pyro metallurgical processes for the removal of iron (Archambo et al, 2020). For leaching techniques to extract minerals for red mud, a neutralizing step with CO_2 can reduce the pH of red mud prior to acid leaching to reduce the amount of acid required for leaching (Rivera et al, 2017). The CO_2 seemed to hinder the iron leach efficiency due to compounds such as calcite and cancrinite forming and depleting available acid that could have been used for iron dissolution.

CO_2 has proven to be effective in removing a portion of the alkalinity of red mud. Experimental work must still be done to discover a method for CO_2 to completely and permanently remove the alkaline solids from red mud. This method of neutralization does provide a sink to utilize excess CO_2 that is produced during the process while still lowering the overall pH.

2.5   Utilizing red mud waste as a valuable material

2.5.1   Iron recovery

Because of the typically high weight percent of iron in red mud, many researchers have sought to extract this value from the waste using a variety of methods. Removing iron from red mud effectively reduces the total amount of red mud that is being discharged. In some cases, iron oxides account for half of the composition of red mud. If the iron is removed, up to half of the weight of red mud is utilized as a value-added product. Discovering alternative methods to produce iron are very important to the mineral processing industry because currently the majority of iron production lies on the

shoulders of the blast furnace. Blast furnaces need to be built to such a large scale to be economically feasible that anytime a furnace fails, there are serious economic consequences.

Direct reduction of hematite present in red mud has been studied intensely. The direct reduction of iron ores reduces the iron oxides but does not separate it from gangue material. The product of an iron direct reduction process can be used as a feed for steelmaking in an electric arc furnace (Anameric and Kawatra, 2007b). The following Equations (2-19) through (2-22) outline the reduction of iron oxides to iron (Chen, 2017).

$$3Fe_2O_3 + CO \leftrightarrow 2Fe_3O_4 + CO_2 \qquad (2\text{-}19)$$

$$Fe_3O_4 + CO \leftrightarrow 3FeO + CO_2 \qquad (2\text{-}20)$$

$$FeO + CO \leftrightarrow Fe + CO_2 \qquad (2\text{-}21)$$

$$Fe_3O_4 + 4CO \leftrightarrow 3Fe + 4CO_2 \qquad (2\text{-}22)$$
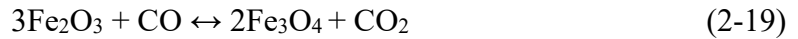
Using self-reducing pellets composed of red mud and varying amounts of crushed coal, iron bearing red mud was reduced and then subjected to a low intensity magnetic separation (Sadangi et al, 2018). It was found that the reduced red mud can be upgraded from 32.87% to 65.93% at 1150 °C for 60 minutes. Following magnetic separation, the iron recovery was found to be 61.85%. Gotsu et al. (2018) used a tube furnace at 550 °C with a reducing atmosphere of CO, CO_2, and N_2 to reduce hematite in red mud to magnetite and separated the iron using dry and wet magnetic separations. The maximum grade of the product was reported to be 60% Fe. A similar study separated iron from red mud by reducing it in an atmosphere of CO and H_2 gases and then used magnetic

separation to remove the magnetic magnetite or metallic iron (Ksiazek et al, 2018). This separation was able to effectively reduce the iron content of red mud by 43%.

Sodium salt additions have been shown to improve the separation of iron from red mud when reduced and then separated magnetically. The salt acts as a catalyst which allows reduced iron crystals in the red mud to grow to larger sizes, which improves efficiency in the magnetic separation step (Wei et al, 2019). The results of Wei et al. (2019) show an increase in iron recovery from 70% to 85% with the addition of sodium salts. Chun et al. (2014) achieved an iron recovery of 92.14%, iron grade of 90.28% and metallization degree of 94.87% with sodium salt roasting. The optimum parameters were 9% sodium sulfate, 9.46% lime, and 16% coal roasted at a temperature of 1150 °C for a residence time of 80 minutes (Chun et al, 2014).

Bhoi et al. (2017) investigated direct reduction of red mud using hydrogen plasma. Dried red mud pellets were reduced with hydrogen plasmas at temperatures between 300 and 800°C. The hydrogen plasma reduces the hematite and magnetite to metallic iron, with 98.23% reduction achieved after 2 hours at 300°C and 99.3% reduction achieved after 1 hour at 800°C. This process stands out from other direct reduction processes because the reducing material, hydrogen plasma can reduce iron at much lower temperatures than typical reductants and has a significantly lower environmental impact (Bhoi et al, 2017).

Yiran et al. (2014) sought to improve the grade of high-grade red mud by using high gradient magnetic separation (HGMS). If iron rich red mud could be upgraded to iron ore pellet grade, then the red mud would be able to be charged into the blast furnace for

conventional iron and steel processes. With a magnetic field strength of 1.2 T and three stages of wet magnetic recovery, the red mud feed was upgraded from 56% to 65% iron (Yiran et al., 2014). This grade is similar to the quality of iron ore pellets that are used in blast furnace iron processing, pellet feed material from the north American iron range after the addition of flux has an iron content of 57.8% (McDonald and Kawatra, 2017). In the pelletization process, additives like flux and binders are mixed with the pellet to improve compression strength at the disadvantage of lowering the overall iron grade in the pellet (Srivastava et al., 2013).

Another method for removal of iron from red mud is the generation of pig iron nuggets. This method begins with rolling self-reducing pellets containing a reducing agent such as coal or coke within them and firing them at high temperatures above 1400 ℃. At these temperatures, the reducing material removes oxygen from the iron oxides to form metallic iron. The variables that play the largest role in the iron nugget process are the furnace temperature and residence time. Anameric and Kawatra (2007a) developed a model from the Arrhenius equation to determine the required parameters in order to make pig iron nuggets. Incentives for industry to implement this process include the following.

1.   Use of iron reducing reagents other than coking coal (Anameric and Kawatra, 2008).

2.   Lower grade feedstocks like red mud can be used (Srivastava and Kawatra, 2009).

3.   Iron can be produced on a smaller scale (Anameric and Kawatra, 2008).

Figure 2-11 shows the basics on how the process works to reduce and separate iron from red mud. The nugget process differs from blast furnace iron production because the melting iron is achieved through carburization, which decreases the melting temperature (Anameric and Kawatra, 2007c). Following Equations (2-23) through (2-27), the fusible slag forms and iron bonds to carbon in the system to form iron carbide, which has a lower melting point than pure iron, allowing separation based on density (Anameric et al., 2006):

$$CaCO_3 \leftrightarrow CaO + CO_2 \qquad\qquad (2\text{-}23)$$

$$CaO + SiO_2 \leftrightarrow CaSiO_3 \qquad\qquad (2\text{-}24)$$

$$FeO + SiO_2 \leftrightarrow FeSiO_3 \qquad\qquad (2\text{-}25)$$

$$FeSiO_3 + CaO \leftrightarrow CaSiO_3 + FeO \qquad\qquad (2\text{-}26)$$

$$3Fe + C \leftrightarrow Fe_3C \qquad\qquad (2\text{-}27)$$

A

+

Heat

Red mud pellet is heated above 1400 C

B

Denser iron sinks below the slag body

C

Slag

Iron Nugget

Iron nuggets separate from slag
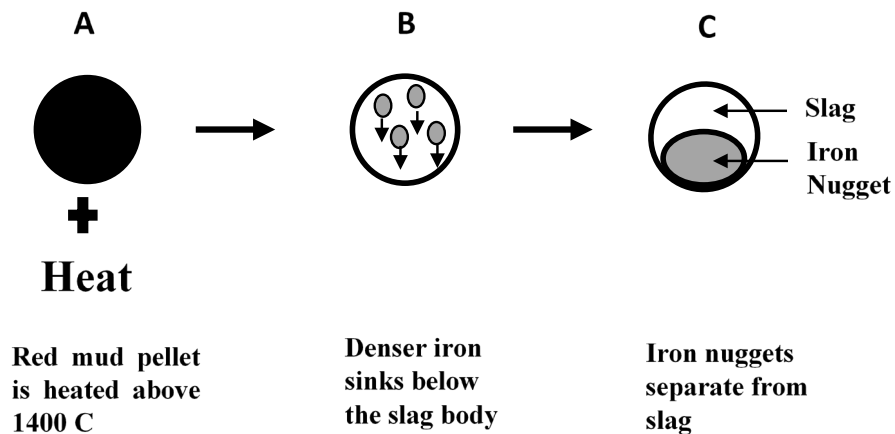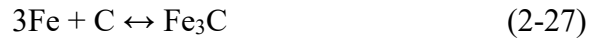
Figure 2-11: The red mud iron nugget process iron separation diagram. (A) The mixed pellet of red mud and a reducing carbon material is heated. (B) the reduced iron begins to sink to the bottom of the pellet. (C) An iron nugget forms separate from the slag body based on density differences.

Iron nuggets have also been generated using powdered wood as the reducing agent. Red mud is rolled into pellets with additives of powdered wood, bentonite, and dolomite flux and then dried in an oven to remove moisture. The pellets are placed into crucibles and placed into a furnace that has been preheated to 1475 degrees Celsius. Figure 2-12 shows a simple flow diagram of the red mud iron nugget experiments.
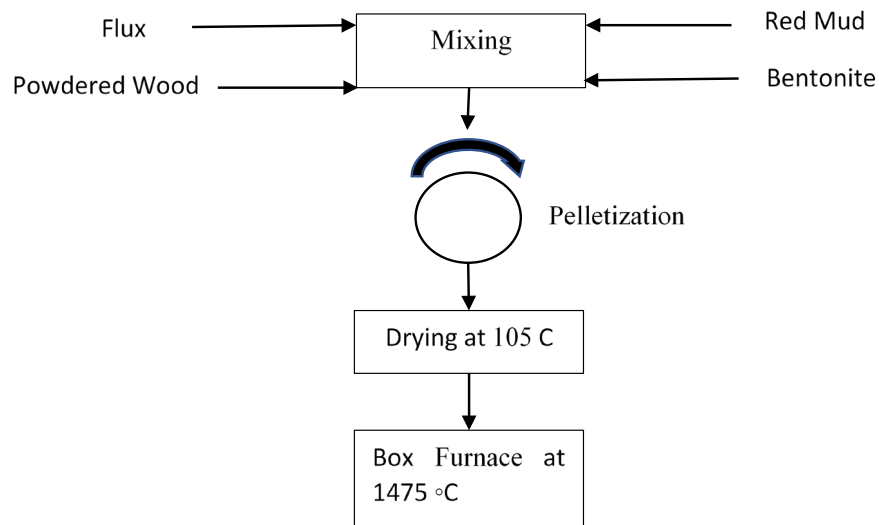
Figure 2-12: Process flow diagram for the red mud iron nugget process (Archambo and Kawatra, 2020)

Iron recovery over 80% was achieved with the iron purity of the nuggets reaching 90% Fe (Archambo and Kawatra, 2020). Iron nuggets were formed over a range of residence times from 30 minutes to 120 minutes with similar iron purities above 90% iron. Microstructure analysis and apparent density measurements of pig iron nuggets shows that the iron is identical to iron produced with a blast furnace (Anameric and Kawatra, 2006). This is a promising method to use low grade feeds such as red mud to create pig iron that can compete with the quality of blast furnace pig iron. Table 2-10 shows the elemental composition of the formed iron nuggets. From the table, the compositions are similar to those of blast furnace pig iron. Figure 2-13 shows the overall iron recovery of the iron nuggets with varying residence time.

Table 2-10: X-Ray Fluorescence (XRF) of red mud iron nuggets chemical composition (Archambo and Kawatra, 2020).

Element	Fe	C	Al	Ca	S	Cr	Ti	Total
Weight Percent, %	90.03	7.739	1.125	0.546	0.421	0.0774	0.0599	100
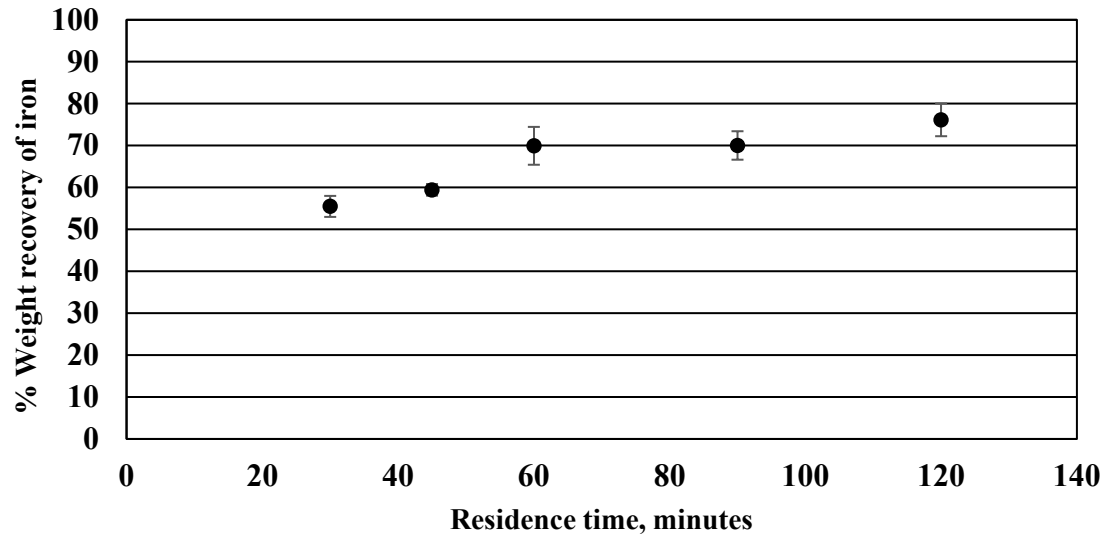
Figure 2-13: Red mud iron nugget process with powdered wood reducing agent. Total weight recovery of iron with changing residence time. (Archambo and Kawatra, 2020)

Using anthracite coal, iron nuggets were produced in a furnace at 1500 °C yielding pig iron with an Fe purity of 96.52% (Guo et al, 2013). Pig iron nuggets have also been generated using thermal plasma technology (Jayasankar et al, 2012). Optimum iron recovery in the nuggets were found to be 71% in the plasma technology research with the optimum conditions being 15-minute residence time, 12% flux by weight percent, in a 35 kW DC arc plasma reactor.

In North America, iron ore is beneficiated using deslime thickening or selective flocculation. A flocculating reagent attaches selectively to iron ore and generates flocs with a larger particle size in a mineral suspension. These larger particles settle to the bottom of a thickening tank more quickly and can be separated. Huang et al (2016) applied this method of iron beneficiation to recovery of iron in red mud. Iron oxide was

flocculated from the red mud using various humic flocculants derived from brown coal. These tests found that 86% of iron could be recovered at a grade of 61%. Important parameters for this study were pH, flocculant dosage, and agitation speed.

Due to the difficulty in dewatering red mud by filtering or thickening for pyrometallurgical extraction, hydrometallurgy seems to be a promising route for iron recovery. There have been a multitude of leaching studies for the extraction of iron from red mud. One study leached iron from bauxite ore before it could be process for alumina production in the Bayer process. First, the bauxite is calcined at a high temperature and then the iron is leached using sulfuric acid. At the optimum conditions, an iron removal efficiency of 47.33% was reached (Li et al, 2018). Ultrasonic waves were used to improve the efficiency of iron leaching in sulfuric acid, increasing the leaching efficiency from <30% to >40% (Lim and Shon, 2015). The drawbacks to acid leaching of iron from red mud is that at such a low pH range, other metals tend to dissolve and leach out of the red mud as well. Many experiments leach combinations of aluminum, titanium, and rare earth elements along with iron and then separate each of them (Lu et al, 2012; Lim et al, 2015; Li et al, 2018). Zhang et al. (2020) leached red mud with hydrochloric acid, mixed with an organic methyl trioctyl ammonium chloride, and then used NaH_2PO_4 to strip the iron from the leach solution selectively. At a concentration of 1.5 mol/L NaH_2PO_4, the maximum stripping efficiency was achieved to be 95.9% (Zhang et al., 2020). The implication here is that iron can be selectively leached from a red mud leachate, which means that other minerals like rare earths can be separated.

Oxalic acid has been selected to leach iron for a number of studies. One such study leached iron from HCl washed red mud using oxalic acid. The leach ratio of iron for this experiment was reported to be 94.15% and the oxalic acid was regenerated so that it can be reused for further use in iron leaching (Yang et al, 2015). A flow diagram for the process can be seen in Figure 2-14.
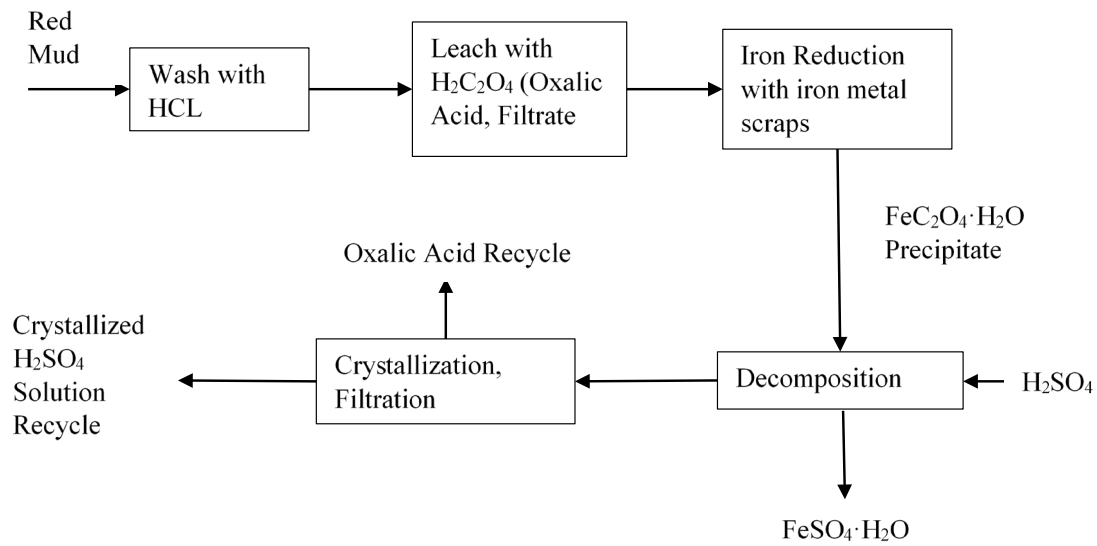
Figure 2-14: Process flow diagram for iron leaching via oxalic acid (Yang, 2015)

 Yang et al (2016) improved upon the process for iron leaching with oxalic acid by adjusting the pH with calcium carbonate to selectively dissolve the iron more efficiently.

In summary, iron found in red mud can be reliably extracted using a variety of pyrometallurgical and hydrometallurgical processes. Recovering iron from red mud can reduce the total amount of disposed red mud by up to 55% by weight depending on the initial concentration in the ore. Smelting and direct reduction processes are an effective

alternative to blast furnace production of iron in terms of iron grade. Leaching processes for iron are also effective, but they also tend to dissolve other valued minerals as well. Effective iron leaching processes must also have a method for purifying the leach solution by extracting the other valued minerals. Iron removal is the most promising method for the reduction of red mud waste.

2.5.2 Titanium recovery

Available in smaller weight percent's than iron in red mud, titanium is another metal that has potential for extraction. This is because titanium is a more expensive metal with a more difficult production process. Titanium rich ores also occur far less frequently in nature than that of iron, which makes finding an alternative source of titanium through concentrated mineral processing waste like red mud more appealing.

Tests to recover titanium with sulfuric acid have shown that 64% of the titanium can be recovered along with amounts of iron and aluminum, a low solid to liquid ratio showed increased titanium recovery while lowering aluminum and iron recovery (Agatzini-Lleonardou et al, 2008). Another study looked to avoid dissolving titanium along with other minerals by using HCl to remove iron and alumina while keeping titanium oxide insoluble to enrich the concentration in the red mud solids. The dissolution reactions of iron and aluminum oxides in the presence of HCl is shown in reactions 2-28 and 2-29 (Kasliwal and Sai, 1999). The reported enrichment of titanium in the leaching step is 0.36.

$$Fe_2O_3 + 6HCl \leftrightarrow 2FeCl_3 + 3H_2O \qquad\qquad (2\text{-}28)$$

$$Al_2O_3 + 6HCl \leftrightarrow 2AlCl_3 + 3H_2O \tag{2-29}$$
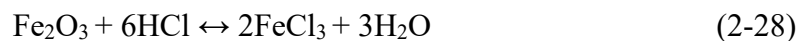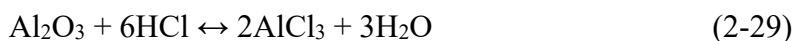
The solids were then roasted with sodium carbonate to form water soluble minerals from the remaining aluminum and silica following reactions 2-30 and 2-31 (Kasliwal and Sai, 1999). An increase in enrichment of titanium after the roasting step was determined to be 0.76 under optimum process conditions of 115-minute residence and 1150 degrees Celsius roasting temperature.

$$Na_2CO_3 + Al_2O_3 \leftrightarrow 2NaAlO_2 + CO_2 \tag{2-30}$$

$$Na_2CO_3 + SiO_2 \leftrightarrow Na_2O \cdot SiO_2 + CO_2 \tag{2-31}$$

A study conducted by (Huang et al, 2016) sought to purify leached titanium from dissolved iron using a precipitate flotation method outlined in Figure 2-15. A majority of iron is removed from red mud using a deslime- thickening process, then the tailings are subjected to a stage of acid leaching with H2SO4. The leachate is then sent to flotation where iron ions attach to a frothing agent, precipitate, and then float. After calcination, the remaining solution is concentrated titanium oxides. The final titanium recovery was 92.7%, and 93% of the iron was rejected (Huang et al, 2016).
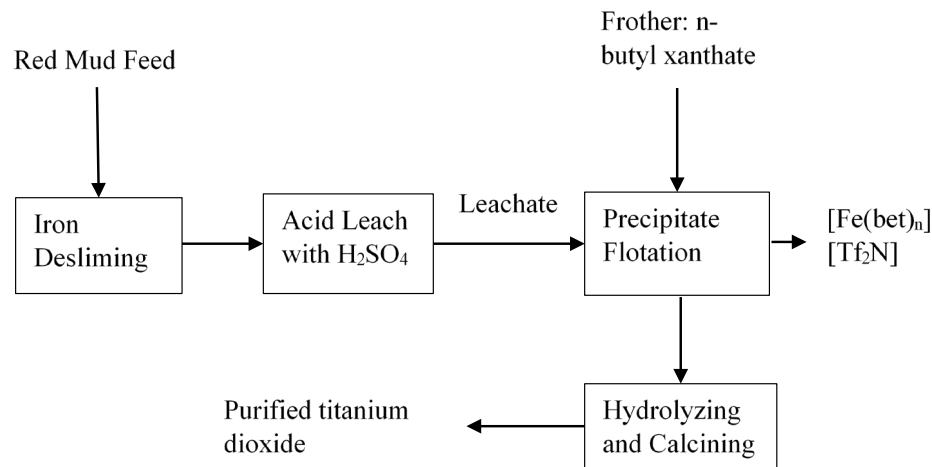
Figure 2-15: Simplified flow diagram for enriching titanium in red mud using precipitation flotation (Huang et al., 2016).

In order for titanium to become a viable byproduct from Bayer red mud, the most promising processes are those that also produce iron through leaching. The development of processes that can separate iron and titanium from the leach solution will be the most beneficial as two valued products are created. Titanium is available in red mud at a much smaller fraction than iron, but its overall value maintains its position as an important mineral in red mud.

2.5.3 Rare Earth element/Scandium/Gallium recovery

The group of elements on the periodic table from atomic numbers 57 to 71 are considered as the rare earth elements. Scandium and yttrium are typically included in this category as well due to similarities in their chemical properties (Balaram, 2019). The rare earth

elements are widely applied in many new and developing technologies. The continuously high demand for rare earths has spurred a huge boom in their production and utilization over recent years. Applications for rare earth elements include a variety of things such as electronics, medicine, technology, and energy (Balaram, 2019). It is clear that these elements are an integral part of our way of life and will continue to be as technology advance further. The issue with these elements is that they do not typically occur in deposits that are high enough in concentration to mine profitably. This is the reason that they were coined as rare earth elements. REES are found in more abundance in two types of deposits, alkaline igneous formations which include minerals like bastnaesite and residual deposits caused by excessive weathering effects including minerals like bauxite (Balaram, 2019).

Red mud is a promising source for critical rare earth elements. It is also worth mentioning that the compositions of rare earths in different red mud samples can vary widely, some elements may be most prevalent in one sample while not appearing in another. This implies that the removal process for rare earths will also depend on the mineralogy of the sample. Red mud may present a viable feedstock for extracting critical rare earth resources.

The predominant methods for rare earth extraction have been in ion exchange methods, extraction with organic solvents, and precipitation of low soluble compounds (Akcil et al, 2018). Most rare earth elements exhibit very similar chemical properties, which makes the separation of rare earths from each other uniquely difficult. One exception to this case it that of cerium, which can become stable at the Ce+4 oxidation state, making it easier to

separate from other rare earths (Meshram and Abhilash, 2019). One such process for the removal of cerium from red mud involves leaching red mud with sulfuric acid followed by solvent extraction with Cyanex 301; 99.9% of cerium was extracted at 3M H_2SO_4, 10 g/L, and 1 hour (Abhilash et al, 2014). Borra et al. (2016) used acid leaching to remove REEs from red mud that had already been smelted to remove iron. The reason for this is that iron also dissolves at the same pH as the REEs and it would require further purification steps to remove the iron. Leaching iron deficient slag from red mud with HCl, sulfuric acid, and nitric acid extracted rare earth elements such as Sc, Y, La, Ce, Nd, Dy, and Ti with limited amounts of iron as a contaminant. A large amount of research that studies extraction of rare earth elements takes the acid leach route to remove rare earth elements along with valuable iron, titanium and aluminum. Some of the works that acid leach red mud is the following: (Ochsenkuehn-Petropoulou et al., 1996; Wang et al., 2013; Abhilash et al., 2014; Alkan et al., 2017, 2018; Davris et al., 2018; Rivera et al., 2018; Zhang et al., 2019). Table 2-11 shows the extraction efficiencies of different red mud leaching experiments.

Table 2-11: Rare earth extraction percent from red mud utilizing different reagents, temperatures, and residence times.

Reference	Dissolving Reagent	Residence Time (min)	Temperature (°C)	Element Extraction %
Alkan et al, 2017	HNO_3, 3M	120	90	Sc 34%

Borra et al, 2015	HNO$_3$, 1N	1440	25	La 35%, Ce20%, Nd 45%, Dy 50%, Y 65%, Sc 45%
Ochsenkuhn-Petropulu et al, 1996	HNO$_3$ 0.5M	30	30	La 35%, Ce 29%, Pr 35%, Nd 52%, Sm 49%, Eu 53%, Gd 49%, Dy 52%, Er 60%, Yb 70%, Y 96%, Sc 80%
Wang et al, 2013	HNO$_3$, 0.5 M	120	23	Sc 80.2
Alkan et al, 2017	HCl, 3M	120	90	Sc 36%
Borra et al, 2015	HCl 1N	1440	25	La 35%, Ce 38%, Nd 45%, Dy 50%, Y 70%, Sc 42%
Ochsenkuhn-Petropulu et al, 1996	HCl, 0.5 M	30	30	La 33%, Ce 32%, Pr 25%, Nd 55%, Sm 57%, Eu 50 %, Gd 37%, Dy 45%, Er 43%, Yb 60%, Y 79%, Sc 68%
Rivera et al, 2018	HCl	1440	25	La 34%, Nd 35%, Y 43%, Sc 36%
Wang et al, 2013	HCl, 0.5 M	120	30	Sc 80.7%
Zhang et al, 2019	HCl	20	75	La 82.3%, Ce 96.9%, Nd 98.3, Y 95.6%, Sc 93.3%

Abhilash et al, 2014	H_2SO_4, 3M	60	35	La 99.9%, Ce 99.9%
Alkan et al, 2017	H_2SO_4, 3M	120	90	Sc 78%
Borra et al, 2015	H_2SO_4, 1N	1440	25	La 25%, Ce 35%, Nd 40%, Dy 45%, Y 60%, Sc 45%
Ochsenkuhn-Petropulu et al, 1996	H_2SO_4, 0.5M	30	30	La 28%, Ce 24%, Pr 29%, Nd 21%, Sm 33%, Eu 37%, Gd 32%, Dy 43%, Er 34%, Yb 52%, Y 77%
Rivera et al, 2018	H_2SO_4	1440	25	La 20%, Nd 19%, Y 22%, Sc 22%
Wang et al, 2013	H_2SO_4, 0.5M	120	30	Sc 83.8%
Ujaczki et al, 2019	$H_2C_2O_4$, 2.5M	1440	80	Ga 40%
Borra et al, 2015	Citric Acid 1N	1440	25	La 20%, Ce 15%, Nd 30%, Dy 35%, Y 50%, Sc 40%
Borra et al, 2015	Acetic Acid 1 N	1440	25	La 15%, Ce 10%, Nd 20%, Dy 15%, Y 20%, Sc 20%
Davris et al, 2016	HbetTf2N	240	150	La 68%, Ce 71%, Nd 71%, Pr 81%, Sm 68%, Eu 77%, Gd

				82%, Dy 52%, Er 71%, Yb 71%, Y 56%, Sc 36%
Davris et al, 2016	HbetTf2N	1440	150	La 85%, Ce 74%, Nd 84%, Pr 82%, Sm 69%, Eu 75%, Gd 81%, Dy 65%, Er 75%, Yb 76%, Y 69%, Sc 43%
Xue et al, 2019	NaOH	720	120	Ga 91.4%
Yagmurlu et al, 2019	H_2SO_4 2.5M H_2O_2 2.5 M	120	75	Ce 60%, Sc 90% , Y 50%

Leaching REE's from red mud using ionic liquids has also been studied. An ionic liquid

is an ionic material that is typically a liquid at room temperature and it is made up

entirely of ions. These ionic liquid solutions can dissolve rare earth oxides and form a

complex, which can then be stripped with an aqueous acid. Davris et al. (2016) utilized

betainium bis(trifluoromethylsulfonyl)imide (HbetTf2N) as an ionic liquid followed by

HCl stripping to leach rare earth elements selectively. The rare earth extraction rate was

found to be 70-85% while also maintaining iron extraction of less than 3% (Davris et al,

2016).

Biosorption routes have also been investigated in depth, different projects have reported

the extraction of Lanthanum, Neodymium, Cerium, Erbium, Europium, Samarium,

Praseodymium, and Dysprosium (Das and Das, 2013). The mechanism that allows

biosorption to occur can be attributed to some of the following factors or a combination:

electrostatic interaction, surface complexation, ion-exchange, and precipitation (Das and Das, 2013). These processes are favorable to high concentration acid leaches because they do not produce hazardous waste products, the biomass materials are typically inexpensive, and the leaching can be performed in-situ. This research has yet to reach the scale of industry however, more research into its effectiveness is necessary.

Research has recently put a heavy focus of extraction of scandium specifically from red mud. Scandium is one of the most expensive rare earth elements with a price of 3,487 USD/Kg in 2020 (Mineral Prices, 2020). One route for scandium recovery is synthesizing scandium phosphate from red mud. This is done by depleting the red mud of iron using Pyrometallurgy and then leaching the slag with hydrogen peroxide and then precipitated to form scandium phosphate. From this study, 85% of the scandium was recovered as scandium phosphate (Yagmurlu et al, 2019).

Another valued element that has potential to be removed from red mud sources is gallium, which tends to occur in red mud at similar quantities to that of scandium. Liu et al. (2018) found that the red mud from the Chalco aluminum plant in Shandong, China contained scandium and gallium at concentrations of 80 ppm and 920 ppm respectively. Based on the image analysis, it was concluded that gallium and scandium are more likely to be present in red mud that is rich in iron oxide and aluminum oxide as they have an affinity to exist near those minerals (Liu et al, 2018). One method for removing gallium from red mud is an alkaline leach process to oxidize all iron species (which have high surface area and coat gallium particles) to Fe_2O_3 to allow for more surface area for leaching; optimized results for this procedure are 91.4% of the gallium can be extracted

from the red mud and the leached solution contains a concentration of 73.44 ppm gallium oxide (Xue et al, 2019).

Samples from the Turkish red mud plant Seydişehir were used in a gallium extraction experiment by alkaline leaching with lime followed by TCA precipitation and carbonation; the concentrate solution contained 3200 ppm gallium (Abdulvaliyev et al, 2015). Another approach looked at acid leaching rather than alkaline leaching for gallium recovery, by dissolving red mud in hydrochloric acid, removing dissolved iron using chlorinated polystyrene resin, followed by an ion exchange step. The averaged results showed that 88.34% of gallium in red mud could be recovered in this way (Lu et al, 2018). Ujaczki et al. (2019) found that oxalic acid can also be used for leaching to recover gallium from red mud in conjunction with adsorption onto zeolite HY; the oxalic acid was able to leach gallium at a concentration of 81.1 ppm at optimal conditions of 2.5M acid concentration, 80-degree Celsius temperature, 21.7 h residence time, and 10 g/L slurry concentration. The zeolite adsorbent was able to remove 99.4% of gallium from the leached solution (Ujaczki et al, 2019).

In summary, red mud contains a large amount of rare earth elements which have been concentrated from bauxite ore during the Bayer process. Utilization of red mud as means of rare earth element production can simultaneously reduce the amount of red mud being disposed while also providing a source for a critical material. The composition of each specific red mud source is an important factor in determining the feasibility of rare earth extraction. Rare earth elements are chemically similar and difficult to separate, so a universal process solution for rare earth extraction in red mud is unlikely. Process

solutions should be optimized on a plant basis in order to extract the most available and most concentrated rare earths in the most efficient way. Ultimately, as demand for new sources of rare earth elements increases, the viability for red mud as the source becomes more likely. Red mud has a large potential to be a supplier of necessary rare earth elements in the near future.

2.5.4 Catalysis

One area that red mud is seeing a sharp increase in utilization research is that of catalysis. This field has a wide range of applicability for the case of red mud. Red mud has been used as a catalyst for tests to remove organics from wastewater. With a high content of iron oxides like hematite, red mud was used to remove organics using the mechanism of iron oxide reducing and catalyzing the reaction sequence (Bento et al, 2016). The results from these tests show that up to 90% of organics were removed from the wastewater with a catalyst reusability for up to 4 cycles (Bento et al, 2016).

Catalysis in oil and gas industries is a field that is growing in prominence. With increasing regulations on flue gas compositions that can be discharged to the environment, many research projects have investigated cost effective methods to remove hazardous gases from flue gas streams. Specifically, for this review, the utilization of red mud as a catalyst for these flue gas removal projects has been investigated. The removal of NO from simulated flue gas was investigated by passing the gas through a catalyst filter coated with red mud; the NO gas can adsorb on to the iron minerals in the red mud (Huangfu et al, 2020). The conversion of NO was found to be 74% without the presence

of other common gases like SO_2 and water, with all of these gases together the conversion increased to over 90% conversion of NO (Huangfu et al, 2020).

Red mud has also seen use as a catalyst in production of fuels. Contamination with sulfur components in fuel is very undesirable for the final product and they must be removed. One project used red mud as a catalyst with hydrogen peroxide and acetic acid to remove dibenzothiophene (DBT) by means of oxidation (Resende et al, 2014). It was also shown that the red mud could be regenerated to up to 97% of its original catalyst activity to be used again (Resende et al, 2014). Hemp oil can be converted to biofuel using pyrolysis techniques with hydrogen gas. It was found that when reduced red mud was used as a catalyst, the produced organic materials contained less reactive organics like alcohols, aldehydes, and acids and a higher amount of stable alkanes, alkenes and aromatics (Karimi et al, 2010). The bio oil produced using red mud as a catalyst also showed that the organic material was more stable over the course of 90 days whereas the untreated bio oil began to degrade and the alkanes, alkenes, and aromatics converted into a higher weight percent of reactive organics that cannot be useful as fuel (Karimi et al, 2010). Ammonia can be converted to hydrogen gas which can be used as a fuel with the help of red mud as a catalyst. The iron present in red mud was reduced to metallic iron and then reacted with ammonia to form nitrogen and hydrogen gas at a production rate varying from 72 to 196 mmol H2 per min with ammonia flow rates varying from 72,000 to 240,000 cm3 NH3 per hour (Kurtoglu and Uzun, 2016). This study offers a use for red mud while also creating a storage mechanism for hydrogen gas, which is dangerous to store.

These processes are very interesting and novel uses for red mud which cover a series of different research fields. The overall utilization of the total amount of stored red mud via these methods will be low compared to other means of utilization. For each catalysis process, only small amounts of material are needed and much of it is regenerated in the process. There is little demand in catalysis for the enormous amount of red mud that is produced in industry.

2.5.5 Construction/Ceramics

Red mud has been considered as a bulk construction material over the years. The bulk utilization of red mud in long-term construction would eliminate the majority of storage costs and environmental hazards. Research is currently ongoing on how to effectively prepare red mud for this usage.

Understanding the effects of different parameters on the strength of red mud for a building material are important. These were investigated in mixtures of red mud and lime, it was found that important parameters to consider are lime content, porosity, dry density, and water content (Kumar and Prasad, 2019). On its own, red mud and its components are not very reactive and do not effectively bind to itself or other materials. Red mud can be sintered in an oven to increase its reactivity. The slag of the sinter tests was used as the starting material for compression tests and a mechanical strength of 40 MPa which can be compared to conventional cements (Arnout et al, 2018).

Red mud has a similar particle size distribution to clays used to make insulation bricks. Red mud can be mixed with sawdust to form similar bricks comparable to standard

insulation bricks, with the best results occurring around a 7.5% saw dust content (Singh et al., 2014; Mandal et al., 2017).

Due to the presence of minerals in red mud such as Fe2O¬3, Al2O3, and silica, red mud has potential to be an ingredient in the production of cement (Liu et al, 2011). One study blended fly ash with red mud for a cement additive in order to reduce the amount of alkali sodium in the product. The compressive strengths of these mixtures were tested over time and it was found that high weight percent of red mud showed a higher initial compressive strength but at long periods of time over 90 days the compressive strength suffered (Montini et al, 2018).

Cement production could be an excellent method for bulk utilization of red mud. Lui et al. (2011) showed that the fine particle size of red mud helps to demonstrate a normal consistency in cements with strong mechanical properties. Lui et al. (2011) noted that many of the experiments that were performed using red mud for cement were all on lab scale and a complete bulk utilization of the total stockpile of red mud is still far away.

The high content of largely inert components in red mud, such as quartz and hematite, give credibility to the idea that red mud can be used as a feed source of material for the ceramics industry. Heating tests to determine the properties of red mud at different temperatures was studied to see how red mud could be specifically applied to the process. It was found that under temperatures of 900 °C red mud was largely inert and the only chemical changes were the evaporation of water and the evolution of CO_2 gas, which makes red mud useful for applications as an inert component for the production of bricks

and tile (Sglavo et al, 2000b). When red mud is fired above temperatures of 900 °C to 1400 °C, aluminum silicates begin to melt and form a liquid phase which can be utilized in ceramics to form materials with high strength and low porosity (Sglavo et al, 2000b).

Work has been done to enhance the properties of red mud itself as a ceramic material, specifically using geopolymer technology. It was shown that when using red mud as the aluminosilicate precursor by submerging the mud alkaline activating solutions with combinations of SiO_2 and Na_2O, the produced geopolymer could be heated as a low temperature ceramic material (Lemougna et al, 2017). The reaction sequence begins with silicon and aluminum minerals dissolving at high pH, where the precursor minerals start to form in the aqueous phase as seen in equations (2-32) through (2-35) (Dimas et al., 2009).

$$(SiO_2, Al_2O_3) + 2NaOH + 5H_2O \rightarrow Si(OH)_4 + 2Al(OH)^-_4 + 2Na^+ \qquad (2\text{-}32)$$

$$Si(OH)_4 + Si(OH)_4 \leftrightarrow (OH)_3Si\text{--}O\text{--}Si(OH)_3 + H_2O \qquad (2\text{-}33)$$

$$Si(OH)_4 + Al(OH)^-_4 \leftrightarrow (OH)_3Si\text{--}O\text{--}Al(^-)(OH)_3 + H_2O \qquad (2\text{-}34)$$

$$2Si(OH)_4 + Al(OH)^-_4 \leftrightarrow (OH)_3Si\text{--}O\text{--}Al(^-)(OH)_2\text{--}O\text{--}Si(OH)_3 + 2H_2O \qquad (2\text{-}35)$$
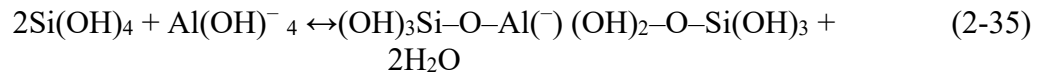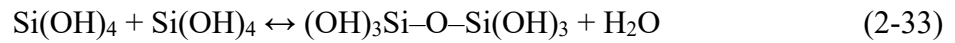
Dimas et al. (2009) found that geopolymers formed using red mud as the precursor, had high compressive strength at 20.5 MPa, 1.28% cold water absorption, and 0 cm3/cm2 per day water permeability. Others studies have been done to determine an ideal weight ratio of red mud for optimal performance of the yielded ceramic products. Drawbacks noted for the process are low flexural strength and weakened structural properties following freezing and thawing cycles (Dimas et al, 2009). On such study determined that out of

mixtures containing 20, 35, and 50% red mud, that the highest weight ratio of red mud fired at a lower optimum sintering temperature which was attributed to Na+ solidification to promote sintering (Pei et al, 2017).

Use of red mud as material for construction can utilize a large amount of red mud with little modification to the dry product. Demand for cement and other construction materials is high and if red mud can be implemented at a high weight percent, the reduction of the red mud stockpile is likely.

2.5.6   Using red mud to remediate soil and water

Red mud has been seen as a material that is detrimental to wildlife and a serious harm to the environment. Some research has gone into actually using red mud to improve the conditions of solid by removing dangerous heavy metal ions. This is possible because red mud that has been neutralized with seawater contains minerals known as hydrotalcites, which can adsorb to heavy toxic elements in solution (Palmer et al, 2010). Results from these experiments were performed with red mud samples from the Gove plant in Australia and it was found the seawater neutralized red mud could remove dangerous metals in aqueous solution like arsenate, vanadate and molybdate (Palmer et al, 2010). Another study conducted arsenic adsorption experiments with raw red mud and red mud that had been activated through heat-treatment and through acid washing. The results showed that arsenic can absorb to regular red mud and activated red mud but the adsorption to activated red mud which contained a lower pH was more effective (Altundogn et al, 2002).

Red mud can be effective at removing dangerous ions from other contaminated sources which is great for cleaning water sources and soils. The issue here is that the red mud that has been used now contains a higher concentration of dangerous metal ions and the storage of the material becomes an issue again. If red mud is used to remediate soil, much thought must put into the storage of red mud with more hazardous metal ions. Current storage techniques can contain the red mud to a certain degree. Remediation of soil and water is unlikely to be a major factor in the total reduction of red mud waste.

2.6 Conclusions

Red mud continues to be a serious issue in regards to the aluminum industry and the state of the environment impacted by mining operations. The variation in composition for red muds around the world creates a difficult problem for a unified method of bulk utilization and extraction of valuable minerals. Almost all red muds do contain a mineral of value that can be extracted, and in most cases, they contain multiple minerals of value that could be removed and in turn reduce the amount of red mud at a profit to industry.

The properties of red mud from the Bayer process make the material very difficult to dispose of and where it is disposed, a large amount of land area is consumed with the potential of soil contamination from caustic levels, toxic, and radioactive elements. Disposal practices have been improved with technology advances in thickening and filtering. This alone is insufficient to deal with the increasing amounts of red mud generated each year. These technologies need to be coupled with new utilization technologies to totally dispel the issue that red mud presents.

The removal of alkalinity from red mud is one of high importance. Methods of pH reduction of red mud have been successful using simple reagents. Carbon dioxide neutralization provides an option for greenhouse gas sequestration in an industry that produces a large amount of CO_2. Adding CO_2 neutralization to red mud at the plant scale would be very easy due to the close proximity of gas emissions to red mud discharge.

Processes that seek to remove iron from red mud can potentially decrease the amount of red mud by 50% by weight. Direct reduction, acid leach, and direct smelting processes have shown that reliable iron grades can be produced from red mud with the added benefit of red mud waste reduction.

Rare earth elements have been found in concentrated quantities in red mud. During a time when finding a source of production for these vital minerals is critical, red mud seeks to become a promising feed stock for secondary production of rare earth metals.

The large amount of laboratory studies shows that there is value in this process waste in the form of low to mid-grade iron ores, titanium ores, rare earths, and residual aluminum. This gives us another reason to look at red mud as a valued feedstock and not just a process waste.

The large stockpile of red mud that has been building since the Bayer processes inception desperately requires utilization options. With the increasing demand for alumina in the world, the amount of red mud being produced every year is growing exponentially. The most reliable way to reduce the stockpile of red mud is projects that rely on bulk utilization of red mud so that there is no waste at the end of the process. The most

promising research and plant-based operations that have been seen are those that include

seawater neutralization of red mud and the use of red mud clays in construction materials.

The industry percent utilization of red mud today is still much lower than the production

rate of red mud. If red mud can effectively be utilized as a valuable material, then the

industry might see reduction of red mud stocks in a much more favorable light.

3 Optimization studies for red mud neutralization with carbon dioxide

3.1 Abstract

Red mud is a caustic aluminum byproduct that must be neutralized in order to process and recover valuable iron. Typically, red mud has a pH of 13 or higher, making it dangerous to handle and for the environment. Carbon dioxide is a greenhouse gas and finding an economically viable utilization method for carbon dioxide is critical for greenhouse gas mitigation. One technique for CO2 utilization is to bubble CO2 into red mud in order to neutralize the caustic sludge. In this study, CO2 was bubbled into a slurry of caustic red mud, and the pH was measured in regular intervals. This study found that CO2 is capable of neutralizing the pH to 7.5. Over large time periods, experimental work has shown that CO2 can effectively reduce the pH of caustic red mud. Neutralization of red mud can also be considered as preprocessing for iron removal. CO2 is stored in red mud as calcium carbonate, which aids the separation of iron. CO2 neutralization also impacts the surface properties of red mud, lowering the zeta potential to zero. This work aims to understand the neutralization of red mud with CO2 and find potential uses for its further processing.

3.2 Introduction

The alumina industry has grown considerably over the last few decades, using the Bayer process to produce valuable alumina from bauxite ore. The problem that grows yearly in the alumina industry is the generation and management of its processing waste. Red mud is produced at very large quantities compared to the alumina that is produced. Up to 2.5

tons of red mud are generated or every ton of alumina made (Patel and Pal, 2015). The Bayer process can be described simply using the flow diagram in Figure 3-1. Red mud is formed after the digestion of bauxite ore in caustic sodium hydroxide, shown in Equation 3-1 (Hind et al, 1999).

$$\text{Al(OH)}_{3\text{ (s)}} + \text{NaOH }_{\text{(aq)}} \leftrightarrow Na^+ + Al(OH)_4^- \qquad\qquad \text{(3-1)}$$
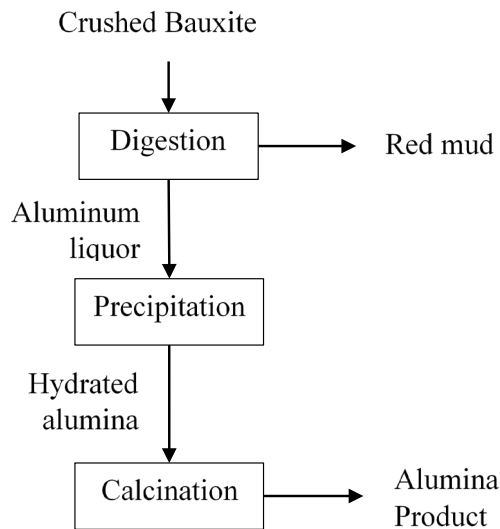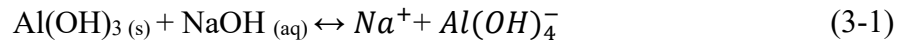
Figure 3-1: Simplified process flow diagram for the Bayer process.

 After the aluminum rich liquor has been separated from the remaining undissolved material, a series of thickening and dewatering steps produce the red mud. Flocculants such as high anionic acrylamide and polyacrylates are added to red mud in order to settle fine solids more quickly (Sankey and Schwarz, 1982). Filtering the red mud using drum filters is also used in order to recover caustic liquor for reuse in the plant (Evans, 2016). The separation and dewatering of red mud can account for 30 to 50% of alumina plant operations (Paramguru et al, 2004). Even with the aid of these dewatering steps, the mud

is still very high in moisture content. The slurry is pumped into lagoon sites where it takes decades for it to dry. The current stockpile of red mud worldwide is estimated to be near 4 billion tons (Wang et al, 2019).

The red mud that is generated in the Bayer process is detrimental to the environment for a variety of reasons. Toxic materials like arsenic, chromium, lead, and zinc have been discovered in excess at red mud spill sites (Rutyers et al, 2011). Red mud also exhibits very high alkalinity due to the residual sodium hydroxide that is left over from the digestion stage of the Bayer process, which makes storage of red mud a potentially dangerous endeavor (Power et al, 2011). When red mud is disposed, for every ton of solids, there is up to 2 tons of liquid with very high alkalinity from 5-20 g/l caustic material (Rai et al, 2012). Other concerns for red mud storage are that of seepage into the groundwater and traveling dust particles that can affect nearby environments (Rai et al, 2012).

Developing a solution to remove the environmental hazard from stockpiling red mud is critical to future sustainable aluminum mining processes. Using neutralization techniques to lower the caustic pH of red mud could prove effective at mitigating the environmental risk. The importance of finding inexpensive reagents to reduce red muds pH are critical for neutralization processes (Klauber et al, 2011).

Carbon dioxide has become a very important gas across every industry because it is a byproduct of many processes and there are currently very few avenues for utilization. The capture and utilization of CO_2 is another critical task for sustainable engineering. In 2019, CO_2 emissions increased by 350 megatons, and the total emissions for that year were

83

estimated to be near 38 gigatons of CO_2 (Olivier and Peters, 2020). Without harsher regulations, there is not much incentive for industry to curb their release of CO_2. CO_2 is an excellent alternative to using acids to neutralize red mud because it is typically produced elsewhere in a mineral processing plant and could be sequestered in red mud rather than being expelled into the atmosphere. Red mud can be neutralized from a relatively cheaper reagent that is typically generated at prices of 25 to 35 $/ton (Valluri and Kawatra, 2021). Most of the time carbon dioxide is generated elsewhere in the same plant, making shipping and logistics simpler.

Red mud can be further processed to remove valuable minerals with the addition of CO_2. Iron can constitute up to 50% of a given red muds weight (Paramguru et al, 2004). The iron can be removed with the addition of a flux using the novel iron nugget process (Archambo and Kawatra, 2020). This process separates the metallic iron from a more viscous slag layer with the aid of a flux material. A flux material is commonly used in steelmaking to remove impurities from molten pig iron. The reaction between red mud and CO_2 can generate flux material in red mud to improve the iron nugget separation.

Research has been done to investigate the ability of carbon dioxide to neutralize red mud slurries, with varying levels of success. Rai et al (2013), neutralized red mud with multiple cycles over a period of 7 weeks. For each cycle, red mud would be treated with CO_2 and left alone for a week, the pH would be measured and it would be treated again with CO_2. It was observed that the pH of the sample would always rise back to the pH range of 9.0 to 9.5 (Rai, 2013). Prior to rare earth element recovery, a neutralization step for the red mud with carbon dioxide was able to lower the pH to 8.6 (Rivera et al, 2017).

Patel and Sahu (2018), were able to achieve similar results by lowering the pH to 8.45. Some experimental work was done with different size fractions of red mud to determine which size can sequester the CO_2 most effectively. The conclusion is that the intermediate size fraction of 30 microns was most effective due to the presence of cancrinite phases (Yadav et al, 2010). pilot scale CO_2 neutralization setup had been implemented at the Kwinana plant in Australia. With vessels that were under pressure, the pH was lowered down to 8.5 but over time the pH rose again to 10.5 (Power et al, 2011). All of these experiments show that red mud can be neutralized with carbon dioxide with the caveat that the pH will rise again after carbonation.

This research investigates the capability of CO_2 to neutralize red mud. Previous works have cited different mechanisms for red muds neutralization and pH rebound. This work aims to determine a more cohesive hypothesis for the red mud neutralization mechanism. Other aspects of neutralized red mud will be explored in this paper that have not been in other publications. The generation of carbonates in neutral red mud is important as a pretreatment to remove iron in further processing. The investigation into the zeta potential of red mud with mineral acids has been studies, this work will explore how the surface of red mud is affected with additions of CO_2 for neutralization. With that knowledge, optimization of red mud neutralization is possible and avenues of further processing of red mud become available.

3.3 Experimental

3.3.1 Materials

The red mud that was used in the following experiments was acquired from an alumina plant located in Louisiana, USA. The plant processes bauxite ore that is mined in Jamaica. The original solids content of the mud sample was found to be near 60% and the particle size distribution can be seen in Figure 3-2. Particle size of the red mud was estimated using a Mictotrac SRA9200. From the figure, the 80% passing size of the red mud sample is 6.5 microns. The phase distribution of the initial red mud samples can be seen in Table 3-1. The red mud consists of large portions of iron bearing minerals such as hematite and goethite. Other large contributions to the phase distribution belong to a number of aluminosilicate clay minerals.
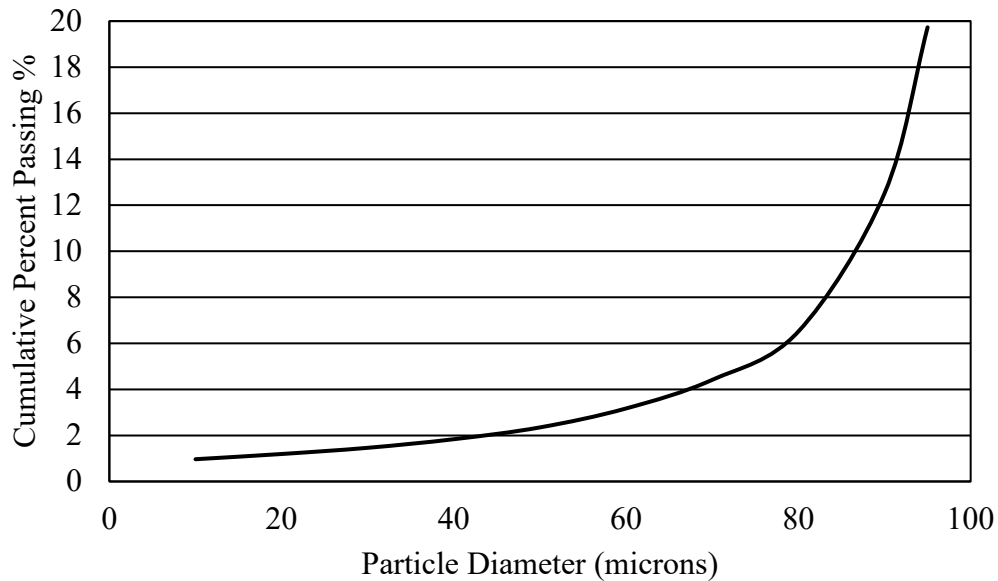
Figure 3-2: Particle Size distribution for the red mud sample used for neutralization experiments

Table 3-1: Chemical distribution of red mud

Component	Chemical Formula	Weight Percent
Hematite	Fe_2O_3	27.3
Sodium Aluminum Silicate Hydrate	$1.08Na_2O \cdot Al_2O_3 \cdot 1.68SiO_2 \cdot 1.8H_2O$	33.9
Goethite	FeO_2H	18.3
Gibbsite	AlO_3	4.4
Anatase	TiO_2	4.6
Rutile	TiO_2	3.8
Calcite	$Ca(CO_3)$	0.2
Quartz	SiO_2	1.6
Sodalite	$Na_4Al_3(SiO_4)_3Cl$	3.4
Sodium Aluminum Silicate Hydrate	$(Na_2O)_{1.31}Al_2O_3(SiO_2)_{2.01}(H_2O)_{1.65}$	2.5

3.3.2 Methods

The neutralization setup for red mud with CO_2 can be visualized in Figure 3-3. Red mud

charges of 800 grams were placed in a 2-liter beaker and distilled water was added at a

1:1 ratio so that the red mud could be mixed until it became homogeneous. The final

solids content of the red mud before neutralization was 30% by weight. A Denver electric

mixer was inserted into the beaker and continuously mixed the red mud at a speed of 900

rpm. The pH of the red mud was monitored using an Oakton pH 700 benchtop meter. The

initial pH of the red mud samples was over 13. A gas dispersion tube was inserted into

the beaker and CO_2 was introduced. During the experiments, the flow rate of CO_2 was

varied from 0.5 – 5 LPM. The neutralization time was also varied between 1- and 6-hour

neutralization cycles and studied under a constant CO_2 flow rate of 1 l/min.
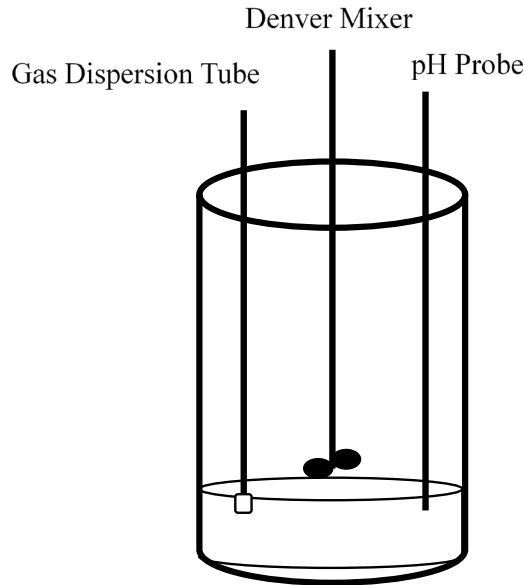
Figure 3-3: Experimental setup for red mud neutralization using CO_2 as a neutralizing

agent

Red mud was sent to X-Ray Diffraction for phase analysis both before and after CO_2

neutralization. Characterization of the samples were done using a Scintag XDS2000

powder diffractometer, configured with a graphite monochromator and IBM compatible

workstation running Scintag DMSNT software in Windows NT environment with scan

parameters of 5.0°/90.0°/0.02°/0.75(s).

Zeta potential measurements were taken using a Malvern Zetasizer Nano ZS. The red

mud samples were inserted via a syringe into a DTS1070 folded capillary cell before

being placed in the zetasizer. Zeta potential measurements were taken over a pH range of

7.5 to 13.2 which was dictated by how far the CO_2 could neutralize the red mud pH.

3.4 Results and Discussion

Neutralization of red mud with CO_2 is possible due to the fact that CO_2 is an acid gas. When the acid gas reacts with basic hydroxide anions the following reactions 3-2 and 3-3 occur in the solution (Sahu, 2010).

$$CO_2(aq) + OH\ (aq) \leftrightarrow HCO_3(aq) \qquad (3\text{-}2)$$

$$HCO_3(aq) \leftrightarrow H^+(aq) + CO_3^{-2}(aq) \qquad (3\text{-}3)$$
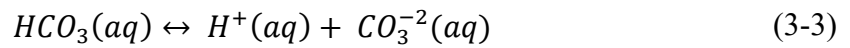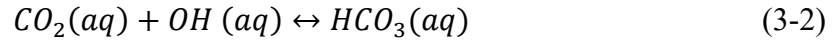
The initial reaction forms bicarbonate ions which can then break down further to generate carbonate ions. This carbonation of the solution is what will lower the pH. As the pH lowers closer to 7, the following reactions 3-4, 3-5, and 3-6 also occur within the red mud slurry (Smith et al, 2003).

$$Al(OH)_4^{-1}(aq) \leftrightarrow Al(OH)_3(s) + OH^{-1}(aq) \qquad (3\text{-}4)$$

$$NaAl(OH)_4(aq) + CO_2(aq) \leftrightarrow NaAl(OH)_2CO_3(s) + H_2O(l) \qquad (3\text{-}5)$$

$$Ca_3Al_2(OH)_{12}(s) + 3CO_2(aq) \qquad (3\text{-}6)$$
$$\leftrightarrow 3CaCO_3(s) + 2Al(OH)_3(s) + 3H_2O(l)$$
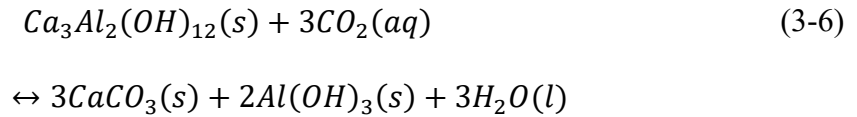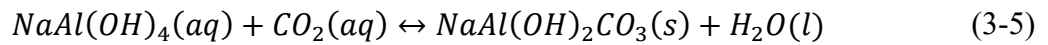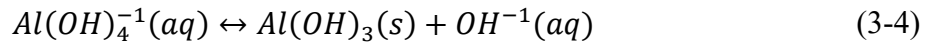
One of the most important alkaline compounds found in red mud that contribute to its high pH is that of tricalcium aluminate, $Ca_3Al_2(OH)_{12}$ (TCA). This mineral reacts with

the carbon dioxide in equation five to create divalent carbonates like calcite. Other minerals play a role in the alkalinity of red mud as well. Going back to the Bayer process, a step occurs before caustic digestion called desilication. The purpose of this step is to not waste the caustic NaOH by only dissolving bauxite in digestion. Desilication transforms mineral clays that would dissolve and contaminate the liquor into insoluble phases at high pH (Archambo and Kawatra, 2020). The issue with red mud neutralization and desilication is that these minerals become unstable and dissolve as CO_2 lowers the pH. This removes alkalinity from them in the form of OH anions, which is counterproductive to neutralization (Power et al, 2011). These minerals that are formed are a range of aluminosilicates such as sodalite and cancrinite (Power et al, 2011).

The effect of introducing CO_2 on the red mud sample can be seen in Figure 3-4. The initial pH begins at 13.2 and quickly descends within the first five minutes. After the initial pH drop from 13 to 10, the reaction appears to slow down and the majority of neutralization time goes to dropping the pH from 10 to 7.5. The steady state value for the pH is achieved after 30 minutes with a flow rate of 1 liter per minute.
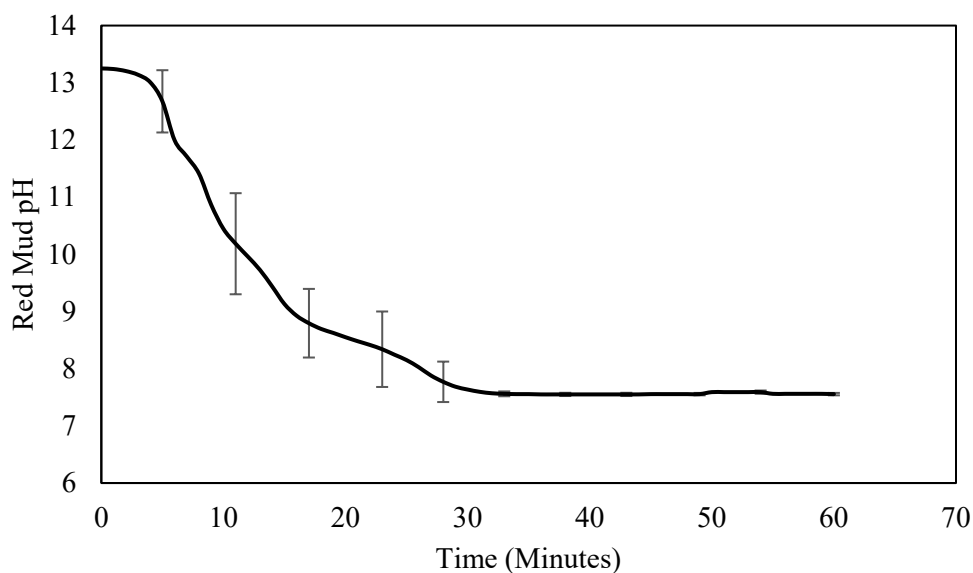
Figure 3-4: Neutralization of red mud with CO_2. Flow rate of 1 liter per minute for 1 hour.

The chemical phases of the neutralized red mud were determined using X-Ray Diffraction. This can be seen in Table 3-2. An increase in carbonates from 0.2% to 2.4% can be seen from the table, in the form of calcite. The carbonate anions that are formed in equation 2 (previously shown) then react with calcium to form calcite. In addition to providing a means to neutralizing red mud, divalent carbonates may provide a further use in downline processing of red mud. For smelting iron nuggets from red mud, the new fraction of carbonate can be used as a flux material in the process to help remove the slag from the iron phase with no additional cost (Archambo and Kawatra, 2020).

Table 3-2: Chemical phase composition of CO_2 neutralized red mud

Chemical Component	Weight Percent, %
Hematite, Fe_2O_3	29.0

Goethite, FeOOH	19.0
Gibbsite, AlO_3	5.6
Anatase, TiO_2	5.0
Rutile, TiO_2	6.5
Calcite, $CaCO_3$	2.4
Sodalite, $Na_4Al_3(SiO_4)_3Cl$	6.1
Sodium Aluminum Silicate Hydrate, $1.08Na_2O\ Al_2O_3\ 1.68SiO_2\ 1.8H_2O$	26.5

After the CO_2 is turned off, the pH was continued to be monitored. Over time, it was noted the pH of neutralized red mud was not stable at its steady state value of 7.50. The rebound of the pH can be seen in Figure 3-5.
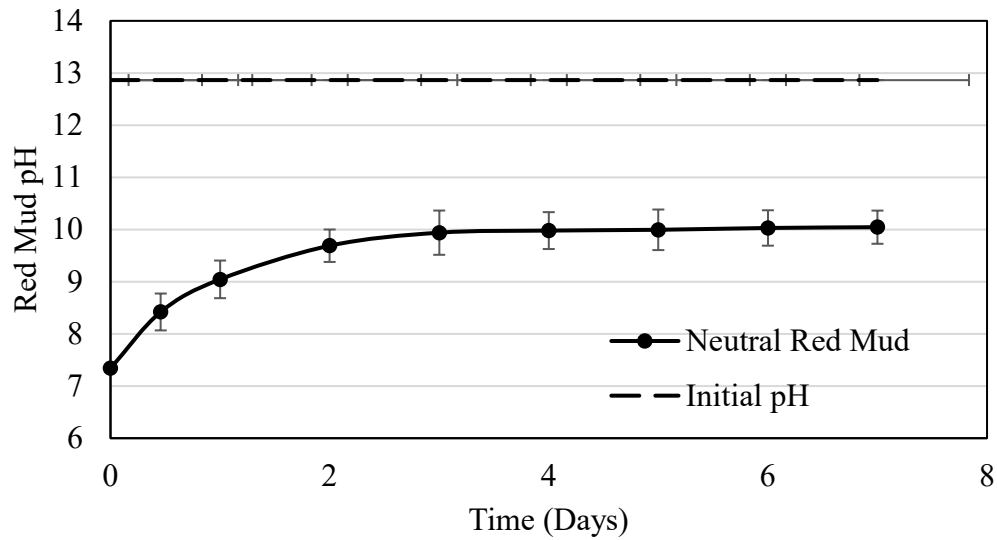
Figure 3-5: CO_2 neutralized red mud pH rebound. Neutralization was done with a CO_2 flow rate of 1 liter per minute. The neutralization cycle lasted for 1 hour and then the gas was turned off. pH of the slurry was measured daily.

From the figure, the pH of the slurry began to rise after the CO_2 was shut off. The increase was largest during the first two days after the experiment. The pH eventually steadied out to near 10. Including the rebound of the pH, the experiment saw an overall pH drop from 12.8 to 10. This is a much better scenario for the disposal of red mud as it will have a lessened negative impact on surrounding settlements and wildlife. The lower pH material may also prove useful for further processing (Archambo and Kawatra, 2020).

The cause of the pH rebound in red mud is not a simple problem, it is a complicated chemistry that even varies between samples of red mud. A summary of the reactions taking place is that of a buffering reaction between alkaline solids in the red mud (Venacio et al, 2013). Smith et al (2003), proposes that the liquor and the solids in red

mud behave differently. The neutralization of the liquor is fast and generates a solution of dissolved bicarbonate, while the solids neutralize much slower due to the presence of the highly alkaline solids such as TCA. If the store of carbonate in the liquor is large enough to neutralize all of the alkaline solids over time, then the pH will rise to 9.5 – 10, a typical pH for carbonate and bicarbonates to buffer at (Smith et al, 2003). If the bicarbonate in the solution is not enough to neutralize the solids, the pH will return to a pH likely close to its original value as the reversible reactions with the alkaline solids will be pushed back (Smith et al, 2003). Another theory is that the large surface area of red mud contributes to the pH rebound. During the typically short neutralization times with CO_2, the alkaline solids are not given the proper amount of time to react, resulting in the rebound of pH (Rai et al, 2013).

To determine what the long-term final effects of the rebound would be on red mud pH, a sample was left alone for 24 weeks or 6 months to determine the final pH that can be expected of neutralized red mud. The rebound effect after 6 months can be seen in Figure 3-6. From the figure, it can be seen that the pH is stable near 10. Based on the previous figure of pH rebound, it can be concluded the rebound of the pH occurs within the first two weeks of neutralization, after that amount of time the rise in pH due to the rebound becomes insignificant.
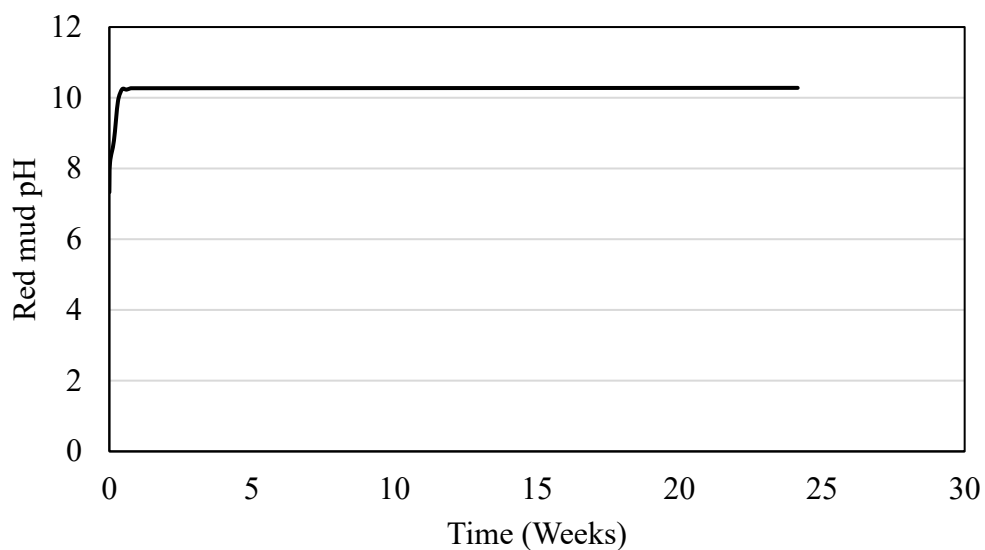
Figure 3-6: Long term effect of pH rebound on the neutralization of red mud with CO_2. Recorded red mud pH up to 24 weeks after initial neutralization at a flow rate of 1 liter per minute.

3.4.1 Effect of CO_2 Flow Rate on pH neutralization

The effect of flow rate on the overall neutralization of the red mud can be seen in Figure 3-7. The pH of the red mud was recorded over the period of 1 hour for each flow rate. All flow rates are able to lower the pH to the same level near 7.50 within a 1-hour time frame. 0.5 liters per minute took the largest amount of time to neutralize, stabilizing after 45 minutes. The 1 liter per minute flow rate was able to neutralize more quickly at around 30 minutes. The flow rate of 5 liters per minute was able to neutralize the red mud the most quickly, only taking about 10 minutes to reach its steady state pH value.
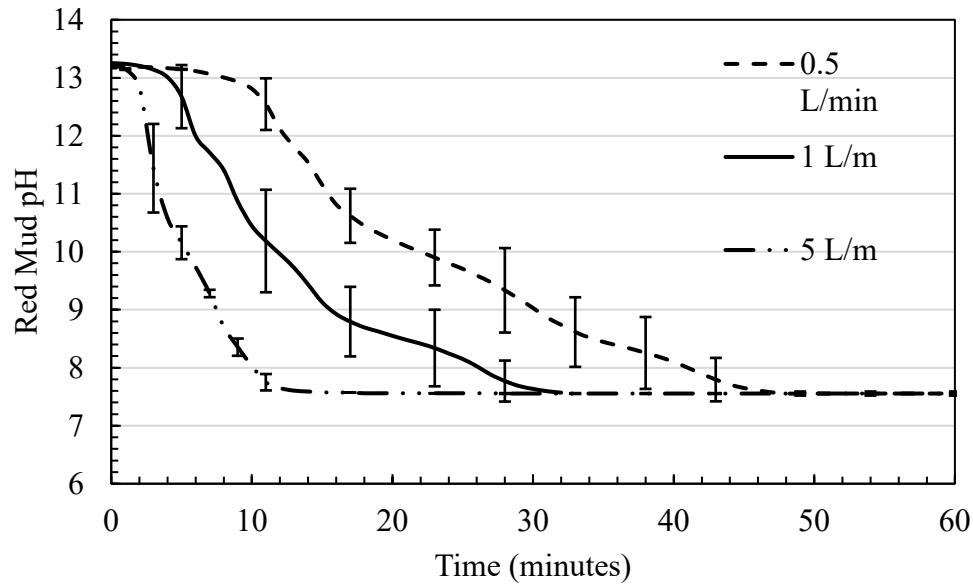
Figure 3-7: Red mud neutralization with CO_2 with flow rates of 0.5, 1, and 5 liters per minute

Table 3-3 shows the amount of CO_2 required for each flow rate to neutralize a red mud sample at standard temperature and pressure while the red mud container is open to the atmosphere. From the table, the flow rate trends linearly with the amount of CO_2 required to neutralize the red mud. On a basis of tons of red mud, up to 144.1 kilograms of CO_2 would be required to neutralize at the highest flow rate. At the lowest flow rate, only 64.9 kilograms of CO_2 would be required.

Due to the neutralizing experiments being open to atmosphere, the true value for the CO_2 sequestered in the red mud is lower than the one given in the table for each flow rate. CO_2 can escape the container and be released into the atmosphere. This table simply shows how much CO_2 would be required to neutralize a sample with this setup on this scale. Based on this logic, the lowest flow rate of CO_2 is most efficient at utilizing and

sequestering CO_2. If CO_2 sequestration is the more important goal, then a lower flow rate should be used to sequester more of the CO_2 as the cost of longer neutralization times. If the fast neutralization of red mud is the priority, then the highest flow rate should be used to lower the pH very quickly at the cost of wasting carbon dioxide in the environment. The optimum flow rate then, with both goals in mind would be the intermediate flow rate. This will neutralize the red mud quickly while also sequestering the CO_2 with a moderate efficiency.

Table 3-3: Amount of CO_2 required in red mud neutralization with varying flow rates

Flow Rate (LPM)	Total Weight CO2 (g)	Kg CO2 per Ton Red Mud
0.5	41.2	64.9
1	54.9	86.5
5	91.5	144.1

The pH was also recorded after the neutralization for the different flow rates to determine if higher or lower rates had an impact on the pH rebound of red mud. The pH rebound for the CO_2 flow rates of 0.5 and 5 liters per minute can be seen in Figure 3-8. The flow rate of 0.5 LPM rebounded more quickly during the first day than the 5 LPM. After 2 days, both flow rates behaved very similarly until the final measurement at 14 days. The final pH of the 0.5 and 5 LPM samples was 9.94 and 9.85 respectively. The higher flow rate of CO_2 was able to slow the rebound initially but ultimately the pH becomes very similar. The likely cause of this similarity is that with enough CO_2 to complete the forward reaction to carbonate, the pH becomes buffered at values typical to carbonate solutions

(Smith et al, 2003). Then, as long as the neutralization time is long enough for any flow rate, the pH will find its end point near 10, similar to what is seen in Figure 5.
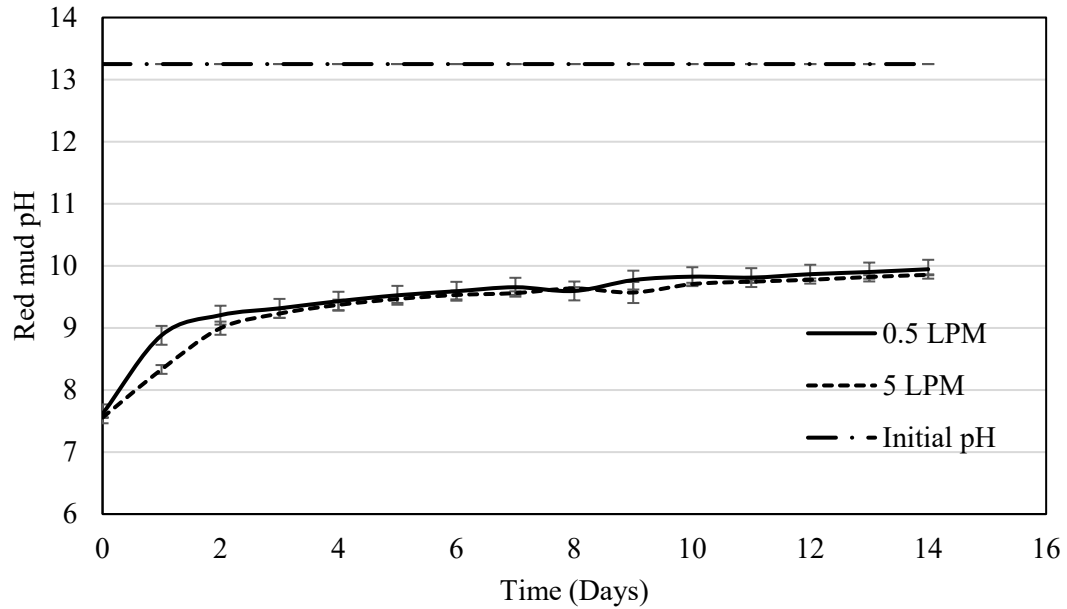
Figure 3-8: pH rebound of CO_2 neutralized red mud at varied flow rates. pH was recorded daily after neutralization for 14 days.

3.4.2   Effect of Neutralization time on red mud pH

According to work done by Rai et al (2013), the rebound in pH can be attributed to the small particle size and subsequent large surface area of red mud. The surface area of red mud can be ranged from 13-16 m2/g (Paramguru et al, 2004). This would indicate that the CO_2 does not have enough time to react with all of the red mud particles in short amount of neutralization. Previous studies have not investigated the effect of longer exposure of red mud to CO_2. Smith et al (2003), also notes that incomplete neutralization of solids materials in red mud slurries is the cause of pH rebound.

This experiment exposes the red mud to a much longer neutralization cycle of six hours with a constant flow rate of 1 liter per minute in order to determine if the large surface area of red mud is contributing the pH rebound. After the six-hour neutralization, the pH was recorded for 14 days. The rebound of pH for the six-hour neutralization cycle can be seen in Figure 3-9. From the figure, the red mud behaves similarly to other experiments in terms of its pH rebound. The pH rise is fastest within the first two days after neutralization. The final pH recorded after 14 days was 9.75, which is lower than 10.04, the value of pH for 1 hour of neutralization. The effect of neutralization time on the final pH of red mud shows that the pH can be slightly lowered but not by a large amount. The amount of CO_2 required to reduce the pH rebound is likely not efficient enough to have this as the most optimal condition.
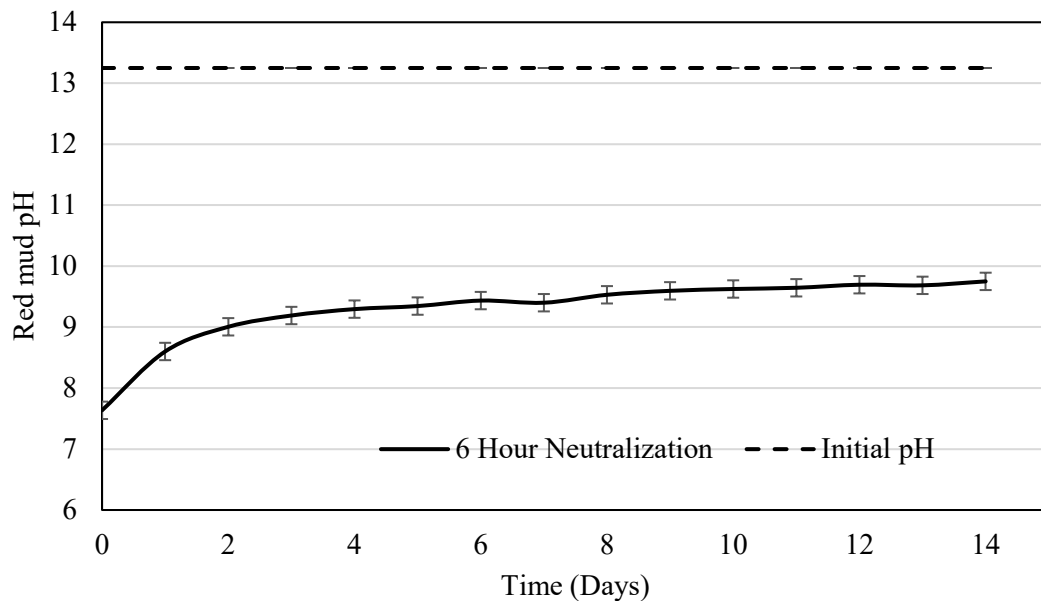
Figure 3-9: Red mud pH after being neutralized with CO_2 for 6 hours. Flow rate of CO_2 was held constant at 1 LPM. pH was recorded daily for 14 days.

3.4.3 Effect of CO$_2$ neutralization on red mud zeta potential

Red mud exhibits typical surface properties of a dispersed slurry, which implies a low settling rate of solids for dewatering (Alam et al, 2018). In order to enhance the dewatering of red mud, current practices employ the addition of flocculants. These chemicals act as a glue and bridge small particles together to create larger conglomerate particles. These larger diameter particles then settle more quickly. Typical reagents used in red mud flocculation are anionic polyacrylamides, polyacrylates, and corn starch (Sankey and Schwarz, 1982).

The effect that carbon dioxide has on the surface properties of red mud may have interesting implications for processing technologies of the waste. Manipulation of the effective surface charge of red mud may be able to dissipate the dispersion properties of caustic red mud. The zeta potential of red mud is one way to measure the effective surface charge of particles in a slurry by measuring the electric potential at the shear plane of a particle (Carlson and Kawatra, 2013). The surface charge density of particles can be broken down into different layers to understand what the zeta potential is measuring. When a particle is moved, the area where the bulk fluid leaves and the fluid near the particle stays in place is called the shear plane, this is where the electric potential is measured as the zeta potential (Carlson and Kawatra, 2013). This can be seen in Figure 3-10.
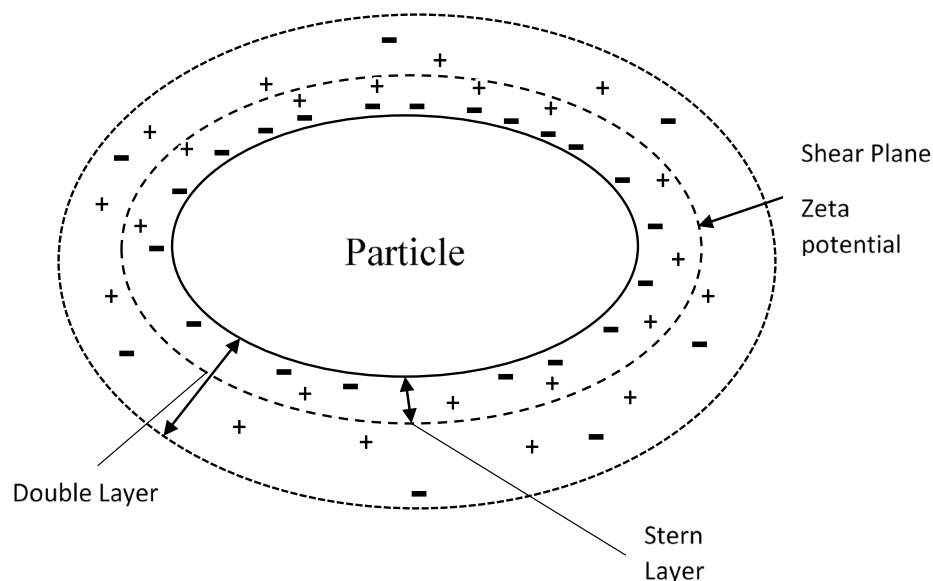
Figure 3-10: Visual explanation of the electric double layer. The zeta potential is the electric potential measured at the shear plane.

Experimental work that was conducted by Rao and Reddy (2017), shows that when red mud is neutralized with acid there is a significant change in the zeta potential of the material. The implication of this study is that when red mud is neutralized, the zeta potential may favor more flocculating conditions which can improve dewatering. Using carbon dioxide as the acidic material to neutralize red mud may show similar results.

The zeta potential was plotted against pH of CO_2 neutralized red mud in Figure 3-11. In its initial state at a pH above 13, the red mud has a high negative value for zeta potential which indicates that it is in a dispersing condition. In the dispersed slurry, all of the particles have a like charge which causes electrostatic repulsion and prevents agglomeration for settling. From the figure, as the pH drops the zeta potential approaches zero. Close to the zero point of the figure is where flocculating conditions occur. Zeta

potentials near zero, along with cohesive and adhesive forces imbalances, and van der

waals forces are factors that impact agglomeration of particles and improve settling

times.
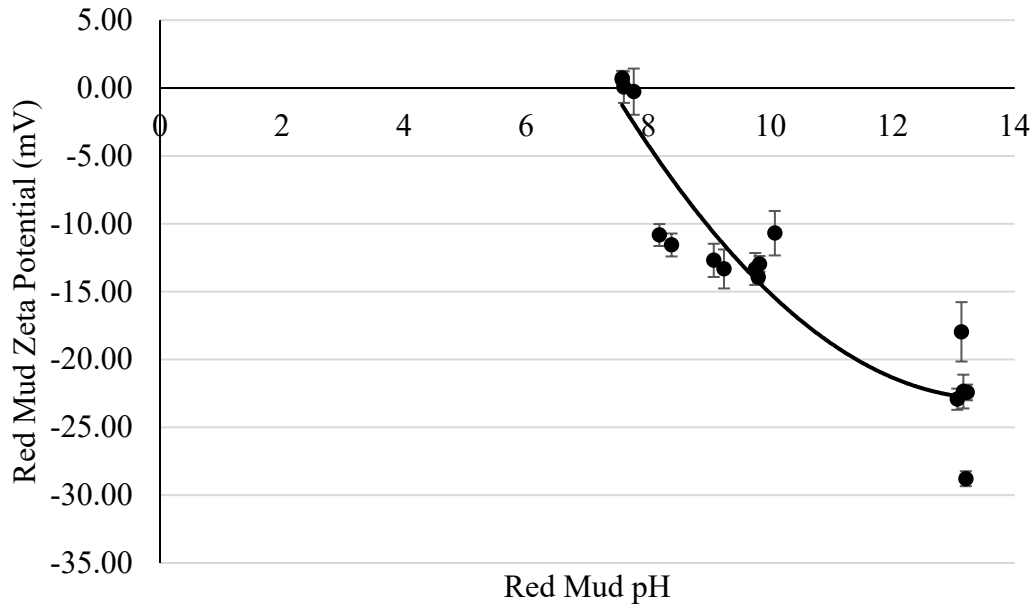
Figure 3-11: Zeta potential vs pH of red mud before and after neutralization with CO_2.

After pH neutralization, the pH of red mud rises again due to the complex internal

chemistry of the slurry (Smith et al, 2003). The zeta potentials measured at the rebound

of the red mud neutralization were a large negative number, but not quite as severe as the

initial values of red mud. It would be advisable then to dewater red mud quickly after

neutralization in order to achieve the most efficient performance.

3.5 Conclusions

Use of CO_2 with caustic red mud provides a simple method to neutralize the high slurry pH. Initially, the pH can be reduced to 7.5. Experiments show that variation in flow rate of CO_2 can decrease the time needed to neutralize red mud. The pH rebounds after each neutralization cycle to near 10. Longer exposure times of CO_2 to the red mud samples did not significantly reduce or slow the rebound of red mud. The more likely cause of pH rebound is that alkalinity is converted into carbonates which then buffer the slurry back to typical carbonate pH. Despite the pH rebound, the overall reduction of red mud pH is more than 3 points on the pH scale, which makes neutral red mud a much safer material to handle.

The alkalinity of red is reduced and calcium carbonate is generated. Calcium carbonate was generated in red mud at a weight percent of 2.5%. This lower alkalinity red mud can be used further to remove iron. The carbonates that are generated during neutralization can be effective reagents in downline processing of red mud to remove valuable minerals like iron. The carbonates can act as a fluxing agent to remove slags from the iron phase in smelting.

Zeta potential measurements approach zero for neutralized red mud. This indicates that dewatering may be more effective when red mud is reduced to a neutral pH range. The neutralized red mud, with reduced alkalinity, poses a smaller threat to the environment. Carbon dioxide is affectively sequestered in red mud, reducing the emissions of greenhouse gases into the atmosphere.

4 Utilization of Bauxite Residue: Recovering Iron Values Using the Iron Nugget Process[2]

4.1 Abstract

Red mud waste from aluminum processing was utilized as a material for extraction of iron. Red mud contains a high amount of iron, comparable to feedstock to North American iron mines, and extracting this iron value is paramount. The iron nugget process can extract iron from the iron minerals in red mud. The nugget process is a one-step alternative to the blast furnace which simultaneously reduces and separates metallic iron from the red mud. A mixture of powdered hard wood and soft wood was used as the reducing agent. Resulting iron nuggets have an iron grade that is comparable to blast furnace pig iron.

4.2 Introduction

Bauxite residue (red mud) is an aluminum processing waste that contains valuable minerals and can be exploited as a feedstock. Red mud is an environmental problem for industry due to its high pH, small particle size, and high disposal costs. Bauxite Residue, more commonly referred to as red mud is a potential source of valuable minerals such as iron, aluminum, titanium, and rare earth metals. In this paper, the term red mud will be used. Worldwide, more than 4 billion tons of bauxite residue has been produced over the

---

course of 120 years. This accumulated waste continues to increase by a rate of around

120 million tonnes per year (Power, 2011). These wastes are difficult and costly to

dispose of for aluminum producing companies. Red mud is a slurry of very fine particles,

making drying and disposal a difficult task. The complication is the caustic nature of the

red mud; most red mud wastes have a pH in the range of 11 to 13.

The Bayer Process treats bauxite ore to produces alumina. Red mud is a byproduct

created as a result of the process. Following the digestion of bauxite in sodium hydroxide

(NaOH), the green liquor containing dissolved aluminates is removed so that it can be

further processed. The remaining solids are dosed with flocculants in a series of thickener

tanks in order to increase the solids content before discharge to the red mud containment

reservoirs. Red mud disposal is not a negligible part of the process for alumina

production, removal of red mud accounts for 30 – 50% of operations in any given

alumina facility (Paramguru, 2004). Studies have been done to optimize the Bayer

process using a technique called mechanical activation which increases reactivity of

aluminum oxide particles through milling by increasing surface area. Increasing

reactivity could reduce the large amount of caustic needed in the Bayer process, but this

work has only been done at the laboratory scale (Alex, 2016).

Removing the environmental hazard of red mud is beneficial for those who work with the

material and those who live near the reservoirs. Red mud storage reservoirs can collapse

and cause serious damage to the surrounding area. In 2010, a red mud dam collapsed in

Ajka, Hungary and spilled 700,000 cubic meters of red mud into the town. This tragedy

killed 10 people and many others were treated for chemical burns for being in contact with the hazardous material (Ruyters, 2011).

Bulk utilization of red mud has been expanded into many different research areas. Most prominently, red mud can be used as a component to make cement, with various mixtures including lime, bauxite, and gypsum (Liu, 2011). Mixing red mud with other components prove to be a promising gateway towards making stronger construction materials. Mixing red mud with lime increases the mixtures compressive strength due to pozzolanic reactions with calcium ions and available silica in the red mud (Sujeet, 2019). One method for the construction industry is to create insulating bricks from red mud by mixing with sawdust to improve porosity for thermal conductivity (Mandal, 2017), (Singh, 2014). Synthesis of geopolymers with red mud has been researched for practical applications such as pH regulation for wastewater treatment and bioreactors (Novais, 2018). For polluted soils containing high amounts of heavy elements such as Pb, Cu, Zn etc., red mud has been successful in tests as a material that can remove available heavy metals from soil (Zhou, 2017). One approach to removing this hazard is the neutralization of red mud using CO_2 as an acid gas. This technology actually achieves multiple goals at once (Power, 2011).

1. It reduces the hazard of red mud and makes it a more valuable feedstock.
2. It provides a sink for carbon emissions to reduce greenhouse gases.
3. Improve the quality of used process water
4. Reduce the risk of groundwater contamination

Red mud has a chemical composition that varies widely and very often contains valuable minerals. These mineral compositions change because the ore bodies at each location are different. Table 4-1 shows red mud compositions throughout the world. As can be seen, the mineral composition varies significantly from location to location, but in general the values range for each mineral are as follows: Fe_2O_3, 20 – 60%; Al_2O_3, 10-30%; SiO_2, 2-20%, Na_2O, 2-10%; CaO, 2-8%, TiO_2, trace-28% (Paramguru, 2004). For these ore bodies, hematite and goethite are the main chemical components. These are both iron bearing minerals, which will add value to the red mud if a utilization process is developed.

Table 4-1: Red mud compositions from various plants and laboratories around the world. Elemental compositions determined by XRF. Redrawn from (Grafe, 2011) and (Sutar, 2014)

Bauxite Origin	Refinery	Al_2O_3% By Wt	Fe_2O_3% By Wt	SiO_2% By Wt	TiO_2% By Wt	CaO% By Wt	Na_2O% By Wt
USA	RMC	18.4	35.5	8.5	6.31	7.73	6.1
Canada	ALCAN	20.61	31.60	8.89	6.23	1.66	10.26
China	Chalco	18.36	6.81	14.49	10.45	25.22	5.53
Southern Brazil	Laboratory	6.8	71.9	1.35	7.8	3.2	0.4
Jamaica	Laboratory	2.34	62.1	1.3	12.9	15.9	0.8
India	Damanjodi	14.8	54.8	6.4	3.7	2.5	4.8
India	Korba	19.4	27.9	7.3	16.4	11.8	3.3

Greece	Alumina De Greece	15.6	42.5	9.2	5.9	19.7	2.4

Extracting value of red mud is critical to reducing the amount of waste produced. Red mud could serve as an iron feedstock comparable to the iron ore feed stocks for Midwestern mining facilities. Determining how to economically extract this iron value is key to eliminating a large fraction of this mineral waste. Utilized red mud will not need to be stored in large impoundments for decades while it dries out and a new source of iron for steelmaking would be available. Work has been done to utilize red mud as a construction material by a process called geopolymerization; the red mud can be made into building material like bricks through this process to minimize waste of aluminum processing further (Dimas, 2009).

The primary method for making steel has always been the blast furnace. This method uses iron ore pellets, coke, and flux to make metallic pig iron. This process has its drawbacks and limitations (Zervas, 1996):

1. The metallurgical coke required as a reducing agent for iron reduction is becoming more difficult to obtain due to environmental restrictions.

2. Efficiency of the blast furnace can only be achieved at the large scale, so small-scale blast furnace operations are not possible. This makes any change in supply of iron ore feed and demand for steel produced to be a detriment to the economics of the process.

To effectively compete with the blast furnace, a process would have to be one which can operate on a small scale and effectively handle iron feed stocks with widely varying

grades. A large flaw that the blast furnace has is that it can only be done economically on a very large scale, so any alternative that can operate on a small scale is favorable. The direct reduction process can effectively reduce iron ore, but the sponge iron that is created still contains a large amount of impurities that must be separated for steel production. Recovery of iron via the direct reduction pathway has been investigated. Reduction roasting of red mud mixed with coal, followed by magnetic separation was able to generate an iron concentrate of 65.93% iron with 61.85% recovery (Sandangi, 2018).

The process that can achieve these goals, both reduction and separation, is the iron nugget process (Anameric, 2006). The nugget process works in a single step to reduce iron oxides to metallic iron and separate them from the gangue minerals at furnace temperatures at 1425°C. A reducing agent containing carbon is mixed into a pellet with iron ore and it is heated to high temperatures. Iron oxides are converted to metallic iron- and as the iron melts it separates from the slag layer (Anameric, 2006). Iron nuggets have been studied using iron ores such as magnetite or hematite as a feed stock. Investigations on the compositions of the slag formed during the process say that in order for a good separation, the gangue material must have a low liquidus temperature to separate from the iron. This can be done with the help of flux and binder additions (Mourao, 2010). A continuous process was developed for production of pig iron from iron ore using microwaves at 2.45 GHz (Hara, 2011). Mixed carbon pellets have also been formed with aluminum oxide, the product of the Bayer process to form metallic aluminum using vacuum reduction; the energy required to reduce aluminum in this way currently is far

greater than that of the current method of aluminum production, the Hall-Heroult process (Halmann, 2014).

The iron nugget process can handle very low-grade ores with little to no beneficiation, impurities are all removed in a single step. The iron nugget process is therefore ideal for handling red mud, which is essentially impossible to process via the blast furnace route to its disagreeable characteristics. The fine particle size prevents effective filtration or density separations in any reasonable or economical amount of time (Power, 2011). Due to the presence of chemical additives such as surfactants to aid in the thickening of red mud, surface separations in mineral processing such as selective flocculation or flotation are also ineffective (Power, 2011). Pig iron has been recovered from red mud using different furnace and heating technologies. Pig iron has been formed from red mud using thermal plasma heating with graphite as the reducing material in the pellet; this resulted in a maximum iron recovery of 71% (Jayasankar, 2011). Iron nuggets were also formed from red mud by Guo (2013), which yielded iron nuggets with 96.52% iron from an ore containing 63.20% hematite. Carbon graphite was used as the reducing material. A much cheaper source of carbon that can be used from production of nuggets from red mud is powdered wood. Powdered wood has seen little research done in its ability to act as a reducing agent for iron. This research investigates the effectiveness of the iron nugget process on red mud using powdered wood as the reductant, which has not yet been studied. Overall, there has been very little initiative to extract iron from bauxite tailings at all. The novelty of this process both gives value to a waste product while also removing red mud as an environmental and safety hazard.

4.3   Experimental

4.3.1   Materials

At Michigan Technological University, a sample of red mud was obtained for the valorization project. This sample ore was mined in Jamaica and processed in an alumina facility in Louisiana. The ore was sampled at a low solids content of about 50% percent solids.

Particle size analysis was completed with a laboratory MicroTrac SRA 9200 laser diffraction. Figure 4-1 shows the results for the particle size distribution. The sample had a D80 of 10 µm. This is a typical result for size of red mud.
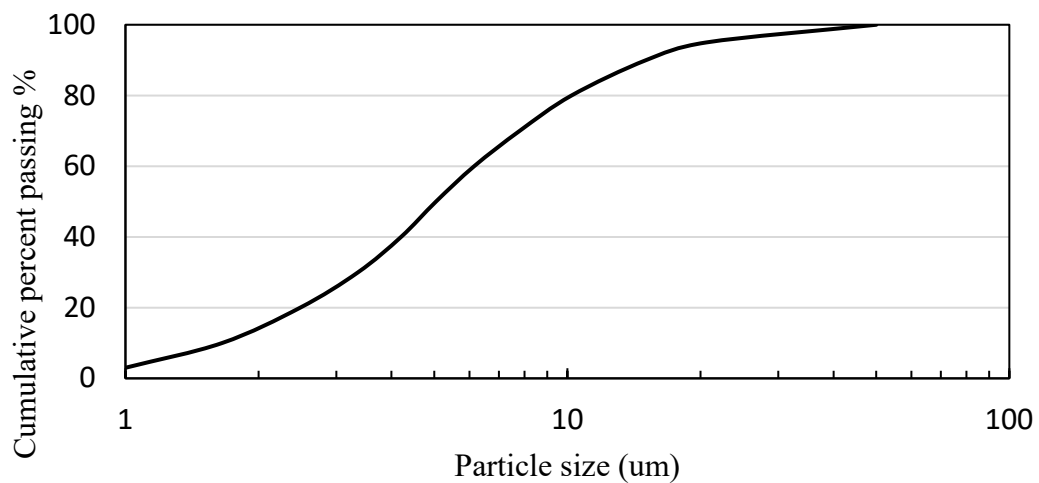
Figure 4-1: Particle size distribution of the Jamaican red mud sample

Elemental compositions were found using X-Ray Fluorescence as shown in Table 4-2. From the table, iron, aluminum, and silicon are the most prevalent elements with the rest being minor contributors. This technique is unable to detect elements lighter than sodium,

so any of these elements are absent from the analysis. Many of the elements shown from XRF are actually in oxidized forms but the device will not detect oxygen. From the XRF data, the mineral phases can be more easily identified using another technique, X-Ray Diffraction.

Table 4-2: XRF elemental compositions of Jamaican red mud

Element	Weight %
Fe	50.97
Al	15.253
Si	10.258
Na	7.611
Ag	7.621
Ti	4.303
Ca	1.583
Si	0.156
Cr	0.013
Zr	0.035

The mineral composition of the red mud samples was determined using X-ray diffraction (XRD). The compositions were found using a Scintag XDS 2000 powder diffractometer. Figure 4-2 shows the raw diffraction data. From the phase composition breakdown in Table 4-3, it can be seen that the two most common components are both iron bearing minerals, hematite and goethite. Residual aluminum and silicates are also present in the sample; as multiple different complex mineral phases.
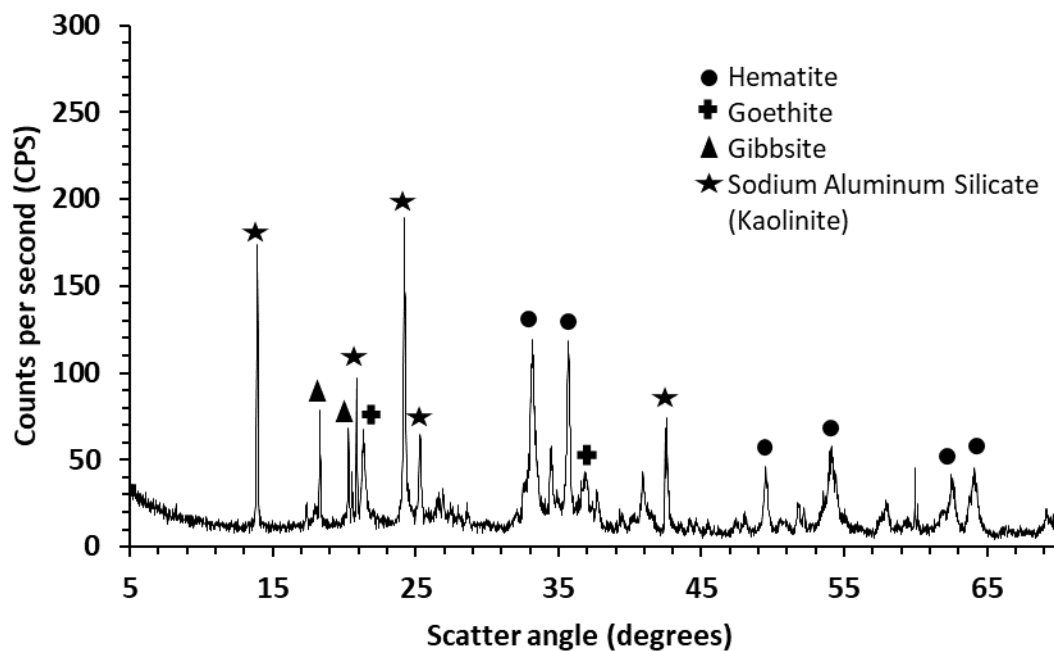
Figure 4-2: Raw X-Ray diffraction pattern for the bauxite residue sample (major components labeled)

Table 4-3: Phase composition of red mud by weight percent

Component	Chemical Formula	Weight Percent
Hematite	Fe_2O_3	14.0
Sodium Aluminum Silicate Hydrate	$1.08Na_2O\text{-}Al_2O_3\text{-}1.68SiO_2\text{-}1.8H_2O$	17.3
Goethite	$FeO(OH)$	6.8
Gibbsite	$Al_2O_3 \cdot 3H_2O$	11.5
Chromium Iron Oxide	$CrFeO_3$	10.1

Anatase	TiO_2	2.1
Sodalite	$Na_4Cl(Al_3Si_3O_{12})$	11.6
Perovskite	$CaTiO_3$	4.9
Iron Zirconium	$ZrFe_2$	0.1
Silver Aluminum Silicate	$Ag_{61.1}Al_{69.8}Si_{122.2}O_{384}$	0.2
$Ca_{8.5}NaAl_6O_{18}$	$Ca_{8.5}NaAl_6O_{18}$	21.5
Total		100

In literature, it has been noted that rare earth elements are often contained in high concentrations in red mud residue (Borra, 2015). The presence of rare earths should be investigated in bauxite because most of the REEs are discharged from the Bayer Process in the red mud. Akcil et al described a process that could be used to concentrate rare earth elements in red muds with a high REE concentration. Using ICP-AES (Inductively Coupled Plasma Atomic Emission Spectroscopy) the presence of rare earth elements including scandium was shown to be negligible for this sample of red mud. Table 4-4 shows the results for concentration of rare earth elements in the red mud sample. In this particular red mud sample, however, rare earths were found to be negligible, and were not investigated further.

Table 4-4: Concentration of rare earth elements (REE) including Sc in the Jamaican red mud sample

Rare Earth Element	Concentration (ppm)
Lanthanum (La)	0.02
Cerium (Ce)	0.02
Neodymium (Nd)	0.02
Scandium (Sc)	0.01
Praseodymium (Pr)	< 0.01

Previous work (Anameric, 2006) with the iron nugget project showed that metallic iron could be produced using iron ore feed stock pellets with a coal reducing agent. In this study, the iron ore feed stock was substituted with the iron bearing red mud. This research also utilizes a different reducing agent, a powdered hard and soft wood mixture. The carbon content of the powdered wood sample was determined in triplicate using a Costech 4010 Elemental Analyzer to be 50.16 ±0.11% Carbon. Moisture content of the powdered wood sample was measured to be 6.83%.

4.3.2   Methods

4.3.2.1   Sample Preparation

A sample of red mud was dried in a drying oven at 105 °C to remove all moisture so that it could be pelletized. A process flow diagram for the nugget furnace experiments is show in Figure 4-3. The following samples were added together and mixed in a mixing bowl at the following total weight percentages:

Powdered wood with moisture: 10% by weight

Dry Red Mud: 81.84% by weight

Dolomite: 7.5 % by weight

Bentonite Clay: 0.66% by weight

The red mud and wood were mixed with 7.5% dolomite flux to help encourage slag separation and with 0.66% bentonite for stronger pellet strength. The mixed material was then fed into a pelletizing drum where pellets formed to a diameter of 3 mesh and were then screened and dried in a drying oven. The dry pellets were placed into crucibles, placed into a Micropyretics MXI high temperature box furnace preheated to 1475 °C. The temperature was kept constant for all experiments due to the limitations of the furnace available in the laboratory. Pellets were placed into the furnace for varying residence times and removed to cool quickly on a bed of sand. Determining the heating rate of the pellet sample is valuable but due to the limitations of the experimental setup, it is not present in this paper. A thermal couple could not be safely placed into the furnace while the crucible was placed so the heating gradient of the pellets themselves could not be determined.
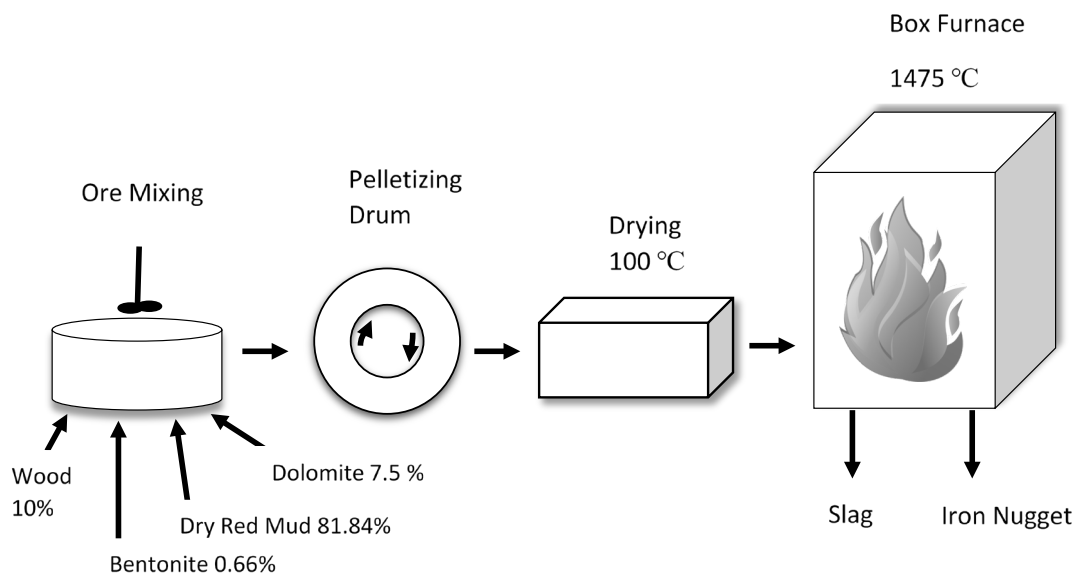
Figure 4-3: Process flow diagram for the red mud iron nugget experiments

4.3.2.2   Iron Content Analysis

Iron content of each sample was determined using ultraviolet spectroscopy. Iron nuggets

and slags were digested in 20 mL of concentrated 12M hydrochloric acid (HCl) and

diluted in distilled water. The iron nuggets were diluted to 1000 mL and the slags were

diluted to 100 mL. 0.1 mL of that solution was transferred to a 50 mL volumetric flask

and diluted again with distilled water. Hydroxylamine hydrochloride was added in excess

to reduce all iron ions from the +3 to the +2 state. Ammonium acetate was added as a pH

buffer and 1-10 phenanthroline as an indicator. The absorbance of the solution was

measured using UV-VIS spectroscopy, set at a single wavelength of 510 nm. Iron content

can be calculated by the relationship of light absorbance to concentration (Day, 1991).

4.4 Results and Discussion

Red mud pellets placed into a preheated 1475 °C begin to react with the mixed carbon source immediately after being placed in the pre-heated furnace. The powdered wood decomposes and form gases that will react with iron oxides. The reactions for the thermal decomposition of the reducing material is as follows from Equations 4-1 through 4-6 (Anameric, 2006):

$$Carbon\ Source\ \rightarrow CO, CO2, H2, N2, C_nH_m, C \qquad (4\text{-}1)$$

$$C + O_2 \leftrightarrow CO_2 \qquad (4\text{-}2)$$

$$CO_2 + C \leftrightarrow 2CO \qquad (4\text{-}3)$$

$$C + \frac{1}{2}O_2 \leftrightarrow CO \qquad (4\text{-}4)$$

$$CH_4 + CO_2 \leftrightarrow 2CO + 2H_2 \qquad (4\text{-}5)$$

$$C + H_2O \leftrightarrow CO + H_2 \qquad (4\text{-}6)$$
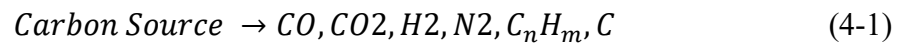
The mechanism that reduces iron oxides is complex and occurs in multiple steps. The reduction of hematite to metallic iron can be thought of as a multistep reaction or several single step reactions. Hematite reduces to magnetite, then magnetite to wustite, and wustite to iron. The reduction of hematite to magnetite is the fastest; the reduction reactions occur as follows (Chen, 2017). As a form of direct reduction of iron, iron oxides in the presence of an excess of reducing substance can reduce at low temperatures relative to blast furnace operation. Direct reduction of iron oxides begins to occur at temperatures above 900 °C (Fruehan, 1998). In the pellet, the close contact of iron oxides to the reactive sites of the reducing agent improves the utilization of the reductant in the pellets by increasing the rate of reactions (Anameric, 2006).

At furnace temperatures exceeding 1200 °C, the slag in the pellet's melts. Important slag forming reactions are shown below with Equations 4-11 through 4-15 (Anameric, 2006). After the reduction reactions occur, the liquidus temperature of the metal decreases due to carburization of the metal as shown in equation 4-15. This allows the slag separation to be achieved by forming two immiscible liquid phases. Density and surface tension effects are the driving forces in this separation (Anameric, 2006).

$$CaCO_3 \leftrightarrow CaO + CO_2 \qquad (4\text{-}11)$$

$$CaO + SiO_2 \leftrightarrow CaSiO_3 \qquad (4\text{-}12)$$

$$FeO + SiO_2 \leftrightarrow FeSiO_3 \qquad (4\text{-}13)$$

$$FeSiO_3 + CaO \leftrightarrow CaSiO_3 + FeO \qquad (4\text{-}14)$$

$$3Fe + C \leftrightarrow Fe_3C \qquad (4\text{-}15)$$
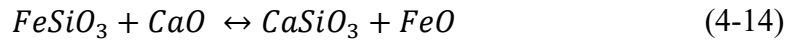
A total mass balance for this process is shown with Equation 4-16. F, C, T, and G represents the feed, concentrate, tailings, and gases respectively. An iron balance is represented in Equation 4-17 where lower-case letters signify weight percent.

$$F = C + T + G \qquad (4\text{-}16)$$

$$Ff = Cc + Tt \qquad (4\text{-}17)$$

Iron nuggets generated from this method fall into three categories, which are dependent on residence time (Anameric, 2006):

1) Direct reduced iron: Single solid product with no slag separation

2) Transition direct reduced iron: liquid and solid-state products with partial slag separation

3) Pig iron nuggets: liquid state products with complete slag separation.

4.4.1   Residence Time Variation

Iron nuggets were produced from dry red mud/powdered wood pellets in the laboratory at Michigan Tech at varying residence times. Red mud pellets were placed fired in the furnace at 1475 °C for 30, 45, 60, 90 and 120 minutes. Table 4-5 shows the elemental composition of the iron nuggets that were formed. They contain the majority of iron which is similar to pig iron with a high carbon content relative to blast furnace pig iron which typically contains 3 to 4.5% (McGannon, 1971). Small amounts of aluminum appear in the nugget due to red mud being rich in aluminum minerals left over from the bauxite. Figure 4-4 shows the resulting iron nugget and slag bodies that formed during the firing process. The iron recovery of the pellets at each of these conditions is recorded in Table 4-6 and Figure 4-5. All remaining iron that is not captured in the iron nugget is contained in the slag body as partially reduced iron oxides.
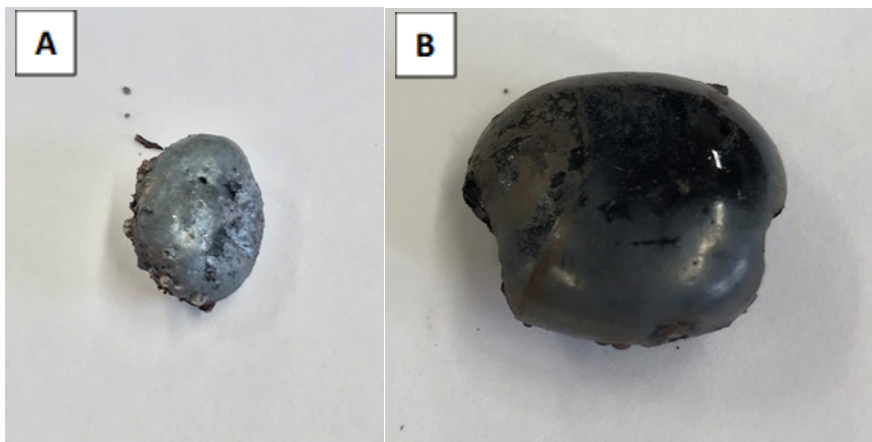
Figure 4-4: Photographs of iron nugget process using red mud. Products were fired at a furnace temperature of 1475 °C with a 120-minute residence time. A) Iron nugget B) Fusible slag

Table 4-5: X-Ray Fluorescence (XRF) of red mud iron nuggets chemical composition.

Element	Fe	C	Al	Ca	S	Cr	Ti	Total
Weight Percent, %	90.03	7.739	1.125	0.546	0.421	0.0774	0.0599	100

Table 4-6: Red mud iron nugget iron recovery. Fired in a furnace heated to 1475 °C.

Furnace Conditions	Residence Time 30 Minute	Residence Time 45 Minute	Residence Time 60 Minute	Residence Time 90 Minute	Residence Time 120 Minute
Iron Recovery %	55.48%	59.43%	69.93%	70.02%	76.14%
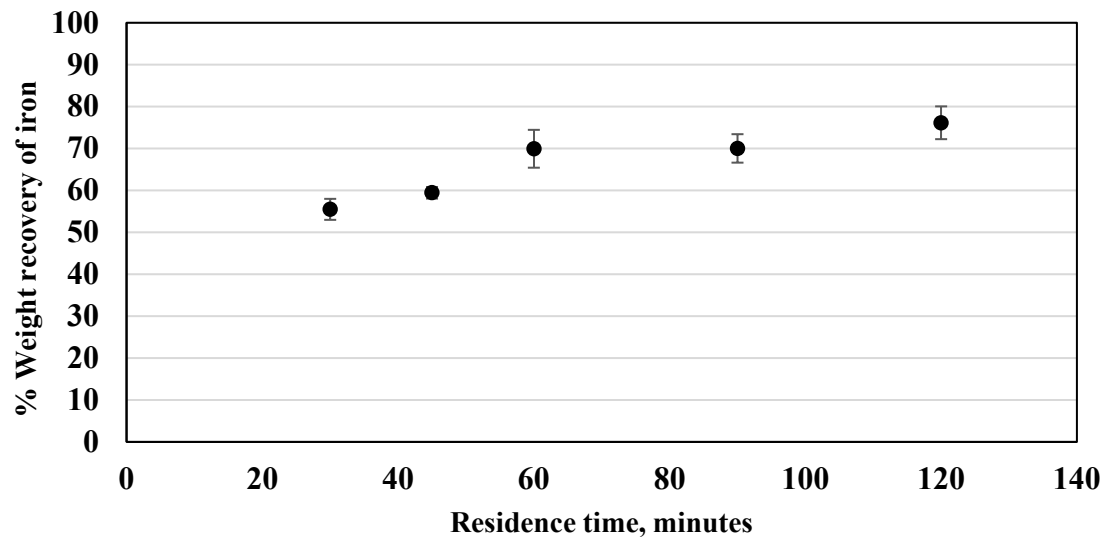
Figure 4-5: Weight recovery of iron from the red mud using the iron nugget process for varying residence times. Error bars represent 95% confidence intervals.

For low residence times under 30 minutes, slag separation was unable to occur. This is due to the iron and the slag not both being completely in the liquid phase, the separation occurs because of density differences between the two fluids. The overall reduction of hematite to metallic iron occurs more quickly than the slag separation. Tanako (1996) showed the reduction time for their self-reducing pellets at temperatures near 1000 ℃ were reduced completely after 20 minutes. If one or both are not fluids, then the separation will be incomplete. Residence times above 30 minutes showed an iron separation. With more time to melt and separate, the reduced and melted iron is allowed to sick to the bottom of the crucible. Lower iron content at lower residence times can be attributed to entrainment of slags in the iron nugget body that have not been able to properly separate.

The iron nuggets produced via the nugget process have an iron content higher than 90%. Most tests showed comparable results with blast furnace pig iron in regards to iron content. Generally, when pig iron is produced it has a purity of over 90% iron (Fruehan, 1998). Nugget process iron is similar to blast furnace iron in terms of carbonation as well, with high amount of carbon appearing in the nugget. For all residence times, iron content exceeded 90%. With increasing residence time, the grade of the iron nuggets increases.

Overall recovery of iron in the nugget process was also studied, as shown in Table 4 for varying furnace residence times. Recovery varies from 55 to 80%, but in general as residence time increases the recovery of iron increases.

4.4.2 Carbon Content Variation

The amount of reducing material in the feed pellets is an important parameter to consider in the nugget process for red mud. Powdered wood contains much less total weight percent carbon than coal and coke which is also used in self reducing pellets. The sample of powdered hard/soft wood mixture contained 50.16% carbon. Experiments were carried out by changing the weight percent of the wood in the pellets from 1, 5, 10, 20, and 30%. Other parameters were held constant such as residence time, temperature, and flux content at 30 minutes, 1475 °C, and 7.5% respectively. From Figure 4-6, the iron recovery increases with increasing wood content. With low amounts of reducing material, the surface area of contact between the hematite and the wood is small which causes less of the iron to be reduced and recovered in the nugget. In contrast, when the reducing content is high the hematite has a large amount of surface contact with the reducing material which causes a more complete reduction and improved recovery in the iron nugget. The effect of powdered wood percent change is most significant for the lower portion of the graph, where to slope of the change is much higher. From 10 to 30%, the increase in recovery appears linear with a smaller slope. At the point where the slope changes in this graph would be the optimum point for nugget production, which occurs at 10% powdered wood.
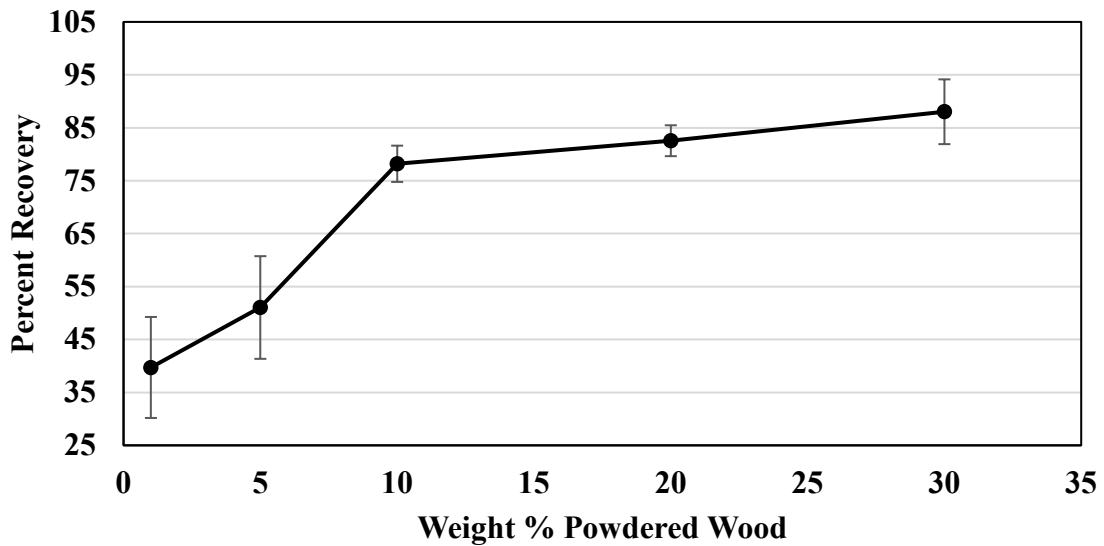
Figure 4-6: Iron recovery from the nugget process with changing powdered wood content by total weight percent. Error bars represent 95% confidence intervals.

4.4.3 Flux Content Variation

In the nugget process, the separation is completed between the liquid phases of iron and slag mainly on differences in density and viscosity. Flux additions to the slag decrease the liquidus temperature at which all of the slag becomes a liquid an in turn decreases the viscosity (Mourao, 2010). Optimizing the addition of flux for each ore body is necessary in order to maximize iron recovery.

Experiments altered the amount of dolomite flux in the feed pellets by total weight percent. 0, 1, 2.5, 5, 7.5, and 10 total weight percent were fired in the furnace and recovery was calculated. Residence time, temperature, and reducing content were held constant at 30 minutes, 1475 °C, and 10% respectively. Figure 4-7 shows the result of

these experiments. At 0% flux content, no iron nuggets were formed. This is caused by materials that have not melted inside the red mud pellet. The liquidus temperature is too high for the slag and no separation can occur.

High amounts of flux over 7.5% saw a steep decrease in iron recovery, this could be due to the composition of the slag becoming too saturated with Mg and Ca. The liquidus temperature of the slag begins to rise again at this point of flux addition and separation from the iron becomes more difficult (Mourao, 2010). The optimal range for flux in the red mud case was from 2.5 to 7.5%. The highest iron recovery was found at 2.5% flux at 80.9% iron recovery.
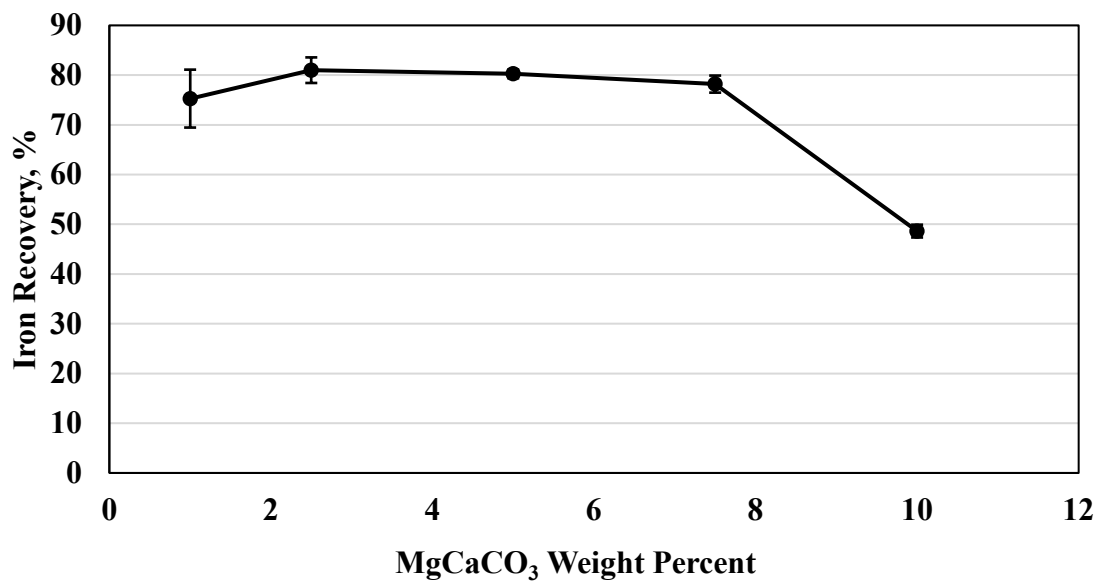
Figure 4-7: Iron recovery from the nugget process with changing dolomite flux by total weight percent. Error bars represent 95% confidence intervals.

4.4.4   Slag Analysis

The slag obtained from the box furnace after physically separation from the iron nugget body was analyzed by x-ray fluorescence and x-ray diffraction. Table 4-7 displays the elemental analysis of the nugget slag. Iron is still present in the sample but is much lower in the case of the slag. The same spread of elements that were present in the red mud feed material are present in the slag with the addition of Mg and Ca that were added with the dolomite flux. Table 4-8 shows the chemical compositions for the slag. We can see that the aluminum silicates were left mainly in the slag, accounting for the majority of the slag's total weight. This implies that side reactions with these compounds are not competing with the iron oxides or appearing in the iron nuggets. The remaining unreacted iron oxides appear in the form of goethite at 8.3%. Supply of CO reducing gas from wood decomposition may be limiting the exposure of reducing gas to iron oxides preventing all of it from being separated. Residual carbon in the forms of carbon and graphite are present in the spectrum. Much of the sodium aluminum silicate from the red mud has been transformed to nepheline.

Table 4-7: XRF elemental composition of red mud nugget slags

Element	Weight %
Fe	16.257
Al	22.705
Si	21.773
Ca	15.363
Na	7.91

Ag	5.672
Ti	6.407
S	0.234
Zr	2.729
Cr	0.116
Mg	0.0534
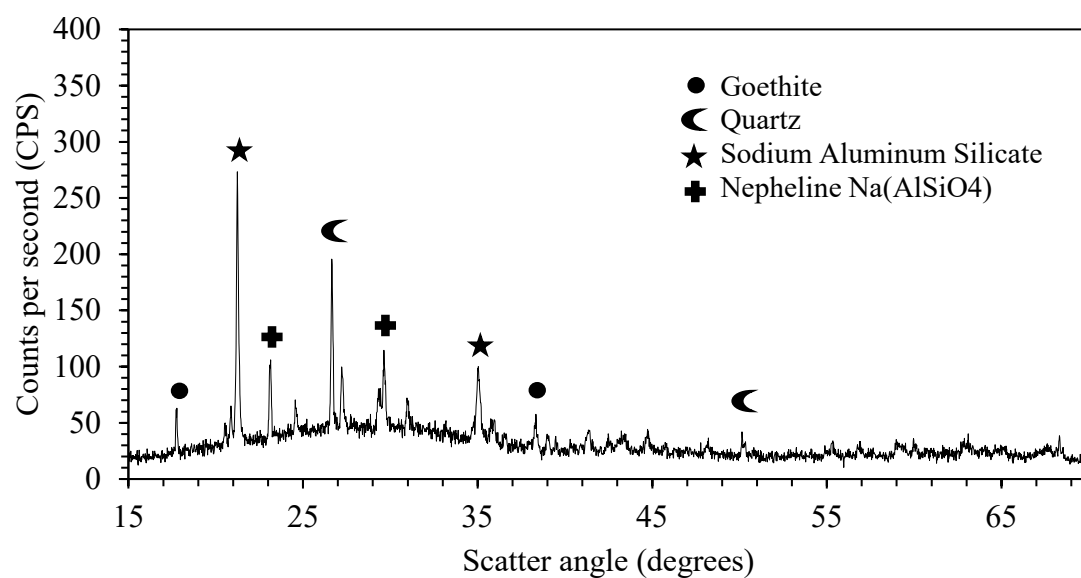
Figure 4-8: Raw X-Ray diffraction pattern for slags produced with the red mud iron nugget process (major peaks labeled)

Table 4-8: Chemical component distribution in red mud iron nugget slags. Pellets fired at 1475 °C for a residence time of 60 minutes

Component	Chemical Formula	Weight Percent
Quartz	SiO_2	3.7
Goethite	$FeO(OH)$	8.3
Nepheline	$NaAlSiO_4$	46.4
Sodium Aluminum Silicate	$NaAlSiO_4$	21.4
Carbon Sulfide	C_3S_4	1.2
Pyrope	$Mg_3Al_2Si_3O_{12}$	8.4
Aluminum Hydroxide	$Al(OH)_3$	2.1
Calcium Iron Oxide	$CaFe_5O_7$	4.3
Calcium Silicon Oxide Nitride	$CaSiN_{1.86}O_{0.21}$	4.1
Total		100.0

In the blast furnace, the goal is to remove all impurities through the slag body. Slag compositions vary depending on several variables including the ore body and furnace conditions. Iron content of blast furnace slags has been investigated on many occasions in attempts to understand and improve the process. The four oxides that are most present in blast furnace slags are alumina, magnesia, lime, and silica. Iron content is typically very low in these slags, ranging from 0.3% to 2% (Josephson,1949). McCaffery et al. (1928) developed a model to calculate compositions of ternary blast furnace slags which were based on an alumina-silica-lime-magnesia system. They calculated compositions for 74

blast furnace slags around the world with FeO compositions ranging from 0.43% to 3.70% (McCaffery et al, 1928).

The iron nugget process generates a large amount of slag due to the comparatively low iron grade of red mud as the feed material. It is important to note that the slag generated has existing industrial applications. The nugget process slag has the potential to be utilized in a variety of industrial situations. For example, blast furnace slag has been known to be utilized in cement, glass sand, slag wool, ceramics, soil treatment, roofing, sewage filter media, paint filler, abrasives, and cast products (Josephson, 1949).

4.5   Conclusions

Hematite and Goethite were found to be present in red mud at an iron grade of 22%, similar to taconite feedstocks in North America. It was found that rare earth elements are present in this red mud sample at concentrations of less than 1 ppm and so no further effort was made to extract them. The iron nugget process was used to extract the iron value from the red mud sample because it can process ores at very low feed grade and produce metallic iron.

Iron nuggets were produced experimentally from red mud using the 1-step iron nugget process. Iron nuggets exceeding 90% iron content, comparable with blast furnace pig iron, were formed at residence times exceeding 30 minutes. The iron recovery was found to be dependent on residence time, reducing material content, and flux content. Recoveries between 55% and 80% with increasing residence time. Iron recovery steeply increases with increasing reducing material with an optimal point at 10% powdered

wood. Optimal flux content was found to be 2.5%. The slag that was generated from this process contained the remaining iron in the form of goethite.

This method is promising due to its ability to work with very low-grade iron ore sources, as opposed to the blast furnace which requires concentrated iron ore pellets to be effective. The nugget process can also be done on a small scale while the blast furnace is notorious for its huge scale of operation. Extra care should be exercised when handling red mud due to its hazardous properties. High pH red mud solutions between 11 and 13 pose a threat to workers and people that are near the waste reservoirs that contain it. Removing iron from red mud increases the value of a process waste while also making it more manageable to dispose. Decreasing the amount of waste from aluminum plants is beneficial because these disposal areas require significant amounts of land area that become unusable do to the caustic nature of red mud.

5 Effects of various flux material additions on red mud iron nugget quality

5.1 Abstract

Iron nuggets can be generated from red mud, a process waste discarded from the alumina making Bayer process. Red mud is a hazardous waste that threatens the aluminum and mining industry. Forming iron nuggets from red mud reduces the overall waste and adds value to the materials. The iron nuggets do not form and separate from the molten slag unless a carbonate flux material is added to the pellet before firing. The flux aids separation by lowering slag viscosity. Previous work with red mud iron nuggets has shown that dolomite additions can be effective as a flux. This study aims to study other carbonate flux materials and determine which is most effective at lowering slag viscosity and improving separation. It was found that magnesium and calcium carbonates improve recovery most effectively.

5.2 Introduction

Red mud contains a high amount of iron that can range from 20%-60% (Paramguru et al, 2004). Currently, the industry treats red mud slurries as a waste material with little inherent value. In reality, red mud is a mixture of concentrated valuable minerals that can be removed for economic gain (Archambo and Kawatra, 2020a). Removal of iron from red mud is critical to reduce the amount of red mud that is being stockpiled worldwide. Current estimates show that the total amount of red mud that is stockpiled in the world is near 4 billion tons and it is increasing every year with larger demand for aluminum products (Wang et al, 2020). Research is currently searching for ways to lower the

amount of red mud, but without economic incentive, the reduction of red mud will be unlikely. Further production of red mud to extract these minerals of value can provide the required economic incentive.

One novel method for removing iron from red mud is the iron nugget process. Unlike the blast furnace, the nugget process reduces and separates metallic iron from the gangue in a single step and can be used on much smaller scales (Anameric and Kawatra, 2006). The iron nugget process is ideal for low grade iron ores such as that of red mud as it can tolerate a larger amount of slag than the blast furnace. Iron is also in a purer state than that of direct reduction or leaching processes, acid leaching in particular tends to also remove other minerals that would contaminate an iron concentrate like titanium or aluminum (Agatzini-Lleonardou et al, 2008).

Archambo and Kawatra (2020b) showed that a flux addition is required in order to produce iron nuggets from red mud. The flux that was used was a dolomite flux. An analysis of different available flux materials, the properties they exhibit, and their industrial pricing will be able to identify how to increases iron recovery in the iron nuggets and produce the valuable product more economically. Better understanding the role that the flux material plays in the generation of the iron nugget will enable the most efficient production of iron. This research will focus on generating iron nuggets using different carbonate flux materials to determine which causes the best separation of iron and which is the most economically viable.

5.3   Materials and Methods

Red mud slurry was received from a Louisiana alumina plant for experimental work. A flow diagram for the experimental process can be seen in Figure 5-1.
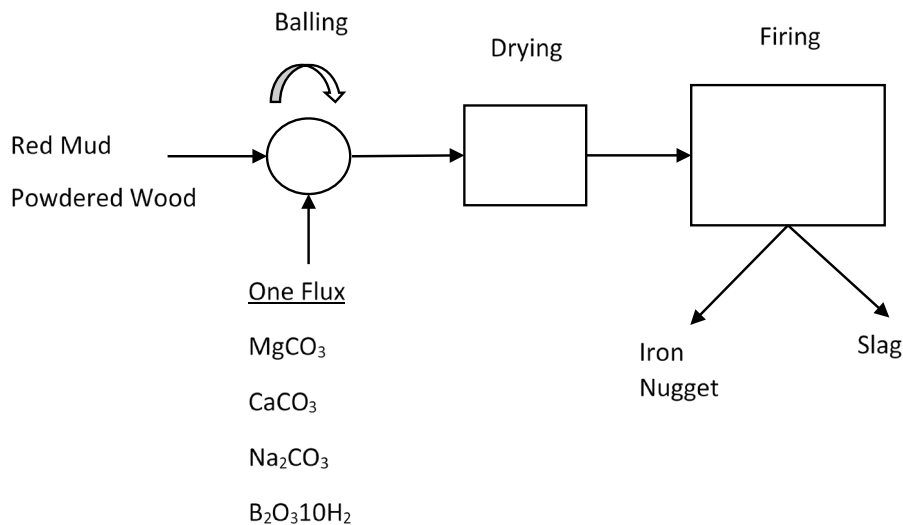
Figure 5-1: Process flow diagram for red mud iron nugget preparation with varied flux materials

The red mud was dried in an oven and rolled into pellets. The red mud was mixed with powdered wood and bentonite clay. Four flux materials were tested in this study and they were added individually to pellet batches and then rolled into large pellets that weighed close to 10 grams each. The rolled pellets were then dried overnight in an oven to remove moisture.

Pellets were placed into graphite crucibles with a bed of anthracite coal to prevent sticking and went into a preheated box furnace at 1475 degrees Celsius for a residence

time of 30 minutes. The iron nuggets were physically separated from the slag and were subjected to iron content determination using spectroscopy techniques. The slag was pulverized in a puck mill and sent for X-Ray diffraction analysis. Diffraction was performed using a Scintag XDS 2000 powder diffractometer.

5.4 Results and Discussion

Iron nuggets can be produced from red mud by first reducing the iron oxides present with a reducing material. Previous research has shown that iron nuggets can be reduced with coal or powdered wood (Anameric and Kawatra, 2006) (Archambo and Kawatra, 2020). Decomposition of the reducing agent occurs via the chemical Equations 5-1 through 5-6 (Archambo and Kawatra, 2020b). The carbon source (coal or wood) is heated to its thermal decomposition temperature where the carbon is converted into CO and CO_2. The carbon monoxide that is produced is the reducing agent that interacts with iron oxides.

$$Carbon\ Source\ \rightarrow CO, CO2, H2, N2, C_nH_m, C \tag{5-1}$$

$$C + O_2 \leftrightarrow CO_2 \tag{5-2}$$

$$CO_2 + C \leftrightarrow 2CO \tag{5-3}$$

$$C + \frac{1}{2}O_2 \leftrightarrow CO \tag{5-4}$$

$$CH_4 + CO_2 \leftrightarrow 2CO + 2H_2 \tag{5-5}$$

$$C + H_2O \leftrightarrow CO + H_2 \tag{5-6}$$
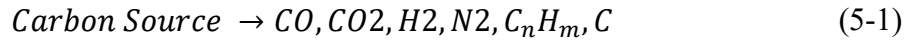
Iron oxide reduction to metallic iron is shown in Equations (5-7) through (5-10) (Chen, 2017).

$$Fe_2O_3 + \frac{1}{3}CO \rightarrow \frac{2}{3}Fe_3O_4 + \frac{1}{3}CO_2 \tag{5-7}$$

$$Fe_3O_4 + CO \rightarrow 3FeO + CO_2 \tag{5-8}$$

$$FeO + CO \rightarrow Fe + CO_2 \tag{5-9}$$

$$Fe_3O_4 + 4CO \rightarrow 3Fe + 4CO_2 \tag{5-10}$$
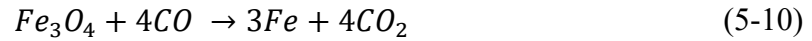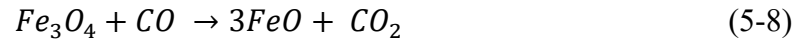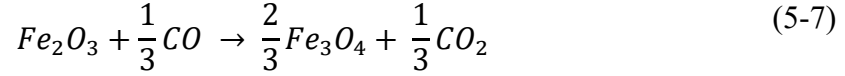
While iron is being reduced, the impurities in the pellet are forming the slag layer. Anameric and Kawatra (2006) outlined some of the important slag forming equations as can be seen in Equations (5-11) through (5-16). In the case of red mud nugget slag, the much more complex and diverse chemical phases will also lend to additional reactions that are occurring in the slag. It is critical that both the iron and slag achieve a liquid phase in the nugget process for the separation to occur. The addition of fluxing materials to the pellet before firing assists in altering the chemical properties of the slag to allow the separation.

$$CaCO_3 \leftrightarrow CaO + CO_2 \tag{5-11}$$

$$CaO + SiO_2 \leftrightarrow CaSiO_3 \tag{5-12}$$

$$SiO_2 + 2C \leftrightarrow Si + 2CO \qquad (5\text{-}13)$$

$$FeO + SiO_2 \leftrightarrow FeSiO_3 \qquad (5\text{-}14)$$

$$FeSiO_3 + CaO \leftrightarrow CaSiO_3 + FeO \qquad (5\text{-}15)$$

$$FeS + CaO + CO \leftrightarrow CaS + FeO + CO \qquad (5\text{-}16)$$
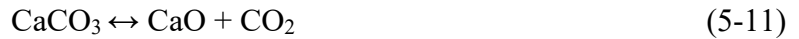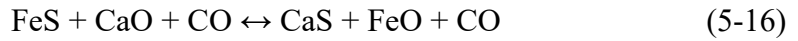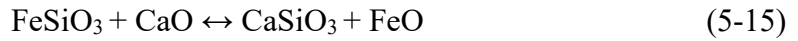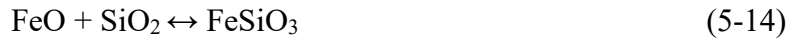
5.4.1 Flux material effect on slag viscosity

The viscosity of the slag is an important factor that determines how well the iron can separate from the slag. In order to produce an iron nugget with the lowest iron bearing slag, the slag viscosity must also be very low. In the nugget process, the molten iron separates from the slag body based on the difference in viscosity of the two phases (Anameric and Kawatra, 2020). The viscosity of the slag can be altered by changing the chemical phase composition of the red mud pellet, this was done by adding different flux materials to the pellet. Figure 5-2 shows the effect of different flux materials on the overall viscosity of the slag. From the table, it can be seen that pellets with no flux addition should have the highest viscosity. Previous work with red mud to make iron nuggets shows that pellets with no flux addition do not generate iron nuggets (Archambo and Kawatra, 2020). Increasing the amount of sodium in the pellet with sodium carbonate is able to lower the slag viscosity to an intermediate effect. Calcium carbonate and magnesium carbonate show similar results being able to greatly reduce the slag viscosity. The fact that they are both divalent cations likely give reason to their similar results.

Borate is estimated to lower the slag viscosity to the greatest extent. Borates are often

used in glass making as an additive.
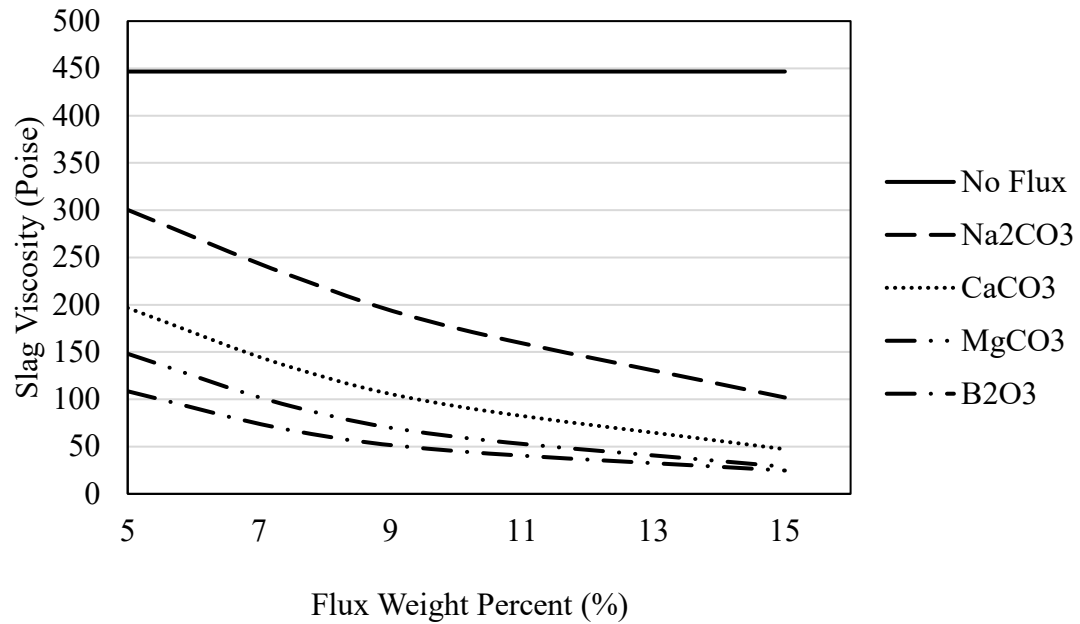
Figure 5-2: Effect of different fluxes for iron nuggets produced with red mud.

Theoretical data simulated using FASTSAGE software and chemical phase compositions

determined by X-Ray Diffraction

5.4.2   X-Ray Diffraction Analysis

X-Ray diffraction was used to analysis the chemical phases that were produced during

the iron nugget process for each separate case of flux additions. Figure 5-3 shows the

chemical phases that appeared in the slag containing magnesium carbonate flux. Sodium

aluminum silicate and nepheline formed in the magnesium bearing slag. The magnesium

itself was sequestered in the form of dolomite and periclase.
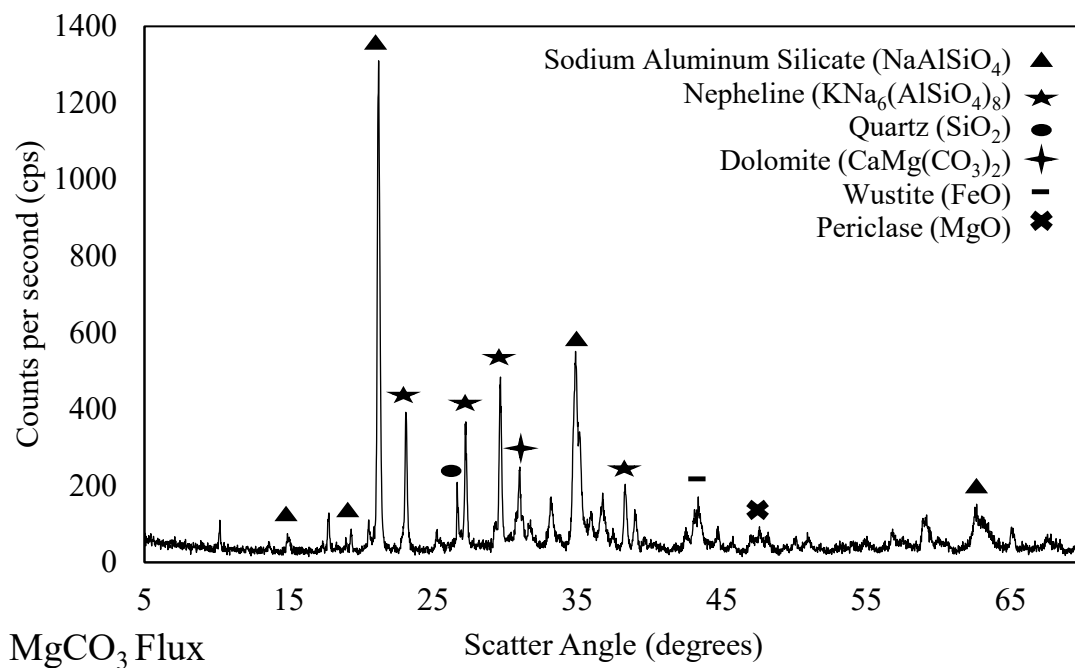
Figure 5-3: X-Ray Diffraction pattern for iron nugget slag with 7.5% MgCO3 added to the pellet as a flux material

The chemical phases for calcium carbonate fluxed slag can be seen in Figure 5-4. The most notable peaks formed with calcium flux are those of sodium aluminum silicate and nepheline. The calcium from the flux has been sequestered in the slag in the forms of calcite and perovskite.
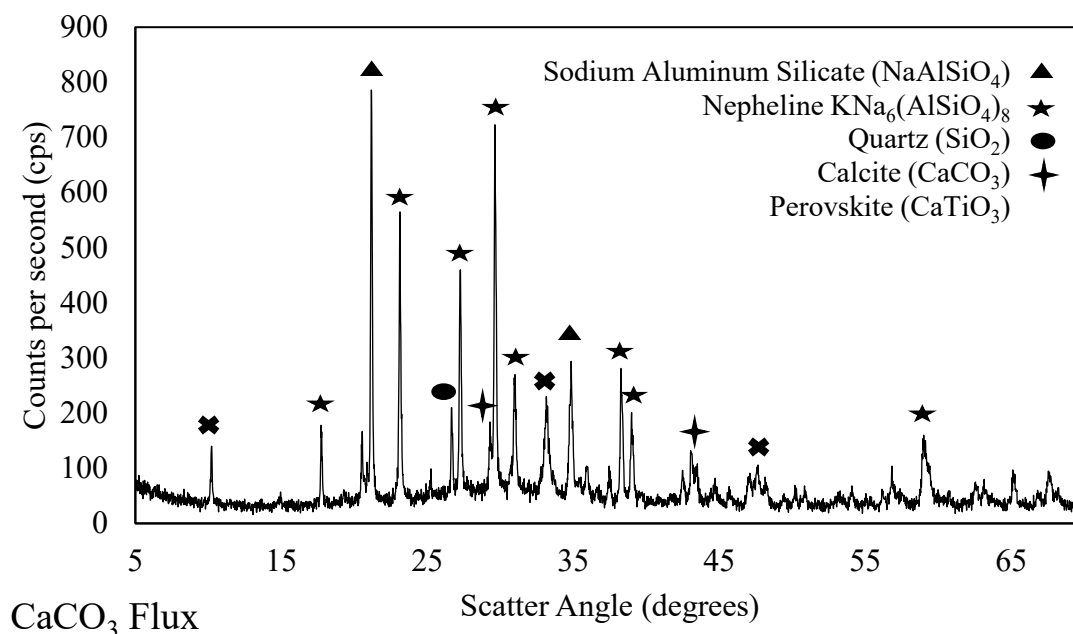
Figure 5-4: X-Ray Diffraction pattern for iron nugget slag with 7.5% CaCO3 added to the pellet as a flux material

The chemical phases for sodium carbonate fluxed slag can be seen in Figure 5-5. The addition of sodium carbonate created a much more intense peak for the chemical phase for sodium aluminum silicate with other smaller contributions by quartz, magnetite, and hematite. Nepheline was not formed from sodium flux as was the case for the previous divalent fluxes. A large amount of sodium is added to crushed bauxite ore in the form of sodium hydroxide, boehmite and diaspore minerals in particular require a more concentrated amount of caustic for dissolution (Adamson, 1963). Large amounts of sodium and other alkali earth metals like potassium have been cited to cause issues during iron production in the blast furnace (Liu et al, 2016). The blast furnace operation

typically seeks to remove as much sodium as possible before reduction. When bentonite

clay is added in iron ore pelletization, even more sodium introduced in the form of

sodium bentonite (Landis and Maubeuge, 2004). It is probable that the introduction of

sodium as a flux material as well will contribute to the higher viscosity and a lower

degree of iron separation.

Na_2Co_3 Flux
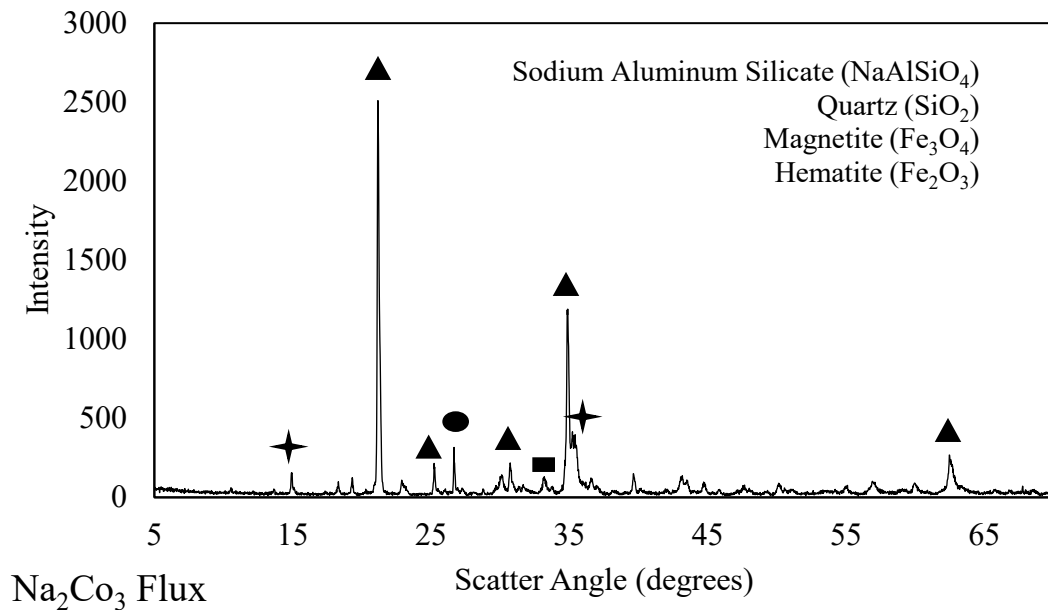
Figure 5-5: X-Ray Diffraction pattern for iron nugget slag with 7.5% Na2CO3 added to

the pellet as a flux material

The chemical phases for borate fluxed slag can be seen in Figure 5-6. The diffraction

pattern for the borate slag is only able to identify peaks that are associated with silica. X-

Ray diffraction is often unable to accurately determine the phase composition of a

material that is amorphous. An amorphous material is one that do not have long range

crystallographic order and in turn produce large humps instead of sharp peaks in a diffraction pattern (Rowe and Brewer, 2018). It can be seen that one of these humps covers the scatter angle from roughly 15 to 40 degrees in the case of the boron slag. Since this phenomenon doesn't occur in the other diffraction patterns of flux additions, this is indicating that the borate has created an amorphous slag during firing. The material does not have a rigidly defined shape with an ordered crystal structure compared to the other fluxed slags that do have crystalline structure. One study on quartz-based slags with the addition of B_2O_3 showed that with increasing borate content, the viscosity of the slag decreased (Wang et al, 2020). This may imply that a different mechanism is driving the separation from iron in the case of borate slags. Wang et al (2020) theorized that borate interacts with silica and removes oxygen to for boroxyl rings and increases the degree of polymerization of the slag.

Quartz (SiO$_2$) ●

B$_4$O$_7$ Flux
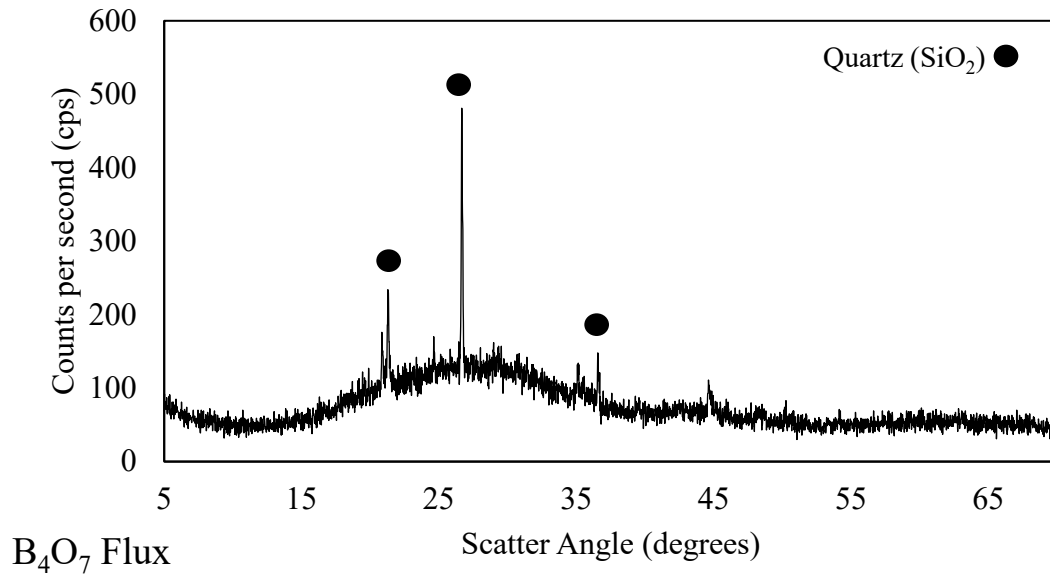
Figure 5-6: X-Ray Diffraction pattern for iron nugget slag with 7.5% B4O7 added to the pellet as a flux material

5.4.3 Grade and Recovery of iron

The experimental results for adding different fluxes to the red mud pellets can be seen in Figures 5-7 and 5-8. Iron grade in the nuggets was the greatest using the sodium carbonate flux, followed by calcium carbonate, magnesium carbonate, and borate performed the worst.

In regards to iron recovery, magnesium and calcium carbonate performed well. Each achieved a recovery above 80%, with magnesium carbonate slightly outperforming calcium. In the case of magnesium oxide flux, when in a molten slag it can release oxygen to simplify the structure of the slag by modifying the silica network (Xing et al, 2020). As expected from the FACTSAGE slag viscosity calculations, sodium carbonate yielded very low recovery below 20%. The is likely due to the fact that the slag viscosity

was not low enough to allow the buoyant forces of the iron to separate completely from

the slag (Shannon et al, 2008). The borate addition to the slag breaks away from the

simulated viscosity calculations, producing the intermediate results for recovery near

60%.
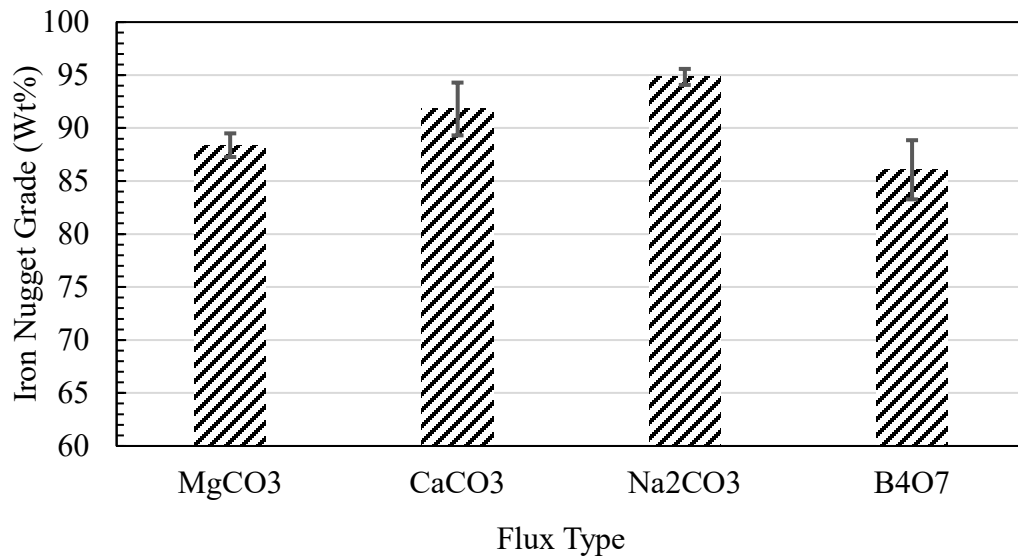
Figure 5-7: Effect of different flux materials on the iron grade of iron nuggets produced
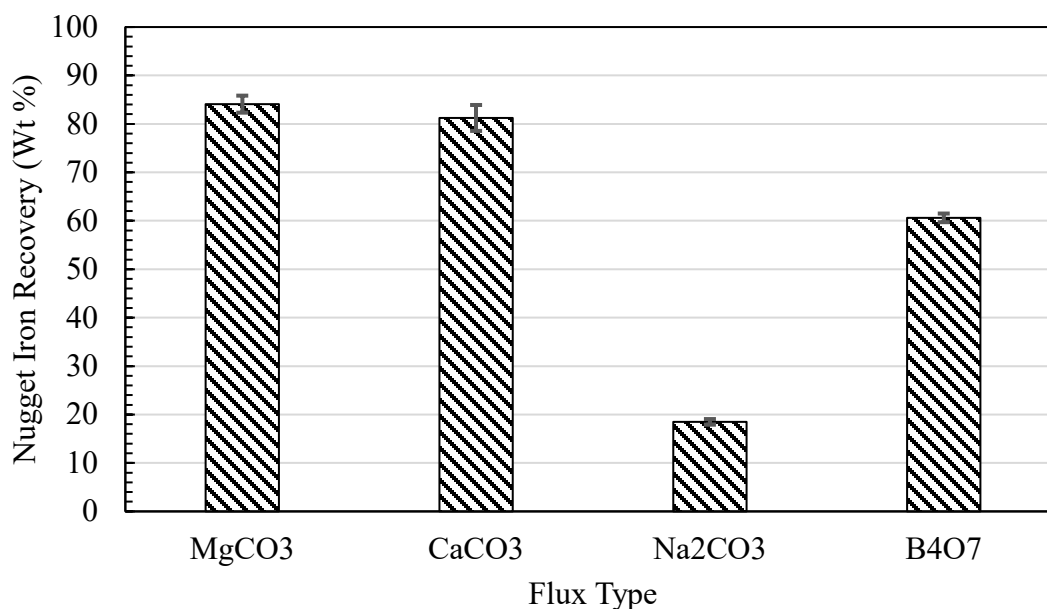
from red mud.

Figure 5-8: Effect of different flux materials on the recovery of iron in iron nuggets generated from red mud.

Along with the recovery of iron as a product, the resulting slag is the new waste material that has been reduced in mass compared to the original red mud. Table 5-1 shows the percent of waste removed by weight using the iron nugget process. The most effective flux for waste reduction was magnesium carbonate, removing 39% of waste. If the iron nugget process were to be used to process iron from the entire stockpile of worldwide red mud, 4 billion tons (Wang et al, 2019), then the new total stockpile would be 2.4 billion tons. Some plants around the world have red muds that contain much higher-grade iron and they would see a waste reduction even larger.

Table 5-1: Waste reduction weight percent of red mud using the iron nugget process

	Percent of waste removed (wt %)	Error (±)

CaCO₃	37.39	0.85
MgCO₃	39.19	1.41
Na₂CO₃	20.27	0.76
B₄O₇	33.07	1.53

5.4.4 Cost of flux reagents

The effectiveness of each flux must also be paired with its availability and pricing when considering which choice is most economic for an industrial process. Table 5-2 shows the pricing data for each of the studied flux materials. In this case, the most effective fluxes, calcium carbonate and magnesium carbonate, are also the cheapest to purchase industrially. Sodium carbonate is nearly twice as expensive and sodium borate decahydrate is more than three times more expensive. Despite being effective at reducing the viscosity of the slag and improving iron recovery, it is still a cost to purchase and add the flux material to the red mud pellets. If the carbonate flux could be generated from costless reagents such as CO_2 in the plant, it would be extremely advantageous.

Table 5-2: Industrial bulk price data for fluxing reagents used in the nugget process

Name	Calcium Carbonate	Magnesium Carbonate	Sodium Carbonate	Sodium Borate Decahydrate
Chemical Formula	$CaCO_3$	$MgCO_3$	Na_2CO_3	NaB_4O_7 $10H_2O$
Industrial Price ($/Ton)	80	80	150	300
Date	10/28/2020	10/28/2020	10/28/2020	10/28/2020

Source	Alibaba	Alibaba	Alibaba	Alibaba
URL	https://offer.alibaba.com/cps/e1f5f93f?tp1=5bc719a63ad4e			

5.5 Conclusions

Flux addition plays a significant role in the iron nugget process for red mud. Fired pellets that contained no flux did not form separate molten iron and slag layers. The flux material impacts the viscosity of the slag and the lower the viscosity the better the separation. Of the fluxes tested in this study it was found that magnesium carbonate and calcium carbonate performed the best achieving iron recoveries of 84% and 81% respectively. Sodium carbonate was not an effective flux due to the fact that it was not able to lower the slag viscosity enough for separation. The use of borate as a flux material generated an amorphous slag whereas the others were crystalline. The amorphous nature of the borate slag also prevented separation of iron from the slag body. From a cost perspective, Magnesium and calcium fluxes are comparable. If the flux can be generated from costless reagents in the plant such as CO_2, the expenditures for flux reagents can be removed.

6 Using CO₂ Neutralized Red mud to Generate Iron Nuggets

6.1 Abstract

Alumina plant waste, or red mud is a problem due to the large amount of waste generated and the hazardous properties it exhibits. Much research has gone into studying the material for its better waste disposal and processing of valuable minerals. Research at Michigan Tech has shown that iron can be removed from red mud using the iron nugget process with the addition of flux materials. The addition of CO_2 can reduce the pH while simultaneously generating carbonate flux material. Combining the iron nugget process with red mud neutralization of CO_2 can remove valuable iron from red mud, remove hazardous alkalinity, and reduce the need for reagent additions such as flux for nugget smelting. CO_2 neutralized red mud was used to generate iron nuggets of similar quality of high pH red mud and blast furnace pig iron without the addition of a flux material.

6.2 Introduction

Mineral processing waste management has and continues to be a challenge across the mining industry. The handling of such wastes is an environmental, logistical, and economic problem which is always seeking to be improved upon. In the case of alumina processing the obstacle is especially high. The Bayer process used to make alumina, generates waste at a rate of 175.5 million tons per year (Archambo and Kawatra, 2020). For every ton of alumina product made, between 1.5 to 2.5 tons of processing waste are generated (Borra et al, 2016). This waste is named red mud; and disposal of it is a huge task for the operation. Its disposal typically consists of 30- 50% of the total plant's operations (Paramguru, 2004). The red mud can either be thickened and pumped into

147

land-based impoundments or be discharged into nearby bodies of water. Countries with small amounts of available land area choose the latter such as Japan, France, and Greece (Rai et al, 2012). Most alumina plants however, have moved to thickening the red mud to a higher solids content and disposing in an enclosure on land.

Red mud is a dangerous waste product for many different reasons, so its correct disposal is paramount. The bauxite ore used in alumina processing is subjected to high temperature dissolution in sodium hydroxide. After this step, the undissolved solids are washed off with residual caustic and that becomes the red mud. The pH of red mud is typically above 11; due to the large amount of caustic used in processing (Grafe et al, 2011). Concentrated amounts of radioactive elements such as thorium and uranium have been identified in some red mud samples (Damayanti and Khareunissa, 2016). Many other toxic elements such as As, Cr, Hg, Pb, and Zn are also concentrated in red mud which poses as danger to human health and the safety of the environment (Rutyers et al, 2011). These characteristics of red mud show that it needs to be handled carefully and dealt with in a way that allows for the safety of people and the environment. The compilation of these factors has given red mud the reputation as a hazardous waste.

The viewpoint of seeing red mud as purely as waste product is incorrect. Red mud is composed of a multitude of minerals that can be further processed for profit. Major chemical phase ranges for red mud around the world can be seen in Table 6-1. The variation in composition of red mud is large, but many sources of red mud have iron grades hovering near 50%. These grades of iron are higher than iron grade feedstocks in the north American iron range. Residual aluminum can also be present at a large quantity

148

which may find use in a recycle stream into the alumina plant for enhanced recovery. Titanium bearing elements are also common among many red muds, which could be processed into titanium-based products.

Table 6-1: Composition ranges of major minerals in red mud wastes (Archambo and Kawatra, 2020).

Mineral Component	Weight % Range
Fe_2O_3	4-55
TiO_2	2-17
Al_2O_3	6-27
SiO_2	3-24

Removal of the iron value from red mud provides a number of benefits. With red mud that constitutes more than 50% iron, the removal of iron reduces that amount of waste disposed by 50%. Reduction of mineral processing waste by such a large margin would allow for much less land area to be consumed as a waste dump. Economic incentive to produce iron as a byproduct from a waste is another bonus.

Research has shown that iron can be removed from red mud by various methods. Iron in red mud can be reduced directly at temperatures above 500 Celsius in the presence of a reducing atmosphere of CO, N2, and CO_2 (Gotsu et al, 2018). Another study was conducted with a reducing atmosphere of CO and H2 in order to reduce red mud iron by 43% (Ksiazek et al, 2018). Red mud that has been subjected to direct reduction

techniques will also need to employ a secondary separation step in order to remove the metallic iron from the gangue. In most cases, magnetic separation is chosen to separate the metallic iron from the gangue. Several studies have shown that acid leaching is a viable option to remove iron from red mud (Li et al, 2018), (Zhang et al, 2020), (Yang et al, 2015). Leaching under acidic conditions also removes other minerals however, making a pure iron extract difficult to achieve.

The iron nugget process is one that can effectively reduce iron oxides, melt the metallic iron, and separate the iron from the slag in a single step (Anameric and Kawatra, 2006). The iron that is produced via this method can be compared to the quality of blast furnace pig iron. A comparison of apparent densities of iron nuggets to various iron sources can be seen in Table 6-2. From the table, iron nuggets produced from both red mud and magnetite ore are able to produce iron with apparent densities near 7. Blast furnace pig iron apparent densities are near 7.2, while higher grades of iron and steel are above 7.5. Pig iron and iron nugget apparent densities are lower because of the higher carbon content that is present in each of these irons. The carbon content of iron is lowered inside of the basic oxygen furnace.

Table 6-2: Apparent densities of various forms of iron compared to iron nuggets produced at Michigan Technological University.

Material	Density	Reference
Red mud iron nugget with wood	6.95	Archambo and Kawatra, 2020
Magnetite iron nugget with coal	6.6-7.06	Anameric and Kawatra, 2007
Magnetite	4.9-5.2	Weiss N.L. 1985
Wustite	6.00	Lide D.R. 2001
Blast Furnace Pig Iron	7.20	Weiss N.L. 1985
Low Carbon White Cast Iron	7.6-7.8	Shackelford et al, 1994
Steel	7.8	Ashby M.F. and Jones D.R. 1986
Iron	7.87	Lide D.R. 2001

Another pathway for improving recovery of iron in the red mud iron nuggets comes from the addition of CO_2 to the red mud slurry. Previous research has shown that red mud can be neutralized to a moderate pH with the addition of CO_2. One experiment employed CO_2 before acid leaching for metal recovery and achieved a pH of 8.6 in the red mud (Rivera et al, 2017). The neutralization of red mud with CO_2 produces calcite as a solid precipitate, which can also be used as a flux material for the iron nugget process (Archambo and Kawatra, 2020).

If flux can be generated naturally by adding CO_2, another waste product that is generated on a large scale at nearly every industrial plant, that puts the iron nugget process in a

great position to capitalize. The addition of CO_2 can potentially eliminate the need of fluxing additives during pelletization for iron nugget production with red mud.

6.3   Materials and Methods

Red mud was provided for experimental work from an alumina plant in Louisiana. The iron nuggets were produced following the process flow diagram shown in Figure 6-1.
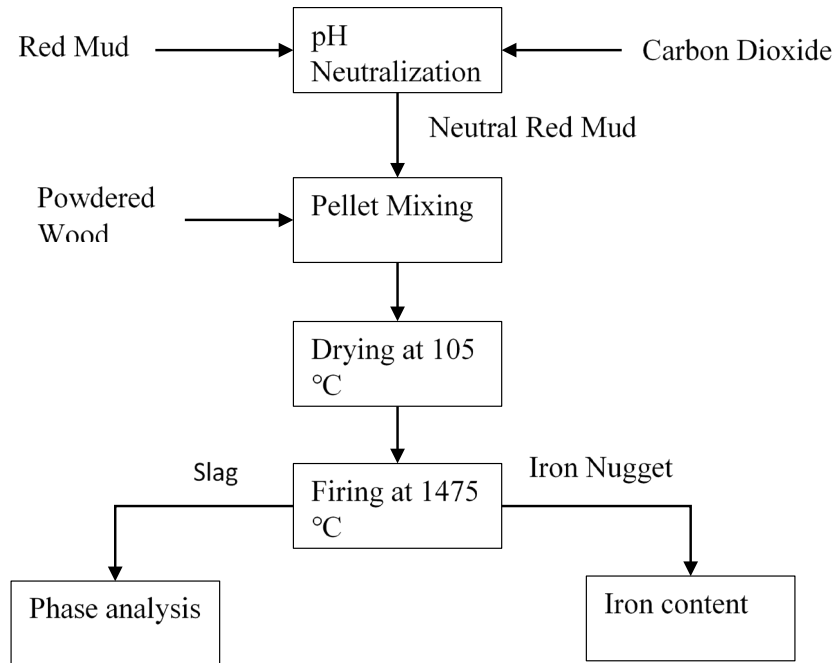
Figure 6-1: Process flow diagram for iron nugget production from neutralized red mud.

Red mud was placed in a 2000 mL beaker with a 1:1 ratio of distilled water and mixed until homogeneous. Carbon dioxide gas was bubbled into the beaker using a gas dispersion tube at a flow rate of 1 liter per minute for 1 hour. Once the pH was brought

down from 13 to 7.5, the slurry was either filtered and dried immediately, or allowed to sit in an open container for 1 week until the pH rose to 10.

Pellets were prepared for high temperature firing. The pellets were composed of 10% powdered wood and 0.66% bentonite clay. The sample was mixed thoroughly and rolled into pellets by hand. The pellets were dried overnight and weighed on the day of firing. Each pellet weighed close to 10 grams.

Pellets were individually placed into crucibles layered with anthracite coal in order to prevent melted samples from sticking to the crucible walls. A Micropyretics MXI high temperature box furnace was used to heat the pellets. The furnace was preheated to 1475 °C. Crucibles were placed into the furnace for constant residence times of 30 minutes. The formed iron nuggets and slag bodies were then subjected to analysis.

Iron content analysis was performed with ultraviolet spectroscopy. X-ray diffraction Scintag XDS 2000 powder diffractometer was used to identify the chemical phase analysis of the samples.

6.4   Results and Discussion

6.4.1   Generation of calcium carbonate during red mud neutralization

Equations 6-1 and 6-2 show that carbonates can be produced as a result of CO_2 neutralization (Sahu et al, 2010). The carbonate anions that are generated can then react with divalent metal cations in solution such as calcium and magnesium to for calcite or dolomite.

$$CO_2(aq) + OH(aq) \leftrightarrow HCO_3(aq) \tag{6-1}$$

$$HCO_3(aq) \leftrightarrow H^+(aq) + CO_3^{-2}(aq) \tag{6-2}$$
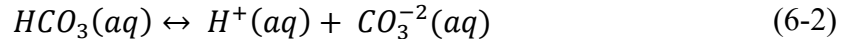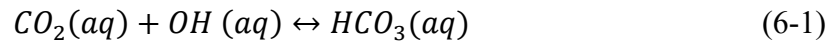
When red mud is neutralized, the pH is not stable at the neutral level and it will rebound once the CO_2 is turned off. Many research projects involving the CO_2 neutralization of red mud cite a rebound of pH after the neutralization cycle is complete (Archambo and Kawatra, 2020), (Rai et al, 2013), (Rivera et al, 2017). Smith et al (2003) contributes the pH rebound to the buffering ability of calcite that is generated via the neutralization.

Rai et al (2013) studied the effect of multiple neutralization cycles of red mud with CO_2 and found that the pH would always rebound to a similar pH. It was also found that multiple cycle neutralization didn't change the amount of calcite that was generated.

Red mud was neutralized to a pH of 7.5 and 10 for nugget making. Table 6-3 Shows the chemical phases present in red mud that has been neutralized with CO_2. As a result of neutralization, calcium carbonate has been produced which should assist in lowering slag viscosity to form iron nuggets. Calcium carbonate was formed at 2.4% weight for these experiments. Iron nuggets had also been generated using a 2.5% dolomite flux in previous works (Archambo and Kawatra, 2020).

Table 6-3: Chemical phases present in red mud that has been neutralized with CO_2

Chemical Component	Weight Percent, %

Calcium Carbonate, $CaCO_3$	2.4
Hematite, Fe_2O_3	29.0
Goethite, FeOOH	19.0
Gibbsite, AlO_3	5.6
Anatase, TiO_2	5.0
Rutile, TiO_2	6.5
Sodalite, $Na_4Al_3(SiO_4)_3Cl$	6.1
Sodium Aluminum Silicate Hydrate, $1.08Na_2O\ Al_2O_3$ $1.68SiO_2\ 1.8H_2O$	26.5

6.4.2 Iron Nugget recovery with CO_2 neutralized red mud

The resulting iron nuggets formed from pH 7.5 and pH 10 CO_2 neutralized nuggets were

compared to a baseline where no neutralization occurred but pure $CaCO_3$ was added to

pellets before firing at a weight percent of the standard 7.5%. Figure 6-2 shows the iron

grade of the resulting pellets. Iron grade at pH 7.5 neutralized red mud are very similar to

that of the baseline results, with grades above 90%. These values compare well with pig

iron that is generated from the conventional blast furnace, which typically produced iron

grades above 90% (Fruehan, 1998).

Iron recovery for the CO_2 neutralized pellets can be seen in Figure 6-3. Compared to the

baseline results, the pH 10 red mud pellets achieved a similar recovery. The baseline

recovered 81% while pH 10 pellets recovered 79%. The pH 7.5 red mud pellets achieved

an iron recovery of 68%. When CO_2 reacts with the red mud slurry system, the calcite flux is not immediately formed. The pH reduction of red mud occurs very quickly as CO_2 is introduced to the system and interacts with available ions in solution, the dissolution of Tricalcium aluminate (TCA) is much slower and occurs over a period of days (Smith et al, 2003). It is the dissolution of TCA that allows calcium carbonates to form following Equation 6-3 (Sahu et al, 2010).

$$3Ca(OH)_2 \cdot 2Al(OH)_{3\,(s)} + 3CO_{2\,(aq)} \leftrightarrow 3CaCO_{3\,(s)} + 2Al(OH)_{3\,(s)} + 3H_2O \qquad (6\text{-}3)$$

pH 7.5 neutralized red mud generated lower recovery of iron due to the fact that it was not given enough time for Equation 6-3 to dissolve the TCA and form calcite. Once the red mud was neutralized, it was immediately dried for pelletization so the TCA couldn't react with an aqueous phase CO_2. The pH 10 neutralized red mud was given a full seven days before it was dried for pelletization. Smith et al (2003) reports that 3 days is required for the neutralized slurry to completely react and generate the maximum amount of calcite.
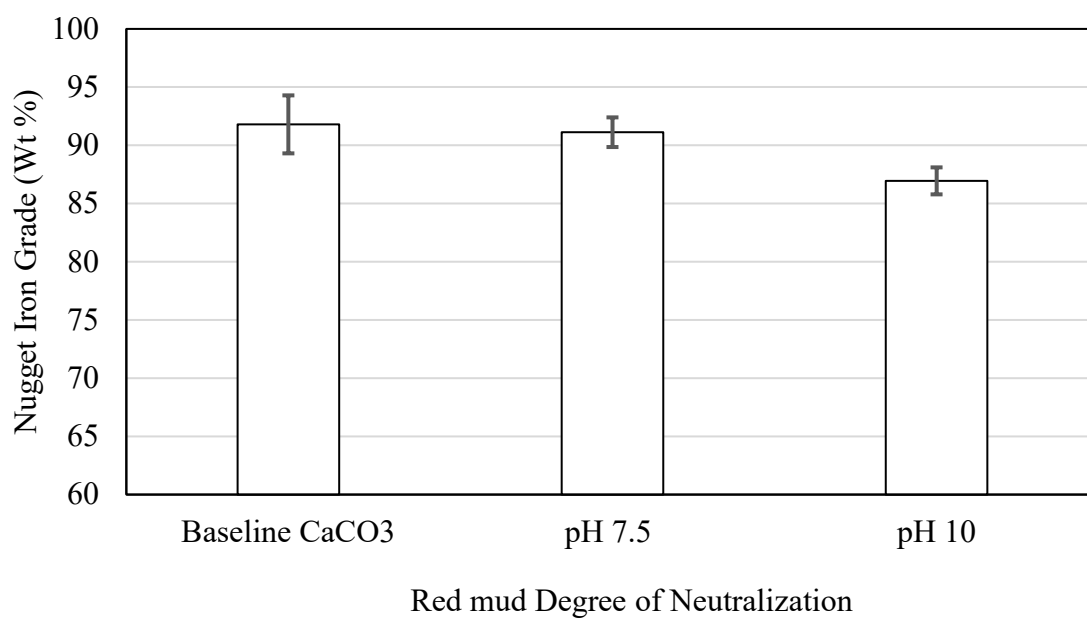
Figure 6-2: Iron nugget grade using carbonate flux generated during CO_2 neutralization of red mud
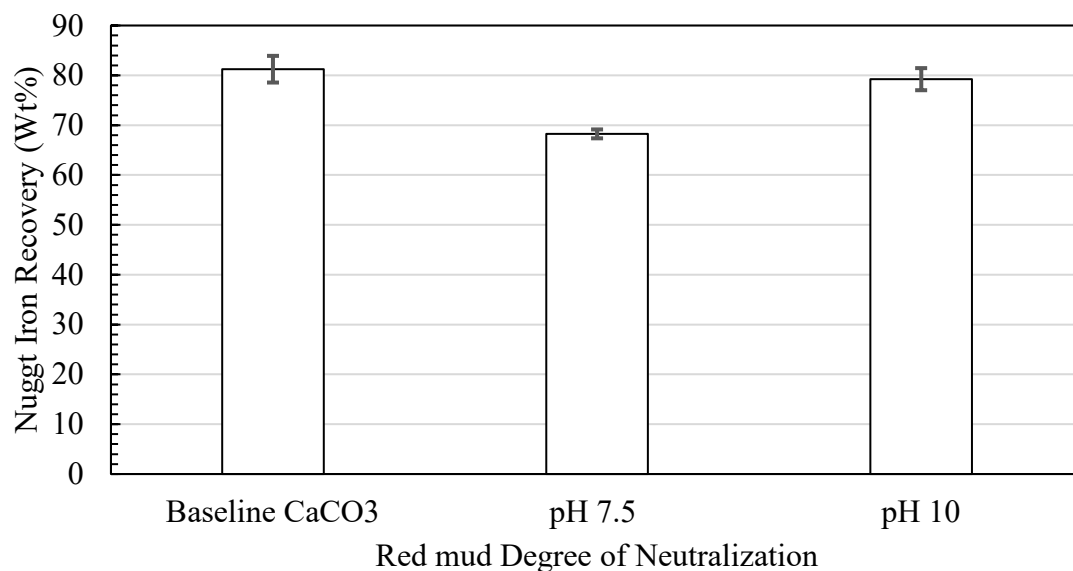
Figure 6-3: Iron recovery in nuggets from red mud that have been neutralized with CO_2 to generate carbonate flux.

The removal of iron from red mud allows a waste material to become more economically feasible and it also reduces the amount of material that it disposed at the end of the process. Table 6-4 shows the overall waste reduction compared to the original red mud. All cases show that waste can be reduced by more than 37% by removing the iron via the iron nugget process. The optimal point, where flux material is generated at a maximum at pH 10 sees the highest waste reduction at nearly 40%. Disposal of red mud in this fashion can greatly limit its negative impact on the environment.

Table 6-4: Waste reduction percent of red mud using the iron nugget process by wt %

	Percent of waste removed (wt %)	Error (±)
pH 7.5 Neutral	37.91	2.04
pH 10 Neutral	39.96	1.41
CaCO₃	37.29	0.85

6.5 Conclusions

Iron nuggets were generated using red mud that had been neutralized with CO_2 prior to

iron extraction. The neutralization formed calcium carbonate that was used as the flux

material for iron nuggets. The red mud was neutralized to pH 7.5 and immediately dried.

Red mud was also neutralized and allowed to rebound for 1 week back to pH 10. Results

showed that both neutral red muds can generate nuggets. The recovery of iron was

highest with the pH 10 red mud. This is because the reaction with aqueous CO_2 and

tricalcium aluminate (TCA) to form calcium carbonate requires time to run to

completion. For nugget production, the rebound of pH is actually favorable to the lowest

pH red mud obtainable. The material that is disposed at the end of the process is also

reduced to nearly 40%. Further processing of iron nugget slags can yield potential for

concentrated valuable minerals such as the elusive rare earth elements.

7 Extraction of rare earth elements from red mud with oxalic acid[3]

7.1 Abstract

Red mud contains large amounts of rare and valuable minerals. Specifically, rare earth elements are present at a concentrated amount in many red mud samples around the world. There is currently only one ore source in the United States that can produce rare earth elements. Pursuing avenues to extract rare earths from red mud is highly advantageous to reduce the amount of red mud being stockpiled, give value to red mud as a waste, and utilize a source for producing rare earths. The iron nugget process effectively increases the concentration of rare earth elements by removing iron. Slag from the iron nugget process upgraded the concentration of rare earth elements by 100%, which makes this a desirable feed for processing. Hydrochloric acid was used to dissolve the rare earth oxides present in the nugget slags, rare earths were then precipitated as a solid using oxalic acid. HCl leach can recover 170 grams of rare earths per ton of red mud nugget slag and Oxalic acid precipitation can recover 45 grams per ton.

7.2 Introduction

Rare earth elements can be found in alumina process waste called red mud. These rare earths can be concentrated by removing iron, which constitutes a large amount of red mud by weight. Many everyday aspects of our society rely on the availability of rare

---

[3] The material contained within this chapter has been submitted to the journal "*Mineral Processing and Extractive Metallurgy Review.*"

earth elements. The rare earth elements have become critical to the expanding world of technology. On the periodic table, the rare earth elements are considered to be elements 57 through 71 including scandium and yttrium. Light rare earth elements (LREE) are the first eight from lanthanum to gadolinium and the heavy rare earth elements (HREE) are the remaining (Krishnamurthy and Gupta, 2016). They are considered rare not because there is a small amount present in the earth but because these elements are rarely found in concentrated ores. Ore bodies that contain high amounts of rare earth elements do exist, however. Bastnaesite ($(REE)CO_3F$) and monazite ($(REE)PO_4$) are minerals that typically contain high concentrations of the light rare earths and xenotime contains heavy rare earth elements (Ganguli and Cook, 2018). The rare earth elements are shown in Table 7-1. All of these elements have a wide variety of applications with critical uses for the military in weapon targeting systems, in nuclear energy, wind, and battery, and in the medical field for imaging.

Table 7-1: Rare earth elements and their typical uses

Element	Atomic Number	Light or Heavy Rare Earth (LREE, HREE)	Uses	Reference
Scandium	21	NA	Ceramics, lasers, and aerospace alloys	Krishnamurthy and Gupta, 2016
Yttrium	39	NA	Molten metal containment ceramics, thermal plasma sprays for aerospace surfaces, superconductors	Krishnamurthy and Gupta, 2016

Lanthanum	57	LREE	Battery and metal alloy, petroleum refining, optics	Ganguli and Cook, 2018
Cerium	58	LREE	Battery and metal alloy, automotive catalyst, ceramics	Ganguli and Cook, 2018
Praseodymium	59	LREE	Ceramics, glasses, pigments	Charalampides et al, 2015
Neodymium	60	LREE	Permanent Magnets	Krishnamurthy and Gupta, 2016
Promethium	61	LREE	Sources for measuring devices, miniature nuclear batteries	Charalampides et al, 2015
Samarium	62	LREE	Permanent magnets, microwave filters, nuclear power	Charalampides et al, 2015
Europium	63	LREE	Phosphors for luminescent characteristics, Targeting and weapon systems	Krishnamurthy and Gupta, 2016
Gadolinium	64	LREE	Visualization of images in medicine. Optical and magnetic detection. Crystal scintillators	Charalampides et al, 2015
Terbium	65	HREE	Fluorescent lamp phosphors, magnets	Haque et al, 2014

Dysprosium	66	HREE	Additive to NdFeB magnets in the electric vehicle and wind energy industries	Krishnamurthy and Gupta, 2016
Holmium	67	HREE	Permanent magnets, nuclear energy, microwave equipment	Ganguli and Cook, 2018
Erbium	68	HREE	Fiber optical amplifiers, high speed optimal communication	Haque et al, 2014
Thulium	69	HREE	Portable X-Ray sources, crystals and laser	Krishnamurthy and Gupta, 2016
Ytterbium	70	HREE	Fluorescent lamps, ceramics, phosphors	Haque et al, 2014
Lutetium	71	HREE	Petroleum refining	Ganguli and Cook, 2018

Rare earth mining and production has grown quickly as innovation in technology has exploded. Table 7-2 shows the production of rare earth oxides by country. The largest producer by far of rare earths is China. Other notable producers in today's market for rare earths are the United States, Myanmar, and Australia. The next largest producer, the Unites States, generates 20% of the rare earths that China does. Currently, in the U.S. these rare earths are only produced from 1 mine in California. The Mountain Pass mine in California was shut down in 2015 due to lower prices for rare earths, which made the U.S. 100% dependent on foreign mined rare earths (Ganguli and Cook, 2018). Since

2018, the Mountain pass mine has begun operating again, but it is the only substantial ore source for directly mining rare earth elements currently in the U.S. This indicates that a push is required to develop methods to extract rare earth elements by other means or secondary sources. Some potential secondary sources of rare earth elements are coal, coal byproducts, iron ore, apatite, phosphate byproducts, cation adsorption clays, recycled materials, and red mud (Peiravi et al, 2021). Utilizing mine tailings from other operations can yield a more profitable margin for the rare earth industry.

Table 7-2: Rare earth oxide reserves and production worldwide (U.S.G.S, 2020)

Country	2019 Rare Earth Oxide Production (Tons)	Estimated Reserves (Tons)
China	132,000	44,000,000
United States	26,000	1,400,000
Burma (Myanmar)	22,000	NA
Australia	21,000	3,300,000
India	3,000	6,900,000
Russia	2,700	12,000,000
Madagascar	2,000	NA
Thailand	1,800	NA
Brazil	1,000	22,000,000
Vietnam	900	22,000,000
Burundi	600	NA

Red mud makes for an excellent candidate for rare earth element extraction. It is noted that some red mud wastes contain a concentrated value of rare earth elements (Balaram, 2019). Vind et al (2018) finds that rare earth elements are almost completely transferred to the waste of the Bayer process and in turn, concentrating them significantly. Jamaican bauxite residue in particular contains a significant amount of rare earth elements. Wagh and Pinnock (1987) report that Jamaican red mud contains between 1690 to 2760 ppm of total rare earth elements. The hazardous nature of red mud combined with the difficulties of processing it economically have been problematic for the aluminum industry. However, if the red mud represents a cache of valuable rare earth elements, then the cost of processing it to remove the rare earths and reduce the total volume of red mud can potentially be offset.

There has been a great deal of research that has gone into how rare earth elements can be leached from red mud. Borra et al (2015) investigated a series of acids for acid leaching red mud to recover rare earths in the liquor. Their research found that hydrochloric acid performed the best at ambient temperature for 24-hour residence time and recovered 70-80% of the rare earth elements. Hydrochloric acid and sulfuric acid were tested using a dry digestion of the red mud followed by water leaching; the finding is that HCl was more effective at dissolving the rare earth elements than sulfuric acid (Rivera et al, 2018).

Zhang et al (2019) sought to remove iron and rare earth elements together using a leaching system with hydrochloric acid followed by solvent extraction; the leaching efficiencies for the leaching were above 80%. Cerium, the most abundant of the rare earth elements can be extracted due to its unique ability as a rare earth element to be oxidized

to the Ce^{4+} state. This paves the way for selective dissolution of trivalent rare earths to separate cerium (Meshram and Abhilash, 2019). The most valuable of the rare earth elements, scandium, can be separated from red mud and the rest of the lanthanides using a combined ion exchange – solvent extraction method (Akcil et al, 2018). One proposed method of rare earth extraction that produces no chemical sludge is biosorption, but it has yet to be used industrially on a large scale (Das and Das, 2013).

For most acid leaching processes involving red mud, contaminants can easily dissolve into the leach solution. Aluminum, titanium, and most notably iron also dissolve into solution at low pH during acid leaching. For example, in the research of Borra et al (2015), more than 80% of the iron from red mud was also digested into the leach solution. Other notable works involving the acid digestion of rare earths include (Ochsenkuhn-Petropulu et al, 1996; Walawalkar et al, 2016; Zhang et al, 2019).

In order for an acid leach process for rare earths to work efficiently, contaminating elements such as iron must be removed first before processing rare earths. The removal of iron can significantly reduce the amount of red mud, up to 50% of red mud weight can be removed in some cases by removing the iron (Archambo and Kawatra, 2020). Smelting red mud at 1600 Celsius was able to remove 85% of the iron and much less iron was found in a leachate of the slags with HCl, H_2SO_4, and HNO_3 (Borra et al, 2016). With the iron nugget process, more than 80% of the iron in red mud can be removed at a lower temperature than iron smelting at 1475 Celsius. The removal of iron also occurs in a single step which is a significant improvement to the operations of the blast furnace, the conventional method for pig iron manufacture. Acid leaching the slag of the nugget

166

process is more beneficial because it has no significant amount of iron to contaminate the rare earth concentrate.

Leach solutions of rare earth concentrates need to be processed further to produce a solid rare earth product. Techniques like solvent extraction have been utilized to produce a solid product of rare earths (Liu and Li, 2015; Wang et al, 2013; Zhu et al, 2019). Solvent extraction requires the use of chemical additives that carry significant cost. A better way to produce the solid precipitate would be to form the precipitation from readily available reagents at the plant site. Carbon dioxide can be removed up to 99% from flue gases in a plant with reagents like bicarbonate and the addition of surfactants (Valluri and Kawatra, 2021). Carbon dioxide can be efficiently converted to oxalic acid using electro catalytic reduction and a low amount of electrical energy input; oxalic acid was chosen as the primary product due to the lowest amount of energy input required to produce compared to other sellable commodities (Valluri and Kawatra, 2019). The oxalic acid can react with rare earth ions in a leach solution and precipitate them as rare earth oxalates. This method of rare earth processing is favorable because it is a simple process that requires less equipment than other precipitation methods (Liu et al, 2008). Oxalic acid has seen research with the application of red mud precipitation for iron, where it was precipitated as an iron oxalate (Yang et al, 2015), (Yang et al, 2016). Using red mud iron nugget slags, which are removed from iron, removes the reaction of iron with oxalate which would also contaminate the solid rare earth concentrate. Utilizing a process which removes iron, acid leaches slag, and precipitates solid rare earths could be an effective

method to separate valuable minerals from red mud and purify them to a level of economic value.

7.3 Experimental

7.3.1 Materials

Red mud samples were received from a plant in Louisiana, USA. The red mud had been produced from a bauxite ore that was mined in Jamaica. Initial analysis of the red mud found that it was composed of a particle size distribution less than 10 microns, the moisture content of the sample was 30%, and the pH of the material was higher than 13. The sample also contained a weight percent of iron near 30%.

The iron was extracted from the red mud sample using the iron nugget process (Archambo and Kawatra, 2020). Using this process, up to 80% of the iron is recovered in an iron nugget concentrate. The slag produced from the nugget process contains the remainder of the red mud material. The major chemical phase distribution can be seen in Figure 7-1. Some remaining iron is present in the form of goethite along with a majority of aluminosilicate phases.
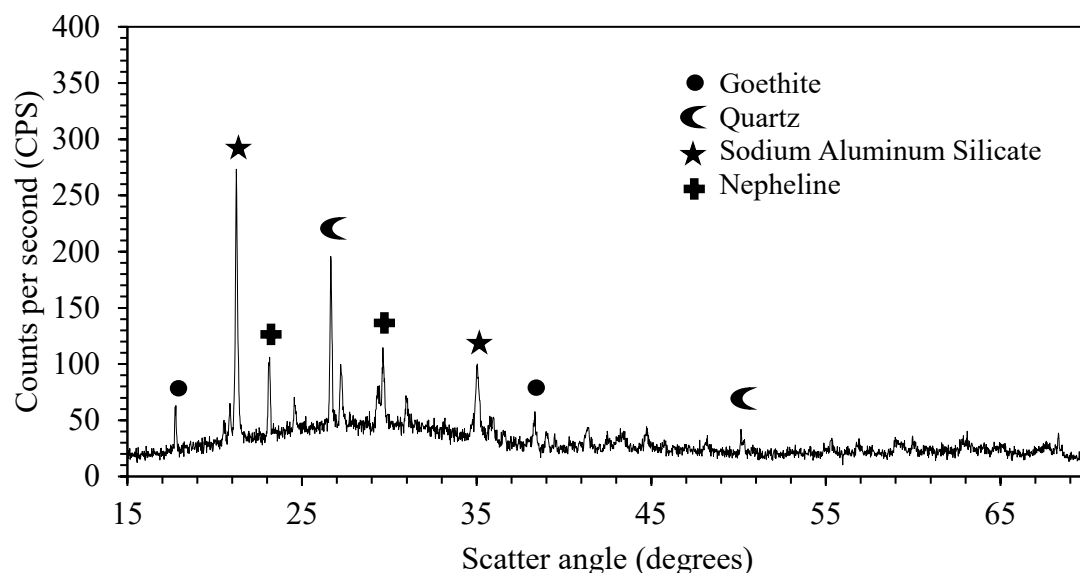
Figure 7-1: X-Ray diffraction pattern for slags produced from the iron nugget process utilizing red mud as a feed.

Inductive coupled plasma (ICP) shows the trace amounts of rare earth elements in the red mud sample and in the iron nugget slag in Table 7-3. From the table, the concentration of rare earth elements had doubled from the original red mud samples. The most concentrated elements are Scandium, Yttrium, Lanthanum, Cerium, and Neodymium. The concentrated nugget slags were used in leaching experiments to remove the rare earths. Nearly all of the rare earth elements are consolidated in the slag phase during the nugget process. Figure 7-2 shows a total rare earth element mass balance around the iron nugget process. The rare earths are recovered at 97% in the slag, the remaining 3% have been incorporated into the iron nugget as trace material at 21.3 ppm. The slag is waste material for the iron nugget process, but rare earth elements have been concentrated in the slag with a recovery of 97%. This implies that the waste material from the nugget process can generate rare earth elements.

Table 7-3: Rare earth element concentrations in parts per million for red mud samples and iron nugget slag samples at Michigan Tech

	Red Mud (ppm)	Nugget Slags (ppm)	Percent Upgraded (%)
Sc	25	35	40
Y	24	45	88
La	12	29	142
Ce	20	48	140
Pr	1.6	4	150
Nd	6	15	150
Sm	1.4	3.2	129
Eu	0.4	0.7	75
Gd	2.1	3.9	86
Tb	0.5	0.8	60
Dy	3.5	6.7	91
Ho	0.9	1.6	78
Er	3.7	5.8	57
Tm	0.7	1.1	57
Yb	5	8.7	74
Lu	1	1.6	60
Total REE	**107.8**	**210.1**	**95**
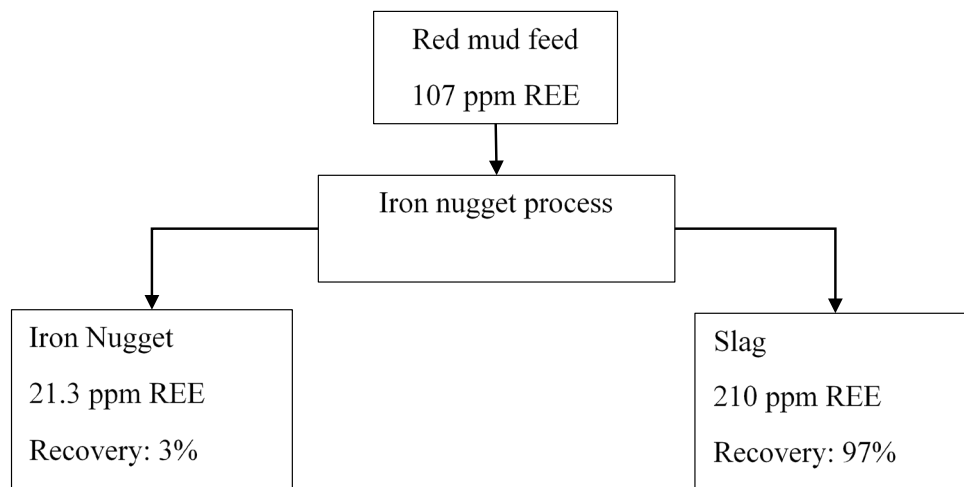
Figure 7-2: Total rare earth element mass balance around the iron nugget process. Concentrations are given in ppm. Recoveries given in weight percent.

7.3.2   Methods

The process flow diagram for the rare earth leaching and precipitation can be seen in Figure 7-3. The powdered slag was weight into 10-gram samples and placed into a 500 mL boiling flask. 12 molar hydrochloric acid was added to the boiling flask at a L/S ratio of 20. A reflux condenser was fitted to the boiling flask and cooled with tap water. The Sample was agitated at a rate of 500 rpm while leaching at a fixed temperature of 90 degrees Celsius. After a residence time of 1 hour, the leach solution was centrifuged to remove any solids and diluted for ICP analysis.

50 mL of leach solution was added to a large beaker and mixed with 50 mL of 0.5M oxalic acid. The pH was then controlled to 2 using sodium hydroxide. The solution was mixed for one hour using a magnetic stir bar at 400 rpm for 1 hour. The sample was then

filtered to remove solid precipitates that formed. Both the solid precipitate and the tailing

liquor was subjected to ICP analysis for rare earth concentrations. All experiments were

done in duplicate for experimental reproducibility.

Red mud iron nugget slag

```
                    ↓
              ┌──────────────┐
              │ Leaching     │
              │ with HCl     │
              └──────────────┘
                    ↓
              ┌──────────────┐
              │ Centrifuge   │──────→  Solid waste
              └──────────────┘
                    ↓
              ┌────────────────────┐
              │ Precipitation with │
              │ Oxalic acid        │
              └────────────────────┘
                    ↓
              ┌──────────────┐                Used leach
              │ Filtration   │──────→         solution
              └──────────────┘
                    ↓
```

REE Oxalate Solid Concentrate
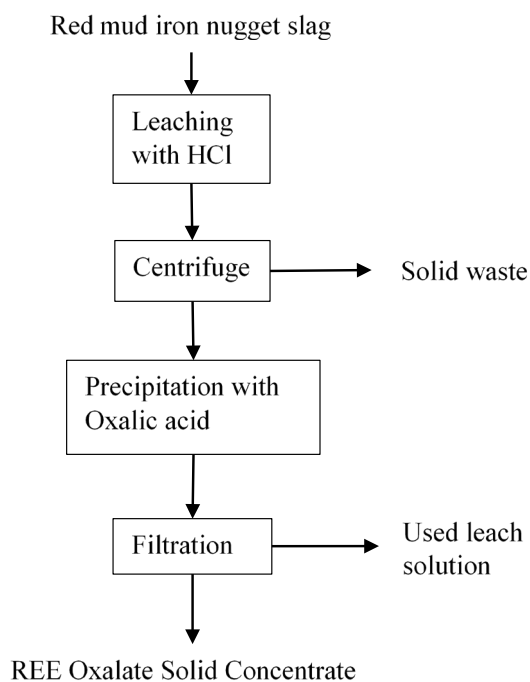
Figure 7-3: Process flow diagram for rare earth element extraction from red mud iron

nugget slags via leaching with HCl and precipitation with oxalic acid

7.4   Results and Discussion

7.4.1   Nugget slag digestion in HCl

The slag from the iron nugget process for red mud was digested in concentrated

hydrochloric acid. The concentration of the leach solution can be seen in Table 7-4. The

concentrations of the rare earth elements in the leach solution are lower than the

concentrations of the solid nugget slags because 20 grams of solids were digested and diluted into 200 mL of acid. During the digestion, it was also noted that silica gel began to form in the boiling flask. Silica gel begins to polymerize at low pH under 1.7 following reactions 7-1 through 7-4 (Rivera et al, 2018). The formation of silica gel is problematic to leaching because the ability to filter the solution is taken away. High concentration of HCl coupled with centrifuging the leachate rather than filtering was sufficient to remove the liquid from the gelled solid silica. A high liquid to solid ratio also reduces the impact of silica gel formation (Borra et al, 2015).

$$M_2SO_4 \text{ (s)} + 4HCl \text{ (l)} + H_2O \text{ (l)} \leftrightarrow 2MCl_2 \text{ (aq)} + H_2O \text{ (l)} + H_4SiO_4 \text{ (aq)} \qquad (7\text{-}1)$$

$$H_4SiO_{4 \text{ (aq)}} + H_2O \leftrightarrow H_3SiO_4 + H_3O \qquad (7\text{-}2)$$

$$H_3SiO_4 + H_4SiO_4 \leftrightarrow OH + H_6Si_2O_7 \qquad (7\text{-}3)$$

$$Si_nO_mOH + H_4SiO_4 \leftrightarrow Si_{n+1}O_{m+2}OH + 2H_2O \qquad (7\text{-}4)$$
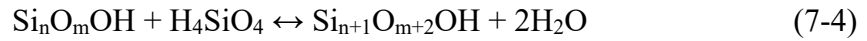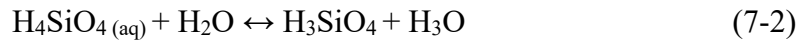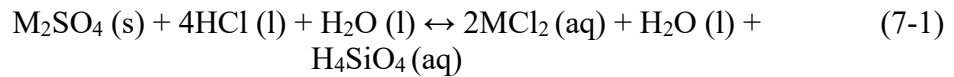
The most prevalent rare earth ions in the solution are Sc, Y, La, and Ce. In general, the highest concentration elements in the acid leachate are the light rare earth elements. The heavy rare earth elements were also dissolved and are present in the leach solution, but they are at a much lower concentration.

Table 7-4: Rare earth element concentration in parts per million (ppm) in 200 mL leach solution of 12M Hydrochloric Acid.

Element	Nugget Slag Concentration (PPM)	HCl Leach Concentration (PPM)	Measurement error (± PPM)
Sc	35	3.545	0.005

Y	45	4.35	0.05
La	29	2.5	0.02
Ce	48	3.96	0.05
Pr	4	0.335	0.005
Nd	15	1.215	0.005
Sm	3.2	0.305	0.005
Eu	0.7	0.065	0.005
Gd	3.9	0.335	0.015
Tb	0.8	0.075	0.005
Dy	6.7	0.635	0.015
Ho	1.6	0.16	0
Er	5.8	0.6	0.02
Tm	1.1	0.105	0.005
Yb	8.7	0.87	0
Lu	1.6	0.145	0.005

Table 7-5 and Figure 7-4 show the results of rare earth leaching in terms of total rare earth recovery. Under these process conditions, the extraction of rare earths was successful. Elements such as scandium (Sc), holmium (Ho), erbium (Er), and ytterbium (Yb) achieved over 95% recovery. The lowest recovery was from neodymium and cerium which were near 80%. Each of these elements are extracted to differing degrees due to their differences in ionic radii and the minerals they might be associated with (Borra et al, 2015). The total recovery of all rare earth elements together was found to be 90.41%.

Elements with low initial concentrations in the nugget slag such as europium and terbium had higher degrees of error. This is likely due to the concentrations being near the low end of the detection range for the ICP to identify accurately. The majority of the rare earths however, contain a small degree of error. The acid leach was able to remove most of the rare earth elements and put them in the leach solution so that they can be recovered as a precipitate with the addition of oxalic acid.

Table 7-5: Rare earth recoveries in weight percent from red mud nugget slag via acid leaching with 200 mL of 12M Hydrochloric acid.

Element	Recovery (%)	Error (±%)
Sc	98.42	0.59
Y	94.51	1.52
La	84.28	0.28
Ce	80.66	1.39
Pr	81.87	0.84
Nd	79.19	0.03
Sm	93.19	1.95
Eu	90.75	6.56
Gd	83.99	4.14
Tb	91.63	5.68
Dy	92.67	2.61
Ho	97.76	0.45

Er	97.31	3.83
Tm	93.34	4.87
Yb	97.76	0.45
Lu	88.61	3.46
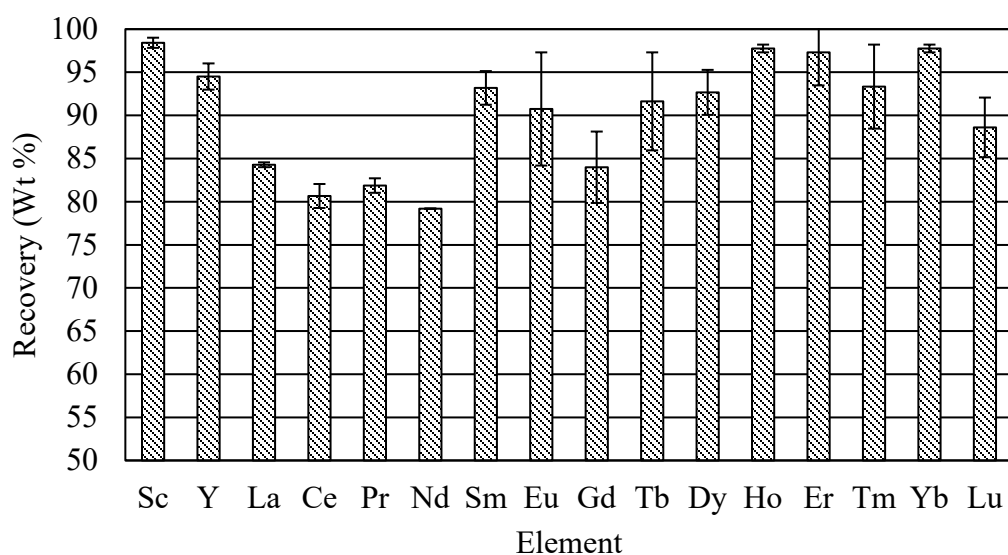
Figure 7-4: Rare earth recoveries in weight percent from the red mud iron nugget slag. Rare earths were recovered in the leach solution of 200 mL 12M Hydrochloric acid.

7.4.2 Rare earth precipitation with oxalic acid

Oxalic acid ($H_2C_2O_4$) was added to the leach solution to generate rare earth precipitate. The following Equation 7-5 shows the generation of rare earth oxalates (Chi and Zu, 1999). Iron can also precipitate using oxalic acid at higher pH, Equations 7-6 and 7-7 show the mechanism for iron precipitation (Yang et al, 2016). Iron precipitation along with other impurities is troublesome to the rare earth separation. The precipitation of the

impurities like iron and aluminum occur at higher pHs above 3. Yang et al (2016) found that significant recovery of iron and aluminum in the rare earth precipitate did not occur until the pH rose above 3.

$$2Re^{3+} + 3H_2C_2O_4 + 10H_2O \leftrightarrow Re_2(C_2O_4)_3 \cdot H_2O + 6H^+ \tag{7-5}$$

$$Fe(C_2O_4)_3^{-3} \leftrightarrow 3(C_2O_4)_4^{-2} + Fe^{3+} \tag{7-6}$$

$$Fe^{3+} + 3OH^- \leftrightarrow Fe(OH)_{3\ (s)} \tag{7-7}$$
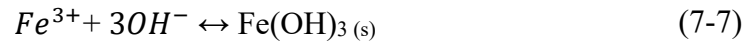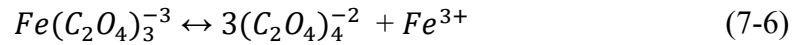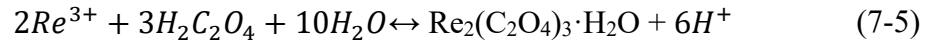
The oxalic acid dissociates into two different ionic phases $HC_2O_4^-$ and $C_2O_4^{2-}$ depending on the pH (Gomes Silva et al, 2019). The balance of these two species is important in maximizing the recovery of rare earths in the precipitate. The optimal pH for rare earth precipitation has been determined to be near 2, the reasons are to maintain the correct ratio of the ionic phases of oxalic acid while also keeping the pH low enough so not to coprecipitate impurities such as iron, aluminum, etc. (Chi and Zhu, 1999).

Table 7-6: Rare earth element recovery in the precipitate with oxalic acid

Element	Recovery (%)	Measurement Error (±%)
Sc	20.73	0.58
Y	25.97	0.47
La	26.15	1.64
Ce	31.11	2.59
Pr	32.64	6.12

Nd	35.84	6.75
Sm	46.20	0.00
Eu	0.00	0.00
Gd	20.40	6.12
Tb	0.00	0.00
Dy	35.39	0.00
Ho	23.08	0.00
Er	17.95	13.68
Tm	0.00	0.00
Yb	26.91	7.07
Lu	15.12	0.00
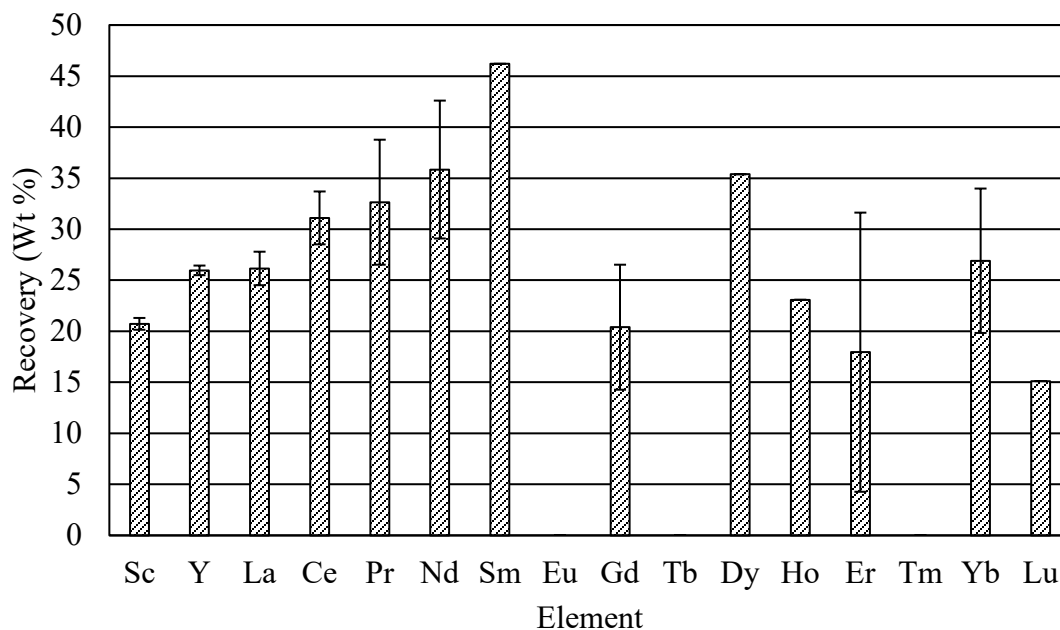
Figure 7-5: Rare earth recovery in the precipitate of oxalic acid. Rare earth precipitate as oxalates. From 0 to 50% recovery. As shown in the graph, Eu, Tb, and Tm could not be recovered

The recovery of rare earth elements in the precipitate can be seen in Table 7-6 and Figure 7-5. The highest recovery was that of samarium at 46%, the majority of elements were recovered between 20 and 35%. The total average recovery of all rare earths in the precipitate was found to be 22.34%. In the case of Eu, Tb, and Tm, the concentration in the precipitate was below the detection limit of the ICP, so it is assumed that none of it was recovered. The recovery was below 50% in the precipitate for all rare earth elements. During the precipitation of rare earth elements in other works, it was found that the initial concentration of rare earths in the leach solution impacted the recovery in the precipitate. The higher the initial concentration of rare earth elements in the leach solution, the higher

the overall recovery in the precipitate (Chi and Xu, 1999). The hypothesis for why initial concentration affects recovery involves the availability of ions to react. In order for Equation 7-5 to proceed, 2 rare earth ions must interact with oxalate ions, when the initial concentration of rare earths is extremely low, it is unlikely that the oxalate will find enough rare earths to form the complex and precipitate.

Experiments in literature that have seen greater success with oxalic acid precipitation had been working with leach samples that were composed of a much higher rare earth initial concentration. Gunes et al (2019), were able to precipitate rare earths from an HCl leach liquor and achieved between 89.5 and 100% precipitation efficiency. The total rare earth concentration was in excess of 32,000 ppm, which is 1600 times higher than the concentration found in this red mud sample. Gomes Silva et al (2019) precipitated rare earth oxalates from rare earth ores which contained between 2 and 6% rare earth oxides. This research was able to recover between 72% and 100% of rare earth elements using oxalic acid precipitation. Other red muds found elsewhere in the world contain significantly more rare earth elements than this sample, in some case more than 2800 ppm (Archambo and Kawatra, 2020). A red mud sample with a higher concentration of rare earths is likely to be a better candidate for oxalic acid precipitation.

The presence of contaminant ions such as Al, Fe, Ca, and Mg have also been shown to negatively impact precipitation efficiency of oxalic acid, when these ions are present, a higher dosage of oxalic acid is required to compensate (Zhang et al, 2020). Red mud leach solutions contain a large number of contaminants, even though the iron has been minimized through extraction in the nugget process, the other contaminant ions are likely

decreasing the leach efficiency significantly. Slags from the iron nugget process have been shown to still contain iron values that weren't recovered, up to 8% by weight (Archambo and Kawatra, 2020).

Table 7-7 shows the production capability of this process for rare earth elements in grams per ton. From the table, the acid leach step can extract 170 grams of rare earth elements per ton of nugget slag and the oxalic acid can precipitate 45 grams of rare earths per ton of nugget slag. Typical recoveries from ion adsorption clays are in excess of 5000 g/ton and 15,000 g/ton for rare earth ores (Talens Peiro and Villalba Mendez, 2013). The values for this particular sample are low due to the low grade of rare earth elements present in this red mud. More concentrated samples of red mud would be able to enhance the kinetics of the oxalic acid precipitation and improve the production capabilities of this rare earth extraction process.

Table 7-7: Rare earth element production from red mud nugget slag. Rare earths were produced with an acid leach step followed by oxalic acid precipitation. Production rate given in grams REE per ton of slag

	REE produced with HCl leach	REE produced with oxalic acid precipitation
Sc	31.4	6.5
Y	38.6	10.0
La	22.2	5.8
Ce	35.1	10.9

Pr	3.0	1.0
Nd	10.8	3.9
Sm	2.7	1.2
Eu	0.6	0.0
Gd	3.0	0.6
Tb	0.7	0.0
Dy	5.6	2.0
Ho	1.4	0.3
Er	5.1	0.9
Tm	0.9	0.0
Yb	7.7	2.1
Lu	1.3	0.0
Total	**170.1**	**45.3**

7.5 Conclusions

Rare earth elements are present in Jamaican red mud. These minerals require immediate attention because they are used heavily in many different technological sectors. The mining and production of these elements has been dominated by China in the last 2 decades which has caused the U.S. and other countries to become dependent. Research must investigate methods to produce rare earth elements on home soil from low grade ores and secondary sources such as red mud.

Rare earths alone may not have value to be processed from red mud, but extracting iron and rare earths may have value. The slags produced from the iron nugget process concentrate the rare earth elements even further, up to double the concentration. Use of a strong acid such as HCl is effective to dissolve rare earth elements found in red mud at recoveries ranging from 80 to 100% depending on the specific element with an average total recovery of 90.41%. The formation of silica gel was combatted by using high liquid to solid ratios with high molarity acid dosages. The precipitation of rare earth oxalates was able to recover between 15 and 50% of the rare earths, depending on the element with the average total recovery at 22.34%. It was found that the initial concentration of rare earths in the acid leach solution impacts the recovery of rare earth oxalates in the precipitate. The low concentration of rare earth elements in this particular sample of red mud impacted to recovery significantly.

Continuing work on this subject should investigate precipitation of rare earths with oxalic acid by upgrading the slags by other means such as solvent extraction first. Utilizing red mud samples that contain a significantly higher rare earth concentrations may also improve recovery of oxalic acid precipitation. Concentrating the rare earths in red mud further by removing more impurities such as titanium, aluminum, and silica may also prove more effective at generating more rare earth oxalate precipitate.

8 Conclusions and Future Work

The purpose of this dissertation was to find methods to produce red mud that is environmentally safe, reduce the amount of red mud that is disposed, and to produce valuable minerals from red mud so that they can compete economically with current industrial practices. In its current form, red mud is a dangerous material with highly alkaline characteristics and concentrations of toxic metals. The growing stockpile of red mud globally is a challenge that needs to be address soon in order to prevent the mining waste from permanently degrading the environment. The high amounts of iron and rare earth elements that are present in red mud can be extracted in order to give the waste material value and reduce the amount of waste that is discarded. Cheap and easily accessible reagents such as CO_2 can be utilized to help prepare red mud for metal extraction.

Carbon dioxide has been shown to be able to significantly reduce the alkalinity of red mud by reducing the pH from 13 to 7.5. The reaction of carbon dioxide with red mud generates calcium carbonate which can be utilized as a flux material for further processing. The calcium carbonate helps to separate iron from red mud using the nugget process. This process can reduce iron and remove it from impurities in a single step. This process has been shown to generate iron nuggets from red mud at qualities similar to blast furnace production. The mechanism of this separation is dependent on the viscosity of the nugget slag, which is significantly improved with the addition of calcium or magnesium fluxes. Iron nuggets can be produced using calcium carbonate that was generated during CO_2 neutralization at similar quality to flux added nuggets. This reduces

184

the need to purchase flux material and allows CO_2 to be sequestered. The amount of material that is disposed of is now up to 40% less than that of the original red mud.

Red mud on its own can contain a concentrated amount of rare earth elements. These metals are critical for many technological sectors of the economy including medicine, military, and renewable energy. The dependence of the rest of the world on China for the production of these metals needs to be broken by production through secondary sources of concentrated rare earths, such as red mud. Iron depleted slags from red mud sent through the iron nugget process is able to double the concentration of rare earth elements. Using hydrochloric acid, 90% of the rare earths were digested into the leach solution. Oxalic acid can be produced cheaply using electrochemical methods from carbon dioxide and can be used as a precipitating reagent to form a pure solid rare earth concentrate. 22.34% of rare earths can be precipitated out of solution using this method with the red mud sample that was used at Michigan Tech. The concentration of the leach solution is an important factor to optimizing recovery in the precipitate. Utilizing this process with higher concentration red muds will likely improve recovery significantly.

Industrial Flue Gas

```
                    Industrial Flue Gas
                          │
                          ▼
            ┌──────────────────────┐
 ┌──────────┤  CO₂                 ◄──────────┐
 │          │  Capture             │          │
 │          └──────────────────────┘          │  CO₂ Recycle
 │                     │                       │
 │                     ▼                       │
 │          ┌──────────────────────┐          │
 Red Mud ──►│  CO₂ Neutralization  │          │
 │          │  of Red Mud          │          │
 │          └──────────────────────┘          │
 │                     │                       │
 │                     ▼                       │
 │          ┌──────────────────────┐          │
 │          │  Iron Nugget Process ├──────────┘──► High Grade
 │          └──────────────────────┘              Metallic Iron
 │                     │
 ▼        Oxalic       ▼
┌────────┐ Acid  ┌──────────────────┐
│ CO₂    │       │ Rare earth       │
│Conver- ├──────►│ extraction with  ├──────► Rare Earth
│sion to │       │ oxalic acid      │        Concentrate
│oxalic  │       └──────────────────┘
│acid    │              │
└────────┘              ▼
                Reduced alumina tailings
```

CO_2 Capture

CO_2 Recycle

Red Mud

CO_2 Neutralization of Red Mud

Iron Nugget Process

High Grade Metallic Iron

CO_2 Conversion to oxalic acid

Oxalic Acid

Rare earth extraction with oxalic acid

Rare Earth Concentrate

Reduced alumina tailings

Figure 8-1: Proposed process flow diagram for efficient utilization of red mud and carbon dioxide

With all of these innovations in mind, Figure 8-1 displays how each of these projects can be put together in a single process. With this process flow, carbon dioxide can be captured and sequestered in the red mud and converted to produced oxalic acid to generate rare earths. The red mud is neutralized with carbon dioxide and then stripped of iron and rare earth values, reducing the amount of waste material by 40%.

To continue the research that began with this dissertation, red mud samples with different compositions should be studied. The chemical phases can vary greatly between red mud samples and the optimization of each process on a particular red mud sample may be different. Determining optimum parameters for carbon dioxide neutralization and the nugget process in varying red mud grades would be beneficial knowledge for the global red mud issue. In addition, red mud samples with rare earth contents below 100 ppm should not be considered for extraction and higher rare earth content muds should be investigated. New methods may be explored to remove valuable minerals from bauxite ore to circumvent the generation of red mud entirely.

9 References

Abdulvaliyev R.A., Akcil A, Gladyshev S.V., Tastanov E.A. , Beisembekova K.O., Akhmadiyeva N.K., and Deveci H. (2015). Gallium and vanadium extraction from red mud of Turkish alumina refinery plant: Hydrogarnet process. *Hydrometallurgy*. Volume 157. 72-77.

Abhilash D, Sinha S, Sinha M.K., and Pandey B.D. (2014). Extraction of lanthanum and cerium from Indian red mud. *International Journal of Mineral Processing*. Volume 127. 70-73.

Adamson A.N., Bloore E.J., and Carr A.R. (1963) Basic Principles of Bayer Process Design. Extractive Metallurgy of Aluminum. *The Minerals, Metals, and Materials Society*. Springer, Cham. 100-117.

Agatzini-Leonardou S, Oustadakis P, Tsakiridis P.E., and Markopoulos C. (2008). Titanium leaching from red mud by diluted sulfuric acid at atmospheric pressure. *Journal of Hazardous Materials*. Volume 157. 579-586.

Akcil A, Akhmadiyeva N, Abdulvaliyev R, Abhilash, and Meshram P. (2018). Overview on extraction and separation of rare earth elements from red mud: Focus on scandium. *Mineral Processing and Extractive Metallurgy Review*. 39(3). 145-151.

Alkan G, Xakalashe B, Yagmurlu B, Kaussen F, and Friedrich B. (2017). Conditioning of red mud for subsequent titanium and scandium recovery- a conceptual design study. *World of Metallurgy*. Volume 70(2). 84-91.

Alkan G, Yagmurlu B, Cakmakoglu S, Hertel T, Kaya S, Gronen L, Stopic S, and Friedrich B. (2018). Novel approach for enhanced scandium and titanium leaching efficiency from bauxite residue with suppressed silica gel. *Scientific Reports*. Volume 8. 5676.

Alex T.C. Kumar R. Roy S.K. and Mehrotra S.P. (2016). Mechanical Activation of Al-oxyhydroxide Minerals-A Review. *Mineral Processing and Extractive Metallurgy Review*. 37:1. 1-26.

Altundoğan H.S., Altundoğan S, Tümen F, and Bildick M. (2002). Arsenic adsorption from aqueous solutions by activated red mud. *Waste management*. Volume 22. 357-63.

Anameric B and Kawatra S.K. (2007a). Conditions for making direct reduced iron, transition direct reduced iron and pig iron nuggets in a laboratory furnace—Temperature-time transformations. *Minerals and Metallurgical Processing*. Volume 24(1). 41.

Anameric B and Kawatra S.K. (2007b). Properties and Features of Direct Reduced Iron. *Mineral Processing and Extractive Metallurgy Review*. Volume 28(1). 59-116.

Anameric B and Kawatra S.K. (2007c). The Microstructure of the pig iron nuggets. *ISIJ International*. Volume 47(1). 53-61.

Anameric B and Kawatra S.K. (2008). Direct iron smelting reduction processes. *Mineral Processing and Extractive Metallurgy Review*. Volume 30(1). 1-51.

Anameric B, Rundman K.B., and Kawatra S.K. (2006). Carburization effects on pig iron nugget making. *Minerals and Metallurgical Processing*. Volume 23(3). 139.

Anameric, B and Kawatra, S. K. (2006). Laboratory study related to the production and processing of pig iron nuggets. *Minerals and Metallurgical Processing*. Volume 23(1). 52-56.

Anameric, B. and Kawatra, S. K. (2006). Pig iron Nuggets versus Blast Furnace Pig Iron. *Sohn International Symposium, Advanced processing of Metals and Materials*. San Diego, Ca USA. August 27-31. Vol 5., 2006, pp. 139-156.

Archambo M and Kawatra S.K. (2020a). Red mud: Fundamentals and new avenues for utilization. "*Mineral Processing and Extractive Metallurgy Review.*" DOI: 10.1080/08827508.2020.1781109

Archambo M, and Kawatra S.K. (2020b). Utilization of Bauxite Residue: Recovering Iron Values Using the Iron Nugget Process. *Mineral Processing and Extractive Metallurgy Review*. DOI: 10.1080/08827508.2020.1720982.

Archambo M, Valluri S.K., and Kawatra S.K. (2020). Pretreatment of red mud with CO_2 for iron recovery. *Annual SME conference*. Phoenix, AZ. February 23-27.

Arnout L, Hertel T, Do Valle L.B., Nelis A, Dormann M, Karachalios T, and Pontikes Y. (2018). Increasing the reactivity of bauxite residue for its use as building material: an alternative thermal activation treatment. *2nd International Bauxite Residue Valorization and Best Practices Conference*. Athens, Greece. 7-10/05/2018.

Balaram V. (2019). Rare Earth Elements: a review of applications, occurrence, exploration, analysis, recycling, and environmental impact. *Geoscience Frontiers*. Volume 10. 1285-1303.

Ballentine F, Lewellyn M.E., and Moffat S.A. (2011). Red Mud Flocculants Used in the Bayer Process. Essential Readings in Light Metals. *The Minerals, Metals, and Materials Society*. Springer, Cham. 425-430.

Balomenos E, Davris P, Pontikes Y, D, Panias D, and Delipaltas A. (2018). Bauxite Residue Handling Practice and Valorization Research in Aluminium of Greece. *2nd International Bauxite Residue Valorization and Best Practices Conference*, 29-37. Athens, Greece.

Balomenos E, Panias D, and Paspaliaris I. (2011). Energy and Exergy Analysis of the Primary Aluminum Production Processes: A Review on Current and Future Sustainability. *Mineral Processing and Extractive Metallurgy Review*. Volume 32(2). 69-89.

Barbosa Botelho A, Hungaro Costa R, Crocce Romano Espinosa D, and Soares Tenorio J.A. (2019). Recovery of Scandium by Leaching Process from Brazilian Red Mud. *Rare Metal Technology*. Springer. 73-79.

Bento N, Santos P, Souza T.E., Oliveira C, and Castro C. (2016). Composites based on PET and red mud residues as catalyst for organic removal from water. *Journal of Hazardous Materials*. Volume 314. 304-311.

Bhoi B, Rajput P, and Mishra C.R. (2017). Production of Green Direct Reduced Iron (DRI) from Red Mud of Indian Origin: A Novel Concept. *Proceedings of 35th International ICSOBA Conference*. Hamburg, Germany. 2-5 October 2017.

Borra C.R., Pontikes Y, Binnemans K, and Van Gerven T. (2015). Leaching of rare earths from bauxite residue (red mud). *Minerals Engineering*. Volume 76. 20-27.

Borra, C.R., Blanpain B, Pontikes Y, Binnemans K, and Van Gerven T. (2016). Recovery of rare earths and other valuable metals from bauxite residue (red mud): a review. *Journal of Sustainable Metallurgy*. Volume 2. 365-86.

Bott R., Langeloh T., and Hahn J. (2008). Advanced Filtration Methods for Pregnant Liquor Purification. Essential Readings in Light Metals. *The Minerals, Metals, and Materials Society*. Springer, Cham. 444-448.

Charalampides G, Vatalis K.I., Apostoplos B, and Ploutarch-Nikolas B. (2015). Rare Earth Elements: Industrial Applications and Economic Dependency of Europe. *Procedia Economic and Finance*. Volume 24. 126-135.

Chaubal M.V. (1990). Physical Chemistry Considerations in Aluminum Hydroxide Precipitation. Essential Readings in Light Metals. *The Minerals, Metals, and Materials Society*. Springer, Cham. 449-508.

Chen, H. Zheng, Z. Chen, Z. Bi, and Xiatao T. (2017). Reduction of hematite (Fe2O3) to metallic iron by CO in a micro fluidized bed reaction analyzer: A multistep kinetics study. *Powder Technology*. Volume 316. 410-420.

Chi R and Xu Z. (1999). A Solution Chemistry Approach to the Study of Rare Earth Element Precipitation by Oxalic Acid. *Metallurgical and Materials Transactions B*. Volume 30B. 189-195.

Chun T.J., Zhu D.Q., Pan J, and He Z. (2014). Preparation of metallic iron powder from red mud by sodium salt roasting and magnetic separation. *Canadian Metallurgical Quarterly*. Volume 53(2). 183-189.

Cristol B and Greenhalgh R. (2018). QAL Bauxite Residue Storage Using Seawater Neutralization. *2nd International Bauxite Residue Valorization and Best Practices Conference*. Athens, Greece. 7-10/05/2018.

Damayanti R, and Khareunissa H. (2016). Composition and characteristics of red mud: a case study on tayan bauxite residue from alumina processing plant at west kalimantan. *Indonesian Mining Journal*. Volume 19. 179-190.

Das N, and Das D. (2013). Recovery of rare earth metals through biosorption: an overview. *Journal of rare earths*. Volume 31(10). 933.

Davris P, Balomenos E, Panias D, and Paspaliaris I. (2016). Selective leaching of rare earth elements from bauxite residue (red mud), using a functionalized hydrophobic ionic liquid. *Hydrometallurgy*. Volume 164. 125-135.

Davris P, Marinos D, Balomenos E, Panias D, and Paspaliiaris I. (2018) Hydrometallurgical extraction of scandium from bauxite residue based on sulfuric acid

process. *2nd International Bauxite Residue Valorization and Best Practices Conference*. Athens, Greece. 7-10/05/2018.

Day R.A., and Underwood A.L. (1991). *Quantitative Analysis*. Determination of Iron with 1,10-Phenanthroline. Sixth Edition. P 720.

Deady E.A., Mouchos E, Goodenough K, Williamson B.J., and Wall F. (2016). A review of the potential for rare-earth element resources from European red muds: examples from Seydişehir, Turkey and Parnassus-Giona, Greece. *Mineralogical Magazine*. Volume 80(1). 43-61.

Dimas D, Giannopoulou I.P., and Panias D. (2009). Utilization of alumina red mud for synthesis of inorganic polymeric materials. *Mineral Processing and Extractive Metallurgy Review*. Volume 30(3). 211-239.

Ding W, Jun-Hui X, Yang P, Si-Yue S, and Tao C. (2019). Iron Extraction from Red Mud using Roasting with Sodium Salt. *Mineral Processing and Extractive Metallurgy Review*.

Evans K. (2016). The History, Challenges, and New Developments in the Management and Use of Bauxite Residue. *Journal of Sustainable Metallurgy*. Volume 2. 316-331.

Fruehan, R. J., & AISE Steel Foundation. (1998). The making, shaping, and treating of steel. Pittsburgh, PA: *AISE Steel Foundation*.

Ganguli R and Cook D.R. (2018). Rare Earths: A review of the landscape. *MRS Energy and Sustainability: A Review Journal*. Doi:10.1557/mre.2018.7

Gawu S. K. Y., Amissah E. E., and Kuma J. S. (2012). The Proposed Alumina Industry And How To Mitigate Against The Red Mud Footprint In Ghana. *Journal of Urban and Environmental Engineering*. Volume 6. Page 48-56.

Glenister D.J. and Abbot T.M. (1989). Dewatering and Dry Disposal of Fine Bauxite Residue. Dewatering Practice and Technology. Brisbane, Australia.

Gomes Silva R., Morais C.A., Teixeira L.V., and Oliveira E.D. (2019). Selective Precipitation of High-Quality Rare Earth Oxalates or Carbonates from a Purified Sulfuric Liquor Containing Soluble Impurities. *Mining, Metallurgy, and Exploration*. Volume 36. 967-977.

Good Philip and Fursman O.C. (1968). Centrifugal Dewatering of Jamaican red mud. U. S. Department of the Interior, Bureau of Mines.

Gotsu S, Mishra B, and Martins G. (2018). Extraction of iron from red mud: low temperature reduction to magnetite and magnetic separation. *2nd International Bauxite Residue Valorization and Best Practices Conference*. Athens, Greece. 7-10/05/2018.

Grafe M., Power G., and Klauber C. (2011). Bauxite residue issues: III. Alkalinity and associated chemistry. *Hydrometallurgy*. Volume 108. 60-79.

Gunes H, Obuz H.E., and Alkan M. (2019). Selective precipitation of Th and Rare Earth Elements from HCl Leach Liquor. *Rare Metal Technology*. DOI: https://doi.org/10.1007/978-3-030-05740-4_9

Guo Y, Gao J, Xu H, Zhou K, And Shi X. (2013). Nuggets Production by Direct Reduction of High Iron Red Mud. *Journal of Iron and Steel Research International*. Volume 20(5). 24-27.

Halmann M, Epstein M, and Steinfeld A. (2012). Vacuum Carbothermic Reduction of Bauxite Components: A Thermodynamic Study. *Mineral Processing and Extractive Metallurgy Review*. Volume 33(3). 190-203.

Halmann M, Steinfeld A, Epstein M, and Vishnevetsky I. (2014). Vacuum Carbothermic reduction of alumina. *Mineral Processing and Extractive Metallurgy Review*. Volume 35(2). 126-135.

Hanahan C, McConchie D, Pohl J, Creelman R, Clark M, and Stocksiek C. (2004). Chemistry of Seawater Neutralization of Bauxite Refinery Residues. *Environmental Engineering Science*. Volume 21(2). 125-138.

Haque N, Hughes A, Lim S, and Vernon C. (2014). Rare Earth Elements: Overview of Mining, Minerology, Uses, Sustainability and Environmental Impact. *Resources*. Volume 3. 614-635.

Hara, K. Hayashi M. Sato, M. and Nagata K. (2011). Continuous Pig Iron Making by Microwave Heating with 12.5 kW at 2.45 GHz. *Journal of Microwave Power and Electromagnetic Energy*, 45 (3).

Hind, A.R., Suresh K.B., and Grocott S.C. (1999). The Surface Chemistry of Bayer Process Solids: a review. *Colloids and Surfaces. A: Physiochemical and Engineering Aspects*. Volume 146. 359-374.

Huang Y, Chai W, Han G, Wang W, and Yang S. (2016). A perspective of stepwise utilization of Bayer red mud: Step two-Extracting and recovering Ti from Ti-enriched tailing with acid leaching and precipitate flotation. *Journal of Hazardous Materials*. Volume 307. 318-327.

Huang Y, Han G, Liu J, and Wang W. (2016). A facile disposal of Bayer red mud based on selective flocculation desliming with organic humics. *Journal of Hazardous Materials*. Volume 301. 46-55.

Huangfu L, Abubakar A, Li C, Li Y, Wang C, Gao S, Liu Z, and Yu J. (2020). Development of Red Mud Coated Catalytic Filter for NOx Removal in the High Temperature Range of 300–450 °C. *Catalysis Letters*. Volume 150. 702-712.

Jayasankar K. Ray P.K., Chaubey A.K., Padhi A., Satapathy B.K., and Mukherjee P.S. (2012). Production of pig iron from red mud waste fines using thermal plasma technology. *International Journal of Minerals, Metallurgy, and Materials*. Volume 19(8). 679.

Josephson G.W, Sillers F, and Runner D.G. (1949). Iron Blast-Furnace Slag Production, Processing, Properties, and Uses. United States Department of the Interior. Bureau of Mines. United States Government Printing Office, Washington.

Karimi E, Briens C, Berruti F, Moloodi S, Tzanetakis T, Thomson M.J., and Schlaf M. (2010). Red Mud as a Catalyst for the Upgrading of Hemp-Seed Pyrolysis Bio-oil. *Energy Fuels*. Volume 24. 6586-6600.

Kasliwal P, and Sai P.S.T. (1999). Enrichment of titanium dioxide in red mud: a kinetic study. *Hydrometallurgy*. Volume 53. 73-87.

Khairul M.A., Zanganeh J, and Moghtaderi B. (2019). The Composition, Recycling, and Utilization of Bayer Red Mud. *Resources, Conservation, and Recycling*. Volume 141. Pages 483-498.

Kotte Jan J. (1981) Bayer Digestion and Predigestion Desilication Reactor Design. Essential Reading in Light Metals. *The Minerals, Metals, and Materials Society*. Springer, Cham. 331-349.

Krishnamurthy N and Gupta C.K. (2016). Extractive Metallurgy of Rare Earths. Second Edition. Taylor and Francis Group. Boca Raton, FL.ISBN: 978-1-4665-7634-6

Ksiazek M, Ringdalen E, Hogaas P.H., and Van Der Eijk C. (2018). Iron removal from bauxite ores. *2nd International Bauxite Residue Valorization and Best Practices Conference*. 7-10/05/2018.

Kumar S, and Prasad A. (2019). Parameters controlling strength of red mud-lime mix. *European Journal of Environmental and Civil Engineering*. Volume 23(6). 743-757.

Kurtoglu S.F. and Uzun A. (2016). Red Mud as an Efficient, Stable, and Cost-Free Catalyst for COx-Free Hydrogen Production from Ammonia. *Scientific Reports*. Volume 6. 32279.

Landis C.R. and Maubeuge K.V. (2004). Activated and natural sodium bentonites and their markets. *Mining Engineering*. Volume 56. 17

Lemougna P.N., Wang K. T., Tang Q, and Cui X. (2017). Synthesis and characterization of low temperature (<800 C) ceramics from red mud geopolymer precursor. *Construction and Building Materials*. Volume 131. 564-573.

Li Y, Haynes R.J., Chandrawana I, and Zhou Y. (2018). Properties of seawater Neutralized Bauxite Residues and Changes in Chemical, Physical, and Microbial Properties induced by additions of gypsum and organic matter. *Journal of Environmental Management*. Volume 223. Page 489-494.

Li Z, Cao Y, Jiang Y, Han G, Fan G, and Chang L. (2018). Removal of Potassium and Iron in Low Grade Bauxite by a Calcination-Acid Leaching Process. *Minerals*. Volume 8. 125.

Lim K, and Shon B. (2008). Metal Components (Fe, Al, and Ti). Recovery from Red Mud by Sulfuric Acid Leaching Assisted with Ultrasonic Waves. *International Journal of Engineering Technology and Advanced Engineering*. Volume 5(2).

Liu C, Li G, Wang R, Yu Z, Li Q, Jing Z, and Zhang Y. (2016). Enhancing the removal of sodium and potassium of sinter by co-containing flue gas circulation sintering process. *7th International Symposium on High Temperature Metallurgical Processing*. 361-368.

Liu W, Chen X, Li W, Yu Y, and Yan K. (2014). Environmental assessment, management, and utilization of red mud in China. *Journal of Cleaner Production*. Volume 84. 606-610.

Liu X, and Zhang N. (2011). Utilization of red mud in cement production: a review. *Waste Management and Research*. Volume 29(10). 1053-1063.

Liu Z and Li H. (2015). Metallurgical process for valuable elements recovery from red mud – a review. *Hydrometallurgy*. Volume 155. 29-43.

Liu Z, Li M, Hu Y, Wang M, and Shi Z. (2008). Preparation of large particle rare earth oxides by precipitation with oxalic acid. *Journal of Rare Earths*. Volume 26. 158.

Liu Z, Zong Y, Li H, and Zhao Z. (2018). Characterization of scandium and gallium in red mud with Time of Flight Secondary Ion Mass Spectrometry (ToF-SIMS) and Electron Probe MicroAnalysis (EPMA). *Minerals Engineering*. Volume 119. 263-273.

Lu F, Xiao T, Lin J, Li A, Long Q, Huang F, Xiao L, Li X, Wang J, Xiao Q, and Chen H. (2018). Recovery of gallium from Bayer red mud through acidic-leaching-ion exchange process under normal atmospheric pressure. *Hydrometallurgy*. Volume 175. 124-132.

Lu R, Zhang Y, Zhou F, and Wang X. (2012). Research of Leaching alumina and iron oxide from Bayer Red mud. *Applied Mechanics and Materials*. Volume 151. 355-359.

Mandal A.K., Verma H.R., and Sinha O.P. (2017). Utilization of aluminum plants waste for production of insulation bricks. *Journal of Cleaner Production*. Volume 162. 949-957.

Martoyan G.A., Karamyan G.G., and Vardan G.A. (2016). New technology of extracting the amount of rare earth metals from the red mud. IOP conference series: *Materials Science and Engineering*. Volume 112.

Mayes W.M., Burke I.T., Gomes H.I., Anton A.D., Molnar M., Feigl V, and Ujaczki E. (2016). Advances in Understanding Environmental Risks of Red Mud After the Ajka Spill, Hungary. *Journal of Sustainable Metallurgy*. Volume 2. 332-343.

McCaffery R.S, Oesterlet J.F, and Schpieo L. (October, 1928) Composition of Blast Furnace Slags. The American Institute of Mining and Metallurgical Engineers. Pittsburgh Meeting. 144-162.

McConchie D, Saenger P, and Fawkes R. (1996). An Environmental Assessment of the Use of Seawater to Neutralize Bauxite Refinery Wastes. Second International Symposium on Extraction and Processing for the Treatment and Minimization of Wastes. The Minerals, Metals, and Materials Society.

McDonald J and Kawatra S.K. (2017). Agglomeration of Hematite Concentrate by Starches. *Mineral Processing and Extractive Metallurgy Review*. Volume 38(1). 1-6.

McGannon H. (1971) The Making, Shaping, and Treating of Steel. Ninth Edition. United States Steel. Herbick and Held. Pittsburg, PN.

Meshram P and Abhilash. (2019). Recovery and Recycling of Cerium from Primary and Secondary Resources- a Critical Review. *Mineral Processing and Extractive Metallurgy Review*. DOI: 10.1080/08827508.2019.1677647

Milacic R, Zuliani T, and Scancar J. (2012). Environmental impact of toxic elements in red mud studied by fractionation and speciation procedures. Science of the total environment. Volume 426. 359-365.

Mineral Prices, (2020). Available from https://mineralprices.com/

Mitsopoulus V.L, and Belanger M. (2006). Thickened Tailings and Red Mud Disposal. Iron Control Technologies. Montreal, Canada.

Montini M, Li X, Rodrigues A.J, Romano R.C.O, Pileggi R.G., and Scrivener K. (2018). Activate fly ash reaction using bauxite residue in blended cement. *2nd International Bauxite Residue Valorization and Best Practices Conference*. Athens, Greece. 7-10/05/2018.

Mourao M. and Cyro T. Effect of Slag Composition on Iron Nuggets Formation from Carbon Composite Pellets. (2010). *Materials Research*. 13(2): 191-195.

Narayanan R.P., Kazantzis N.K., and Emmert M.H. (2019). Process for Scandium Recovery from Jamaican Bauxite Residue: A Probabilistic Economic Assessment. *Materials Today*: Proceedings. Volume 9. 578-586.

Novais, R.M. Innovative use for geopolymers containing high red mud content. (2018). *Proceedings from the 2nd international bauxite residue valorization and best practices conference*. Athens, Greece. 7-10/05/2018.

Ochsenkuhn-Petropulu M, Lyberopulu T, Ochsenkuhn K.M., Parissakis G. (1996). Recovery of lanthanides and yttrium from red mud by selective leaching. *Analytica Chimica Acta*. Volume 319. 249-254.

Olivier J.G.J. and Peters J.A.H.W. (2020). Trend in global CO2 and total greenhouse gas emissions. Netherlands Environmental Assessment Agency. PBL Publishers.

Palmer S.J., Nothling M, Bakon K.H., and Frost R.L. (2010). Thermally activated seawater neutralized red mud used for the removal of arsenate, vanadate, and molybdate from aqueous solutions. *Journal of Colloid and Interface Science*. Volume 342. 147-154.

Paramguru R.K., Rath P.C. and Misra V.N. (2004). Trends in Red Mud Utilization – A Review, *Mineral Processing and Extractive Metallurgy Review*. Volume 26(1). 1- 29.

Pashias N, Boger D.V., Summers K.J., and Glenister D.J. (2000). A Fifty Cent Rheometer for Waste Management of Environmentally Sensitive Ore Tailings. *Mineral Processing and Extractive Metallurgy Review*. Volume 20(1). 115-122.

Patel R.K and Sahu M.K. (2018). Neutralization of red mud using CO_2 sequestration. *2nd international bauxite residue valorization and best practices conference*. Athens, Greece. 7-10/05/2018.

Patel S, and Pal B.K. (2015). Current Status of an Industrial Waste: Red Mud an Overview. *International Journal of Latest Technology in Engineering, Management, and Applied Science (IJLTEMAS)*. ISSN 2278-2540.

Pei D, Li Y, and Cang D. (2017). Na+-solidification behavior of SiO2-Al2O3-CaO-MgO (10 wt%) ceramics prepared from red mud. *Ceramics International*. Volume 43. 16936-16942.

Peiravi M, Dehghani F, Ackah L, Baharlouei A, Godbold J, Liu J, Mohanty M, and Ghosh T. (2021). A Review of Rare-Earth Elements Extraction with Emphasis on Non-conventional Sources: Coal and Coal Byproducts, iron ore tailings, apatite, and phosphate byproducts. *Mining, Metallurgy and Exploration*. Volume 38. 1-26.

Pera J, Boumaza R, and Ambroise J.J. (1996). Development of a pozzolanic pigment from red mud. *Cement and Concrete Research*. Volume 27. 1513-1522.

Pontikes Y and Angelopoulos G.N. (2013). Bauxite residue in cement and cementitious applications: Current status and a possible way forward. *Resources, Conservation, and Recycling*. Volume 73. 53-63.

Power G, Grafe M, and Klauber C. (2011). Bauxite residue issues: I. Current Management, disposal, and storage practices. *Hydrometallurgy*. Volume 108. 33-45.

Rai S, Bahadure S, Chaddha M.J., and Agnihotri A. (2020). Disposal Practices and Utilization of Red Mud (Bauxite Residue): A Review in Indian Context and Abroad. *Journal of Sustainable Metallurgy*. Volume 6. 1-8.

Rai S, Wasewar K, Mishra R.S., Mahindran P, Chadda M.J., Mukhopadhyay J, and Changkoo Y. (2013). Sequestration of carbon dioxide in red mud. *Desalination and water treatment*. Volume 51. 2185-2192.

Rai S, Wasewar K, Mukhopadhyay J, Kyoo Yoo C, and Uslu H. (2012). Neutralization and utilization of red mud for its better waste management. *Archives of Environmental Science*. Volume 6. 13-33.

Resende E.C., Carvalho I, Schlaf M, and Gueriero M.C. (2014). Red Mud waste from the Bayer process as a catalyst for the desulfurization of hydrocarbon fuels. *RSC Advances*. Volume 4. 47287.

Rivera M.R., Ulenaers B, Ounoughene G, Binnemans K, and VanGerven T. (2018). Extraction of rare earths from bauxite residue (red mud) by dry digestion followed by water leaching. *Minerals Engineering*. Volume 119. 82-92.

Rivera R.M, Ghania O, Chenna R.B, Koen B, and Van Gerven T. (2017). Neutralization of bauxite residue by carbon dioxide prior to acidic leaching for metal recovery. *Minerals Engineering*. Volume 112. Page 92-102.

Robertson K. (November, 1 1998) Blast Furnace Slags. Transactions of the American Institute of Mining Engineers.

Rowe M.C. and Brewer B.J. (2018). AMORPH: A statistical program for characterizing amorphous materials by X-ray diffraction. *Computers and Geosciences*. Volume 120. 21-31.

Rutyers S, Mertens J, Vassilieva E, Dehandschutter B, Poffijin A, and Smolders E. (2011). The red mud accident in Ajka (Hungary): Plant toxicity and trace metal bioavailability in red mud contaminated soil. *Environmental Science and Technology*. Volume 45. 1616-1622.

Sahu R.C., Patel R, and Ray B.C. (2010). Neutralization of red mud using CO_2 sequestration cycle. *Journal of Hazardous Materials*. Volume 179. 28-34.

Sandangi J.k., Das S.P., Tripathy A, and Biswal S.K. (2018). Investigation into recovery of iron values from red mud dumps. *Separation Science and Technology*. Volume 53(14). 2186-2191.

Sankey S.E, and Schwarz R.J. (1982). The Structure- Property Relationship of Polymers Used in Red Mud Flocculation. Presentation at the SME-AIME annual meeting. February 14-18 1982. Dallas, Texas.

Scarsella, A, Leong T, and Henriksson B. (2012). A Novel and Environmentally Friendly Process for the Treatment of Bayer Process Residue. *In Proceedings of the 9th International Alumina Quality Workshop*, 171.

Sglavo V.M., Campostrini R, Maurina S, Carturan G, Monagheddu M, Budroni G, and Cocco G. (2000a) Bauxite 'red mud' in the ceramic industry. Part 1: thermal behavior. *Journal of the European Ceramic Society*. Volume 20. 235-244.

Sglavo V.M., Campostrini R, Maurina S, Carturan G, Monagheddu M, Budroni G, and Cocco G. (2000b) Bauxite 'red mud' in the ceramic industry. Part 2: Production of clay-based ceramics. *Journal of the European Ceramic Society*. Volume 20. 245-252.

Shamshad A, Das B. K., and Das S.K. (2018). Dispersion and Sedimentation Characteristics of Red Mud. *Journal of Hazardous, Toxic, and Radioactive Waste*. Volume 22(4).

Shannon G. , White L, and Sridhar S. (2008). Modeling inclusion approach to the steel/slag interface. *Materials Science and Engineering*. A 495. 310-315.

Singh K.K., Singh V.K., Mankhand T.R., and Mandal A.K. (2014). Utilization of Indian Red Mud and Fly Ash with Combustible Additives to prepare Foam Bricks. *Proceedings from the International Conference on Energy, Environment, Materials, and Safety*. December 10-12, 2014.

Singh U, Thawrani S.A., Ansari M.S., Puttewar S.P., and Agnihotri A. (2019). Studies on Beneficiation and Leaching Characteristics of Rare Earth Elements in Indian Red Mud. *Russian Journal of Non Ferrous Metals*. Volume 60(4). 335-340.

Smith, P.G, Pennifold R.M, Davies M.G, and Jamieson E.J. (2003). Reactions of Carbon Dioxide with tri-calcium aluminate. *Hydrometallurgy*. Fifth international conference in honor of professor Ian Ritchie.

Snars K., and Gilkes R.J. (2009). Evaluation of bauxite residues (red muds) of different origins for environmental applications. *Applied Clay Science*. Volume 46. 13-20.

Srikanth S, Ray A.K., Bandopadhyay A, Ravikumar B, and Jha A. (2005). Phase constitution during sintering of red mud and red mud–fly ash mixtures. *Journal of the American Ceramic Society*. Volume 88. 2396-2401.

Srivastava U, and Kawatra S.K. (2009). Strategies for processing low-grade iron ore minerals. *Mineral Processing and Extractive Metallurgy Review*. Volume 30(4). 361-371.

Srivastava U, Eisele T, and Kawatra S.K. (2013). Study of organic and inorganic binders on strength of iron oxide pellets. *Metallurgical and materials transactions*. Volume 44 (4). 1000-1009.

Sujeet Kumar and Arun Prasad. (2019). Parameters controlling strength of red mud-lime mix. *European Journal of Environmental and Civil Engineering*. 23:6 743-757.

Sutar H, Mishra S.C, Sahoo S.K, Chkraverty A.P, and Manharana H.S. (2014) Process of Red Mud Utilization: An Overview. *American Chemical Science Journal*. 4(3): 255-279.

Talens Peiro L and Villalba Mendez G. (2013). Material and Energy Requirement for Rare Earth Production. The Journal of The Minerals, Metals, and Materials Society. Volume 65. DOI: 10.1007/s11837-013-0719-8

Tanako, Cyro and Mourao Marcelo. (January, 1, 1996) Self Reducing Pellets of Wastes from Iron Ore Sinter Plant. Dept. of Metallurgical and Materials Engineering. University of Sao Paolo. The Minerals, Metals, and Materials Society.

Thomas D, and Pei B. (2007). Chemical Reaction Engineering in the Bayer Process. Essential Readings in Light Metals. *The Minerals, Metals, and Materials Society*. Springer, Cham. 118-123.

U.S. Geological Survey, Mineral Commodity Summaries (2019), Access at https://www.usgs.gov/centers/nmic/mineral-commodity-summaries

U.S. Geological Survey, Mineral Commodity Summaries (2020), Access at https://pubs.usgs.gov/periodicals/mcs2020/mcs2020-rare-earths.pdf

Ujaczki E, Courtney R, Cusack P, Chinnam R.K., Clifford S, Curtin T, and O'Donoghue L. (2019). Recovery of Gallium from Bauxite Residue Using Combined Oxalic Acid Leaching with Adsorption onto Zeolite HY. *Journal of Sustainable Metallurgy*. Volume 5. 262-274.

Ujaczki E, Feigl V, Molnar M, Cusack P, Curtin T, Courtney R, O'Donoghue L, Davris P, Hugi C, Evangelou M, Balomenos E, and Lenz M. (2018). Re-using bauxite residues: benefits beyond (critical raw) material recovery. Journal of Chemical Technology and *Biotechnology.* Volume 93(9). 2498-2510.

Ujaczki, E., Zimmerman, Y.-S., Feigl, V., and Lenz, M. (2015). Recovery of rare Earth elements from Hungarian red mud with combined acid leaching and liquid-liquid extraction. *Proceedings of the Bauxite Residue Valorization and Best Practices Conference*. 1–7.

Vachon P, Tyagi R. D., Auclair J.C., and Wilkinson K.J. (1994). Chemical and Biological Leaching of Aluminum from red mud. *Environmental Science and Technology*. Volume 24. 26-30.

Valluri S.K. and Kawatra S.K. (2019). Electro catalytic reduction of CO¬2 to Oxalic acid. *SME Annual Conference and EXPO*. Denver, CO. February 24-27.

Valluri S.K. and Kawatra S.K. (2021). Use of frothers to improve the absorption efficiency of dilute sodium carbonate slurry for post combustion CO2 capture. Fuel Processing Technology. Volume 212.

Vind J, Malfliet A, Blanpain B, Tsakiridis P.E., Tkacyk A.H., Vassiliadou V, and Panias D. (2018). Rare Earth Element Phases in Bauxite Residue. *Minerals*. Volume 8. 77.

Wagh A.S. and Pinnock W.R. (1987). Occurrence of scandium and rare earth elements in Jamaican bauxite waste. *Economic Geology*. Volume 82. 757-761.

Walawalker M, Nichol C.K., and Azimi G. (2016). Process investigation of the acid leaching of rare earth elements from phosphogypsum using HCl, HNO¬3, and H2SO4. *Hydrometallurgy*. Volume 166. 195-204.

Wang W, Dai S, Zhou L, Zhang J, Tian W, and Xu J. (2020). Viscosity and structure of MgO-SiO_2 based slag melt with varying B_2O_3 content. *Ceramics International*. Volume 46. 3631-3636.

Wang L, Sun N, Tang H, and Sun W. (2019). A review on comprehensive utilization of red mud and prospect analysis. *Minerals*. Volume 9(6). 362.

Wang W, Pranolo Y, and Cheng C.Y. (2013). Recovery of scandium from synthetic red mud leach solutions by solvent extraction with D2EHPA. *Separation and Purification Technology*. Volume 108. 96-102.

Wargalla G. and Brandt W. (1981). Processing of Diaspore Bauxites. Essential Readings in Light Metals. *The Minerals, Metals, and Materials Society*. Springer, Cham. 393-401.

Wen Z, Ma S, Zheng S, and Zhang Y. Assessment of Environmental Quality Impacts Caused by Red Mud Storage Facilities in China. *Life of Mine Conference*. Brisbane, Australia. July 12, 2012.

Xing X, Pang Z, Mo C, Wang S, and Ju J. (2020). Effect of MgO and BaO on viscosity and structure of blast furnace slag. *Journal of Non-Crystalline Solids*. Volume 530. 119801.

Xue B, Wei B, Ruan L, Li F, Jiang Y, Tian W, Su B, and Zhou L. (2019). The influencing factor study on the extraction of gallium from red mud. *Hydrometallurgy*. Volume 186. 91-97.

Yadav V.S., Prasad M, Khan J, Amritphale S.S., Singh M, and Raju C.B. (2010). Sequestration of carbon dioxide (CO_2) using red mud. *Journal of Hazardous Materials*. Volume 176. 1044-1050.

Yagmurlu B, Alkan G, Xakalashe B, Schier C, Gronen L, Koiwa I, Dittrich C, and Friedrich B. (2019). Synthesis of scandium phosphate after peroxide assisted leaching of iron depleted bauxite residue (Red Mud) slags. *Scientific Reports*. Volume 9. 11803.

Yang Y, Wang X, Wang M, Wang H, and Xian P. (2015). Recovery of iron from red mud by selective leach with oxalic acid. *Hydrometallurgy*. Volume 157. 239-245.

Yang Y, Wang X, Wang M, Wang H, and Xian P. (2016). Iron recovery from the leached solution of red mud through the application of oxalic acid. *International Journal of Mineral Processing*. Volume 157. 145-151.

Yiran L, Chen H, Wang J, Xu F, and Zhang W. (2014). Research on red mud treatment by a circulating superconducting magnetic separator. *Environmental Technology*. Volume 35(10). 1243-1249.

Zervas, T. McMullan J.T. and Williams B.C. (1996). Developments in Iron and Steel Making. *International Journal of Mineral Processing*. Volume 20. 66-91.

Zhang N, Li H.X., and Liu X.M. (2016). Recovery of scandium from bauxite residue- red mud: a review. *Rare Metals*. Volume 35(12). 887-900.

Zhang W, Noble A, Ji B, and Li Q. (2020). Effects of contaminant metal ions on precipitation of rare earth elements using oxalic acid. *Journal of Rare Earths*. https://doi.org/10.1016/j.jre.2020.11.008.

Zhang X, Zhou K, Chen W, Lei Q, Huang Y, and Peng C. (2019). Recovery of iron and rare earth elements from red mud through an acid leaching-stepwise extraction approach. *Journal of Central South University*. Volume 26(2). 458-466.

Zhang X, Zhou K, Lei Q, Xing Y, Peng C, and Chen W. (2020). Stripping of Fe(III) from Aliquot 336 by NaH2PO4: implication for rare-earth elements recovery from red mud. *Separation Science and Technology*. DOI: 10.1080/01496395.2020.1713814

Zhou, R. Liu, X. Luo, L. Zhou, Y. Wei, J. Chen, A. Tang, L. Wu, H. Deng, Y. Zhang, F. and Wang Y. Remediation of Cu, Pb, Zn, and Cd-contaminated agricultural soil using a combined red mud and compost amendment. (2017). *International Biodeterioration and Biodegradation*. Volume 118. 73-81.

Zhu X, Niu Z, Li W, Zhao H, and Tang Q. (2019). A novel process for recovery of aluminum, iron, vanadium, scandium, titanium and silicon from red mud. *Journal of Environmental Chemical Engineering*. https://doi.org/10.1016/j.jece.2019.103528